Search for pair production of gluinos decaying via stop and sbottom in events with b-jets and large missing transverse momentum in pp collisions at $\sqrt{s} = 13$ TeV with the ATLAS detector

G. Aad *et al.*[*]
(ATLAS Collaboration)

(Received 31 May 2016; published 9 August 2016)

A search for supersymmetry involving the pair production of gluinos decaying via third-generation squarks to the lightest neutralino ($\tilde{\chi}_1^0$) is reported. It uses an LHC proton-proton data set at a center-of-mass energy $\sqrt{s} = 13$ TeV with an integrated luminosity of 3.2 fb^{-1} collected with the ATLAS detector in 2015. The signal is searched for in events containing several energetic jets, of which at least three must be identified as b jets, large missing transverse momentum, and, potentially, isolated electrons or muons. Large-radius jets with a high mass are also used to identify highly boosted top quarks. No excess is found above the predicted background. For $\tilde{\chi}_1^0$ masses below approximately 700 GeV, gluino masses of less than 1.78 TeV and 1.76 TeV are excluded at the 95% C.L. in simplified models of the pair production of gluinos decaying via sbottom and stop, respectively. These results significantly extend the exclusion limits obtained with the $\sqrt{s} = 8$ TeV data set.

DOI: 10.1103/PhysRevD.94.032003

I. INTRODUCTION

Supersymmetry (SUSY) [1–6] is a generalization of space-time symmetries that predicts new bosonic partners to the fermions and new fermionic partners to the bosons of the Standard Model (SM). If R parity is conserved [7], SUSY particles are produced in pairs and the lightest supersymmetric particle (LSP) is stable. The scalar partners of the left- and right-handed quarks, the squarks $\tilde{q}_L$ and $\tilde{q}_R$, can mix to form two mass eigenstates $\tilde{q}_1$ and $\tilde{q}_2$, ordered by increasing mass. SUSY can solve the hierarchy problem [8–11] by preventing "unnatural" fine-tuning in the Higgs sector provided that the superpartners of the top quark (stop, $\tilde{t}_1$ and $\tilde{t}_2$) have masses not too far above the weak scale. Because of the SM weak isospin symmetry, the mass of the left-handed bottom quark scalar partner (sbottom, $\tilde{b}_L$) is tied to the mass of the left-handed top quark scalar partner ($\tilde{t}_L$), and as a consequence the mass of the lightest sbottom $\tilde{b}_1$ is also expected to be close to the weak scale. The fermionic partners of the gluons, the gluinos ($\tilde{g}$), are also constrained by naturalness [12,13] to have a mass around the TeV scale to limit their contributions to the radiative corrections to the stop masses. For these reasons, and because the gluinos are expected to be pair produced with a high cross section at the CERN Large Hadron Collider (LHC), the search for gluino production with decays via stop and sbottom quarks is highly motivated at the LHC.

This paper presents the search for gluino pair production where both gluinos decay either to stops via $\tilde{g} \to \tilde{t}_1 t$ or to sbottoms via $\tilde{g} \to \tilde{b}_1 b$, using a data set of 3.2 fb^{-1} of proton-proton data collected with the ATLAS detector [14] at a center-of-mass energy of $\sqrt{s} = 13$ TeV. Each stop (sbottom) is then assumed to decay to a top (bottom) quark and the LSP: $\tilde{t}_1 \to t\tilde{\chi}_1^0$ ($\tilde{b}_1 \to b\tilde{\chi}_1^0$). The LSP is assumed to be the lightest neutralino $\tilde{\chi}_1^0$, the lightest linear superposition of the superpartners of the neutral electroweak and Higgs bosons. The $\tilde{\chi}_1^0$ interacts only weakly, resulting in final states with substantial missing transverse momentum of magnitude E_T^{miss}. Diagrams of the simplified models [15,16] considered, which are referred to as "Gbb" and "Gtt" in the following, are shown in Figs. 1(a) and 1(b), respectively. The sbottom and stop are assumed to be produced off shell such that the gluinos undergo the three-body decay $\tilde{g} \to b\bar{b}\tilde{\chi}_1^0$ or $\tilde{g} \to t\bar{t}\tilde{\chi}_1^0$, and that the only parameters of the simplified models are the gluino and $\tilde{\chi}_1^0$ masses.[1]

The Gbb experimental signature consists of four energetic b jets (i.e., jets containing b hadrons) and large E_T^{miss}. In order to maintain high signal efficiency, at least three of four required jets must be identified as b jets (b tagged). This requirement is very effective in rejecting $t\bar{t}$ events, which constitute the main background for both the Gbb and Gtt signatures, and which contain only two b jets unless they are produced with additional heavy-flavor jets. The Gtt

[*]Full author list given at the end of the article.

[1]Models with on-shell sbottom and stop were studied in Run 1 [17], and the limits on the gluino and the $\tilde{\chi}_1^0$ masses were found to be mostly independent of the stop and sbottom masses, except when the stop is very light.

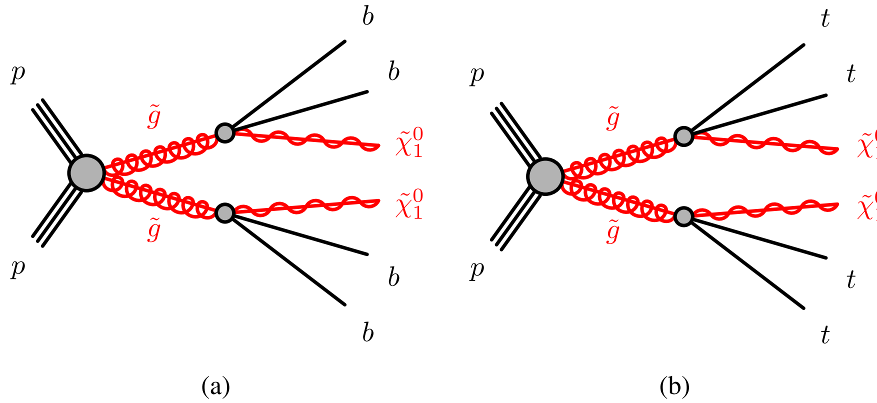

FIG. 1. The decay topologies in the (a) Gbb and (b) Gtt simplified models.

experimental signature also contains four b jets and E_T^{miss}, but yields in addition four W bosons originating from the top quark decays $t \to Wb$. Each W boson can either decay leptonically ($W \to \ell\nu$) or hadronically ($W \to q\bar{q}'$). A Gtt event would therefore possess a high jet multiplicity, with as many as 12 jets originating from top quark decays and, potentially, isolated charged leptons. In this paper, pair-produced gluinos decaying via stop and sbottom quarks are searched for using events with high jet multiplicity, of which at least three must be identified as b jets, large E_T^{miss}, and either zero leptons (referred to as the Gtt 0-lepton channel) or at least one identified charged lepton[2] (referred to as the Gtt 1-lepton channel). For both the Gbb and Gtt models, several signal regions are designed to cover different ranges of gluino and $\tilde{\chi}_1^0$ masses. For the Gtt models with a large mass difference (mass splitting) between the gluino and $\tilde{\chi}_1^0$, the top quarks tend to be highly boosted and their decay products collimated. In the corresponding signal regions, at least one large-radius, trimmed [18] jet, which is reclustered from small-radius jets [19], is required to have a high mass to identify hadronically decaying boosted top quarks.

Pair production of gluinos, with subsequent decays via sbottom quarks, was searched for in ATLAS Run 1 with a similar analysis requiring at least three b-tagged jets [17]. It excluded gluino masses below 1290 GeV for LSP masses below 400 GeV at 95% confidence level (C.L.). That analysis also searched for gluinos decaying via stop quarks in events with at least three b-tagged jets and either zero or at least one identified lepton and obtained the best ATLAS limits for the Gtt models with massless and moderately massive LSP [20]. Gluino masses below 1400 GeV were excluded at 95% C.L. for LSP masses below 400 GeV. Pair-produced gluinos with stop-mediated decays have also been searched for by ATLAS in events with high jet multiplicity [21], events with at least one lepton, many jets, and E_T^{miss} [22], and events containing pairs of same-sign leptons or three leptons [23], the latter obtaining the best ATLAS limit for Gtt models with compressed mass spectra between the gluino and the LSP in Run 1 [20] and having since been performed in Run 2 [24].

Similar searches performed with the CMS experiment using $\sqrt{s} = 8$ TeV [25–30] and $\sqrt{s} = 13$ TeV data [31–34] have produced comparable results to ATLAS searches.

II. ATLAS DETECTOR

The ATLAS detector is a multipurpose particle physics detector with a forward-backward symmetric cylindrical geometry and nearly 4π coverage in solid angle.[3] The inner tracking detector (ID) consists of pixel and silicon microstrip detectors covering the pseudorapidity region $|\eta| < 2.5$, surrounded by a transition radiation tracker, which enhances electron identification in the region $|\eta| < 2.0$. Before the start of Run 2, the new innermost pixel layer, the Insertable B-Layer (IBL) [35], was inserted at a mean sensor radius of 3.3 cm. The ID is surrounded by a thin superconducting solenoid providing an axial 2 T magnetic field and by a fine-granularity lead/liquid-argon (LAr) electromagnetic calorimeter covering $|\eta| < 3.2$. A steel/scintillator-tile calorimeter provides coverage for hadronic showers in the central pseudorapidity range ($|\eta| < 1.7$). The end cap and forward regions ($1.5 < |\eta| < 4.9$) of the hadronic calorimeter are made of LAr active layers with either copper or tungsten as the absorber material. A muon spectrometer with an air-core toroid magnet system surrounds the calorimeters. Three layers of high-precision tracking chambers provide coverage in the range $|\eta| < 2.7$,

[2]The term "lepton" refers exclusively to an electron or a muon in this paper.

[3]ATLAS uses a right-handed coordinate system with its origin at the nominal interaction point in the center of the detector. The positive x axis is defined by the direction from the interaction point to the center of the LHC ring, with the positive y axis pointing upwards, while the beam direction defines the z axis. Cylindrical coordinates (r, ϕ) are used in the transverse plane, ϕ being the azimuthal angle around the z axis. The pseudorapidity η is defined in terms of the polar angle θ by $\eta = -\ln\tan(\theta/2)$.

while dedicated fast chambers allow triggering in the region $|\eta| < 2.4$. The ATLAS trigger system [36] consists of a hardware-based Level-1 trigger followed by a software-based high level trigger.

III. DATA AND SIMULATED EVENT SAMPLES

The data used in this analysis were collected by the ATLAS detector from pp collisions produced by the LHC at a center-of-mass energy of 13 TeV and 25 ns proton bunch spacing. The full data set corresponds to an integrated luminosity of 3.2 fb^{-1} with an associated uncertainty of $\pm 5\%$, after requiring that all detector subsystems were operational during data recording. The measurement of the integrated luminosity is derived, following a methodology similar to that detailed in Ref. [37], from a calibration of the luminosity scale using a pair of x-y beam-separation scans performed in June 2015. Events are required to pass an $E_{\mathrm{T}}^{\mathrm{miss}}$ trigger that is fully efficient for events passing the preselection defined in Sec. V. Each event includes on average 14 additional inelastic pp collisions ("pileup") in the same bunch crossing.

Simulated event samples are used to model the signal and background processes in this analysis. The signal samples for the Gbb and Gtt processes are generated with up to two additional partons using MADGRAPH5_aMC@NLO [38] v2.2.2 at leading order (LO) with CTEQ6L1 [39] parton density function (PDF) sets and interfaced to PYTHIA v8.186 [40] for the modeling of the parton showering, hadronization, and underlying event.

The dominant background in the signal regions is the production of $t\bar{t}$ pairs with additional high-p_{T} jets. The sample for the estimation of this background is generated using the POWHEG-BOX [41,42] generator at next-to-leading order (NLO) with CT10 [43] PDFs and interfaced to PYTHIA v6.428 [44] for showering and hadronization. The decays of heavy-flavor hadrons are modeled using the EVTGEN [45] package. The h_{damp} parameter in POWHEG, which controls the p_{T} of the first additional emission beyond the Born level and thus regulates the p_{T} of the recoil emission against the $t\bar{t}$ system, is set to the mass of the top quark ($m_{\mathrm{top}} = 172.5$ GeV). This setting was found to give the best description of the p_{T} of the $t\bar{t}$ system at $\sqrt{s} = 7$ TeV [46] and $\sqrt{s} = 8$ TeV [47]. All events with at least one semileptonically decaying top quark are included. Fully hadronic $t\bar{t}$ events do not contain sufficient $E_{\mathrm{T}}^{\mathrm{miss}}$ to contribute significantly to the background.

Smaller backgrounds in the signal region come from the production of $t\bar{t}$ pairs in association with $W/Z/h$ and additional jets, single-top production, production of $t\bar{t}t\bar{t}$, $W/Z+$jets and $WW/WZ/ZZ$ (diboson) events. The production of $t\bar{t}$ pairs in association with electroweak vector bosons and $t\bar{t}t\bar{t}$ production are modeled by samples generated using MADGRAPH [48] interfaced to PYTHIA v8.186, while samples to model $t\bar{t}h$ production are generated using MADGRAPH5_aMC@NLO [38] v2.2.1 and showered with HERWIG++ [49] v2.7.1. Single-top production in the s, t, and Wt channels is generated by POWHEG-BOX interfaced to PYTHIA v6.428. $W/Z+$jets and diboson processes are simulated using the SHERPA v2.1.1 [50] generator with CT10 PDF sets. Matrix elements for these processes are calculated using the Comix [51] and OpenLoops [52] generators and merged with the SHERPA parton shower [53] using the ME + PS@NLO prescription [54].

All simulated event samples, with the exception of the Gbb signals, are passed through the full ATLAS detector simulation using GEANT4 [55,56]. The Gbb signal samples are passed through a fast simulation that uses a parametrized description to simulate the response of the calorimeter systems [57]. The simulated events are reconstructed with the same algorithm as that used for data. All PYTHIA v6.428 samples use the PERUGIA2012 [58] set of tuned parameters (tune) for the underlying event, while PYTHIA v8.186 and HERWIG++ showering are run with the A14 [59] and UEEE5 [60] underlying-event tunes, respectively. In-time and out-of-time pileup interactions from the same or nearby bunch crossings are simulated by overlaying additional pp collisions generated by PYTHIA v8.186 on the hard-scattering events. Details of the sample generation and normalization are summarized in Table I. Additional samples with different generators and settings

TABLE I. List of generators used for the different background processes. Information is given about the pQCD highest-order accuracy used for the normalization of the different samples, the underlying-event tunes and PDF sets considered.

Process	Generator + fragmentation/hadronization	Tune	PDF set	Cross-section
$t\bar{t}$	POWHEG-BOX v2 + PYTHIA-6.428	PERUGIA2012	CT10	NNLO + NNLL [61]
Single top	POWHEG-BOX v2 + PYTHIA-6.428	PERUGIA2012	CT10	NNLO + NNLL [62–64]
$t\bar{t}W/t\bar{t}Z$/4-tops	MADGRAPH-2.2.2 + PYTHIA-8.186	A14	NNPDF2.3 [65]	NLO
$t\bar{t}h$	MADGRAPH5_aMC@NLO-2.2.1 + HERWIG++-2.7.1	UEEE5	CT10	NLO [66]
Dibosons WW, WZ, ZZ	SHERPA-2.1.1	Default	CT10	NLO
W/Z+jets	SHERPA-2.1.1	Default	CT10	NNLO [67]

are used to estimate systematic uncertainties on the backgrounds, as described in Sec. VI.

The signal samples are normalized using the best cross sections calculated at NLO in the strong coupling constant, adding the resummation of soft gluon emission at next-to-leading-logarithmic (NLL) accuracy [68–72]. The nominal cross section and the uncertainty are taken from an envelope of cross-section predictions using different PDF sets and factorization and renormalization scales, as described in Ref. [73]. The cross section of gluino pair production in these simplified models is approximately 325 fb for a gluino mass of 1 TeV, falling to 2.8 fb for 1.8 TeV mass gluinos. All background processes are normalized to the best available theoretical calculation for their respective cross sections. The order of this calculation in perturbative QCD (pQCD) for each process is listed in Table I.

IV. OBJECT RECONSTRUCTION

Interaction vertices from the proton-proton collisions are reconstructed from at least two tracks with $p_{\mathrm{T}} > 0.4$ GeV and are required to be consistent with the beam spot envelope. The primary pp interaction vertex is identified as the one with the largest sum of squares of the transverse momenta from associated tracks ($\sum |p_{\mathrm{T,track}}|^2$) [74].

Basic selection criteria are applied to define candidates for electrons, muons, and jets in the event. An overlap removal procedure is applied to these candidates to prevent double counting. Further requirements are then made to select the final signal leptons and jets from the remaining objects. The details of the object selections and of the overlap removal procedure are given below.

Candidate jets are reconstructed from three-dimensional topological energy clusters [75] in the calorimeter using the anti-k_t jet algorithm [76] with a radius parameter of 0.4 (small-R jets). Each topological cluster is calibrated to the electromagnetic scale response prior to jet reconstruction. The reconstructed jets are then calibrated to the particle level by the application of a jet energy scale (JES) derived from simulation and corrections based on 8 TeV data [77,78]. Quality criteria are imposed to reject events that contain at least one jet arising from noncollision sources or detector noise [79]. Further selections are applied to reject jets that originate from pileup interactions [80]. Candidate jets are required to have $p_{\mathrm{T}} > 20$ GeV and $|\eta| < 2.8$. Signal jets, selected after resolving overlaps with electrons and muons, are required to satisfy the stricter requirement of $p_{\mathrm{T}} > 30$ GeV.

A multivariate algorithm using information about the impact parameters of inner detector tracks matched to the jet, the presence of displaced secondary vertices, and the reconstructed flight paths of b and c hadrons inside the jet [81–83] is used to tag b jets. The b tagging working point with an 85% efficiency, as determined from a simulated sample of $t\bar{t}$ events, was found to be optimal. The corresponding rejection factors against jets originating from c quarks, from τ leptons, and from light quarks and gluons in the same sample at this working point are 2.6, 3.8, and 27, respectively.

The candidate small-R jets are used as inputs for further jet reclustering [19] using the anti-k_t algorithm with a radius parameter of 1.0. These reclustered jets are then trimmed [18,19] by removing subjets whose p_{T} falls below $f_{\mathrm{cut}} = 5\%$ of the p_{T} of the original reclustered jet. The resulting large-R jets are used to tag high-p_{T} boosted top quarks in the event. Selected large-R jets are required to have $p_{\mathrm{T}} > 300$ GeV and to have $|\eta| < 2.0$. A large-R jet is tagged as a top candidate if it has a mass above 100 GeV. The mass of the large-R jets is computed from the four-momentum sum of its constituent small-R jets, and the mass of the small-R jets are computed from the four-momentum sum of the topological clusters that make up the jet, which are assumed to be massless. When it is not explicitly stated otherwise, the term "jets" in this paper refers to small-R jets.

Electron candidates are reconstructed from energy clusters in the electromagnetic calorimeter and inner detector tracks and are required to satisfy a set of "loose" quality criteria [84–86]. They are also required to have $|\eta| < 2.47$. Muon candidates are reconstructed from matching tracks in the inner detector and in the muon spectrometer. They are required to meet "medium" quality criteria, as described in Refs. [87,88] and to have $|\eta| < 2.5$. All electron and muon candidates must have $p_{\mathrm{T}} > 20$ GeV and survive the overlap removal procedure. Signal leptons are chosen from the candidates with the following isolation requirement—the scalar sum of p_{T} of additional inner detector tracks in a cone around the lepton track is required to be $<5\%$ of the lepton p_{T}. The angular separation between the lepton and the b jet ensuing from a semileptonic top quark decay narrows as the p_{T} of the top quark increases. This increased collimation is accounted for by varying the radius of the isolation cone as $\max(0.2, 10/p_{\mathrm{T}}^{\mathrm{lep}})$, where $p_{\mathrm{T}}^{\mathrm{lep}}$ is the lepton p_{T} expressed in GeV. Signal electrons are further required to meet the "tight" quality criteria, while signal muons are required to satisfy the same medium quality criteria as the muon candidates. Electrons (muons) are matched to the primary vertex by requiring the transverse impact parameter d_0 to satisfy $|d_0|/\sigma(d_0) < 5$ (3), where $\sigma(d_0)$ is the measured uncertainty in d_0, and the longitudinal impact parameter z_0 to satisfy $|z_0 \sin\theta| < 0.5$ mm. In addition, events containing one or more muon candidates with $|d_0| > 0.2$ mm and $|z_0| > 1$ mm are rejected to suppress cosmic rays.

The overlap removal procedure between muon and jet candidates is designed to remove those muons that are likely to have originated from the decay of hadrons and to retain the overlapping jet. Jets and muons may also appear in close proximity when the jet results from high-p_{T} muon bremsstrahlung, and in such cases the jet should be removed and the muon retained. Such jets are characterized by having very few matching inner detector tracks. Therefore, if the angular distance ΔR between a muon and a jet is within $\min(0.4, 0.04 + 10\ \mathrm{GeV}/p_{\mathrm{T}})$ of the axis of a jet,[4] the muon is removed only if the jet has ≥ 3 matching inner detector tracks. If the jet has fewer than three matching tracks, the jet is removed and the muon is kept [89]. Overlap removal between electron and jet candidates aims to remove jets that are formed primarily from the showering of a prompt electron and to remove electrons that are produced in the decay chains of hadrons. Since electron showers within the cone of a jet contribute to the measured energy of the jet, any overlap between an electron and the jet must be fully resolved. A p_{T} -dependent cone for the purpose of this overlap removal is thus impractical. Consequently, any non-b-tagged jet whose axis lies $\Delta R < 0.2$ from an electron is discarded. If the electron is within $\Delta R = 0.4$ of the axis of any jet remaining after this initial overlap removal procedure, the jet is retained and the electron is removed. Finally, electron candidates that lie $\Delta R < 0.01$ from muon candidates are removed to suppress contributions from muon bremsstrahlung.

The missing transverse momentum ($E_{\mathrm{T}}^{\mathrm{miss}}$) in the event is defined as the magnitude of the negative vector sum transverse momentum (${\vec{p}_{\mathrm{T}}}^{\mathrm{miss}}$) of all selected and calibrated objects in the event, with an extra term added to account for soft energy that is not associated with any of the selected objects. This soft term is calculated from inner detector tracks matched to the primary vertex to make it more resilient to contamination from pileup interactions [90,91] .

Corrections derived from data control samples are applied to simulated events to account for differences between data and simulation in the reconstruction efficiencies, momentum scale, and resolution of leptons [85–87,92] and in the efficiency and false positive rate for identifying b jets [82,83].

V. EVENT SELECTION

The event selection criteria are defined based on kinematic requirements on the objects defined in Sec. IV and on the following event variables.

Two effective mass variables are used, which would typically have much higher values in pair-produced gluino events than in background events. The Gtt signal regions employ the inclusive effective mass $m_{\mathrm{eff}}^{\mathrm{incl}}$,

$$m_{\mathrm{eff}}^{\mathrm{incl}} = \sum_i {p_{\mathrm{T}}}^{\mathrm{jet}_i} + \sum_j {p_{\mathrm{T}}}^{\ell_j} + E_{\mathrm{T}}^{\mathrm{miss}},$$

where the first and second sums are over the signal jets and leptons, respectively. The signal regions for the Gbb models, for which four high-p_{T} b jets are expected, are defined using $m_{\mathrm{eff}}^{4\mathrm{j}}$,

$$m_{\mathrm{eff}}^{4\mathrm{j}} = \sum_{i\leq 4} {p_{\mathrm{T}}}^{\mathrm{jet}_i} + E_{\mathrm{T}}^{\mathrm{miss}},$$

where the sum is over the four highest-p_{T} (leading) signal jets in the event.

In regions with at least one signal lepton, the transverse mass m_{T} of the leading signal lepton (ℓ) and $E_{\mathrm{T}}^{\mathrm{miss}}$ is used to discriminate between the signal and backgrounds from semileptonic $t\bar{t}$ and $W+$jets events,

$$m_{\mathrm{T}} = \sqrt{2 p_{\mathrm{T}}^{\ell} E_{\mathrm{T}}^{\mathrm{miss}} \{1 - \cos[\Delta\phi({\vec{p}_{\mathrm{T}}}^{\mathrm{miss}}, \ell)]\}}.$$

Neglecting resolution effects, m_{T} is bounded from above by the W boson mass for these backgrounds and typically has higher values for Gtt events. Another useful transverse mass variable is $m_{\mathrm{T,min}}^{b\text{-jets}}$, the minimum transverse mass formed by $E_{\mathrm{T}}^{\mathrm{miss}}$ and any of the three leading b-tagged jets in the event,

$$m_{\mathrm{T,min}}^{b\text{-jets}} = \min_{i\leq 3}\left(\sqrt{2 p_{\mathrm{T}}^{b\text{-jet}_i} E_{\mathrm{T}}^{\mathrm{miss}} \{1 - \cos[\Delta\phi({\vec{p}_{\mathrm{T}}}^{\mathrm{miss}}, b\text{-jet}_i)]\}}\right).$$

It is bounded below the top quark mass for semileptonic $t\bar{t}$ events while peaking at higher values for Gbb and Gtt events.

The signal regions require either zero or at least one lepton. The requirement of a signal lepton, with the additional requirements on jets, $E_{\mathrm{T}}^{\mathrm{miss}}$, and event variables described in Sec. VA, render the multijet background negligible for the ≥ 1-lepton signal regions. For the 0-lepton signal regions, the minimum azimuthal angle between ${\vec{p}_{\mathrm{T}}}^{\mathrm{miss}}$ and the leading four small-R jets in the event, $\Delta\phi_{\mathrm{min}}^{4\mathrm{j}}$, is required to be greater than 0.4,

$$\Delta\phi_{\mathrm{min}}^{4\mathrm{j}} = \min(|\phi_{\mathrm{jet}_1} - \phi_{{\vec{p}_{\mathrm{T}}}^{\mathrm{miss}}}|, \ldots, |\phi_{\mathrm{jet}_4} - \phi_{{\vec{p}_{\mathrm{T}}}^{\mathrm{miss}}}|) > 0.4.$$

This requirement ensures that the multijet background, which can produce large $E_{\mathrm{T}}^{\mathrm{miss}}$ if containing poorly measured jets or neutrinos emitted close to the axis of a jet, is also negligible in the 0-lepton signal regions (along with the other requirements on jets, $E_{\mathrm{T}}^{\mathrm{miss}}$, and event variables described in Sec. VA).

Figure 2 shows the kinematic distributions of $E_{\mathrm{T}}^{\mathrm{miss}}$, $m_{\mathrm{eff}}^{\mathrm{incl}}$, $m_{\mathrm{T,min}}^{b\text{-jets}}$, and m_{T} for a preselection that requires $E_{\mathrm{T}}^{\mathrm{miss}} > 200$ GeV, at least four signal jets of which at least three must be b tagged, and $\Delta\phi_{\mathrm{min}}^{4\mathrm{j}} > 0.4$. Figure 3 shows the multiplicity of signal jets, b-tagged signal jets, top-tagged large-R jets, and signal leptons in the preselection.

[4] $\Delta R = \sqrt{(\Delta\eta)^2 + (\Delta\phi)^2}$ defines the distance between objects in (η, ϕ) space.

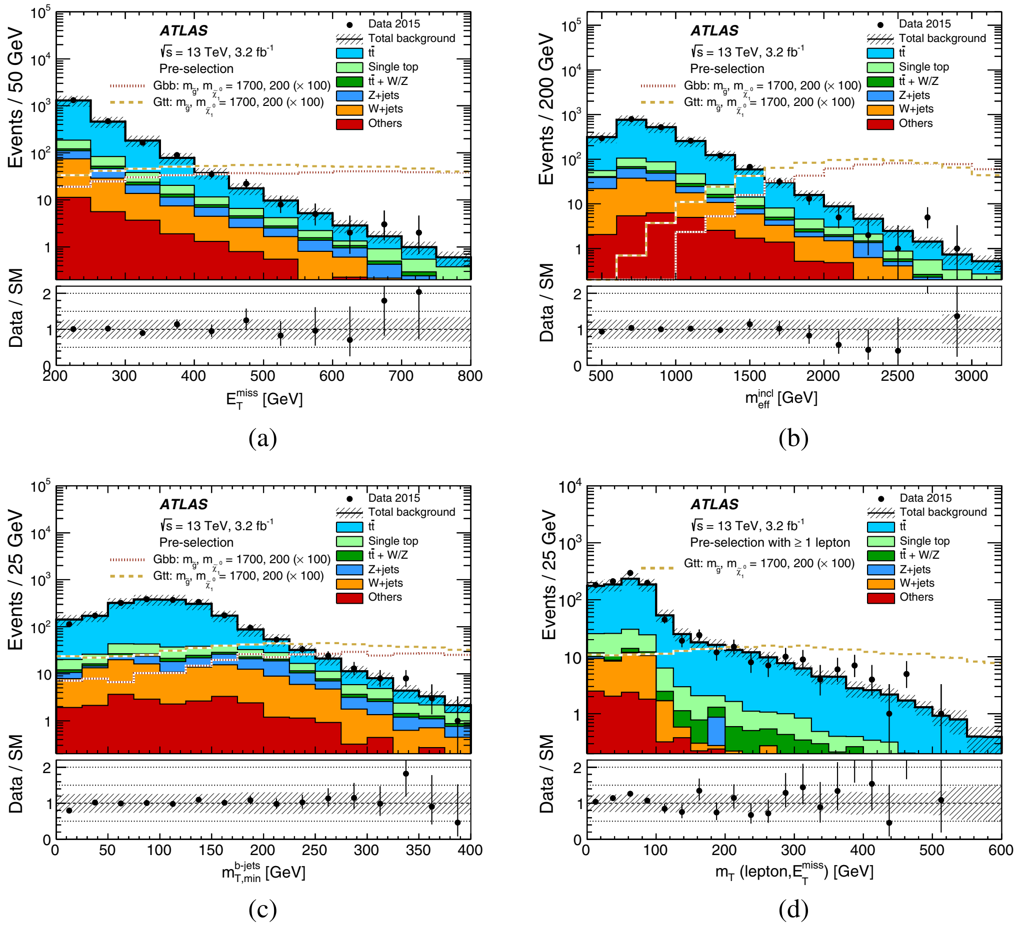

FIG. 2. Distributions of kinematic variables in the preselection region described in the text: (a) $E_{\mathrm{T}}^{\mathrm{miss}}$, (b) $m_{\mathrm{eff}}^{\mathrm{incl}}$, (c) $m_{T,\mathrm{min}}^{b\text{-jets}}$, and (d) m_{T} (for preselected events with at least one signal lepton). The statistical and experimental systematic uncertainties are included in the uncertainty band, where the systematic uncertainties are defined in Sec. VI. The lower part of each figure shows the ratio of data to the background prediction. All backgrounds (including $t\bar{t}$) are normalized using the best available theoretical calculation described in Sec. III. The background category "Others" includes $t\bar{t}h$, $t\bar{t}t\bar{t}$, and diboson events. Example signal models with cross sections enhanced by a factor of 100 are overlaid for comparison.

Good agreement between data and simulation is observed. Example signal models with enhanced cross sections are overlaid for comparison.

A. Signal regions

The signal regions are designed by optimizing the expected signal discovery reach for the 2015 data set. They are defined in the leftmost column of Tables II, III, and IV for the Gbb, Gtt 0-lepton, and Gtt 1-lepton channels, respectively, and are discussed below. These tables also contain the definition of the control regions used to normalize the $t\bar{t}$ background, discussed in Sec. V B, and the validation regions used to cross-check the background estimate and which are discussed in Section V C. The following region nomenclature is used in the remainder of the paper. Signal, control, and validation region names start with the prefix "SR," "CR," and "VR," respectively, and with the type of validation region specified for the Gtt validation regions. The name of the region is completed by the type of model targeted and a letter corresponding to the level of mass splitting between the gluino and the LSP. For example the validation region that cross-checks the extrapolation over m_{T} for the Gtt 1-lepton region A is denoted by "VR-m_{T}-Gtt-1L-A."

The experimental signature for the Gbb model is characterized by four high-p_{T} b jets, large $E_{\mathrm{T}}^{\mathrm{miss}}$, and no leptons [Fig. 1(a)]. The following requirements are applied to all Gbb signal regions. Events containing a candidate lepton are vetoed and at least four signal small-R jets are required, of which at least three must be b tagged. The remaining multijet background is rejected by requiring $\Delta\phi_{\mathrm{min}}^{4\mathrm{j}} > 0.4$. The Gbb signal regions are described in the leftmost column of Table II. The three signal regions A, B, and C are designed to cover Gbb models with large ($\gtrsim$1 TeV), moderate (between $\approx$200 GeV and $\approx$1 TeV), and small ($\lesssim$200 GeV) mass splittings between the gluino

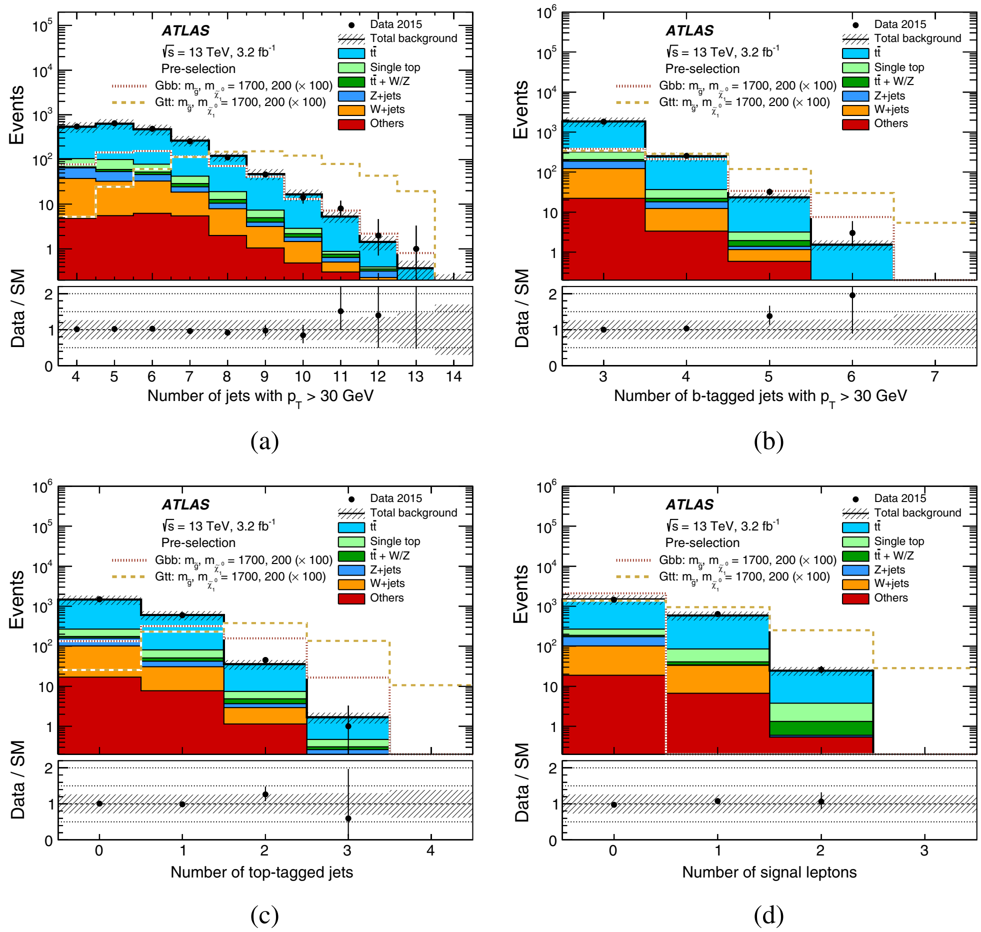

FIG. 3. Distributions of the number of (a) signal jets, (b) b-tagged jets, (c) top-tagged large-R jets, and (d) signal leptons in the preselection region described in the text. The statistical and experimental systematic uncertainties are included in the uncertainty band, where the systematic uncertainties are defined in Sec. VI. The lower part of each figure shows the ratio of data to the background prediction. All backgrounds (including $t\bar{t}$) are normalized using the best available theoretical calculation described in Sec. III. The background category "Others" includes $t\bar{t}h$, $t\bar{t}t\bar{t}$, and diboson events. Example signal models with cross sections enhanced by a factor of 100 are overlaid for comparison.

and the LSP, respectively. All regions feature stringent cuts on E_T^{miss}, m_{eff}^{4j}, and the jet transverse momentum $p_T{}^{\mathrm{jet}}$.

The experimental signature for the Gtt model is characterized by several high-p_T jets of which four are b jets, large E_T^{miss}, and potentially leptons [Fig. 1(b)]. The Gtt signal regions are classified into regions with a signal lepton veto (0-lepton channel) and regions with at least one signal lepton (1-lepton channel). The Gtt 0-lepton signal regions are defined in the leftmost column of Table III. In all Gtt 0-lepton signal regions at least eight signal jets, $\Delta\phi_{\mathrm{min}}^{4j} > 0.4$ and $m_{\mathrm{T,min}}^{b\text{−jets}} > 80$ GeV are required. Three Gtt 0-lepton signal regions are defined to cover Gtt models with decreasing mass splitting between the gluino and the sum of the mass of the two top quarks and the LSP: A ($\gtrsim$1 TeV), B (between $\approx$200 GeV and $\approx$1 TeV), and C ($\lesssim$200 GeV). In the large and moderate mass splitting scenarios, the top quarks tend to have a large p_T, and at least one top-tagged large-R jet is required ($N^{\mathrm{top}} \geq 1$). The requirements on E_T^{miss} and $m_{\mathrm{eff}}^{\mathrm{incl}}$ decrease with the mass splitting between the gluino and the LSP. However, the required number of b-tagged jets $N^{b\text{-jet}}$ is tightened to four for the lower mass splitting regions B and C in order to maintain a high background rejection despite the softer signal kinematics.

The Gtt 1-lepton signal regions are defined in the leftmost column of Table IV. Two signal regions A and B are defined to cover Gtt models with decreasing mass difference between the gluino and the LSP. In all signal regions at least one signal lepton, at least six signal jets ($p_T{}^{\mathrm{jet}} > 30$ GeV), and $m_T > 150$ GeV are required. Region A has tighter requirements on $m_{\mathrm{eff}}^{\mathrm{incl}}$ ($m_{\mathrm{eff}}^{\mathrm{incl}} >$ 1100 GeV) and the number of top-tagged large-R jets ($N^{\mathrm{top}} \geq 1$). Region B has a softer requirement on $m_{\mathrm{eff}}^{\mathrm{incl}}$ than region A, but it features a tighter cut on E_T^{miss} to achieve a satisfactory background rejection without requiring a top-tagged large-R jet.

TABLE II. Definitions of the Gbb signal, control, and validation regions. The unit of all kinematic variables is GeV except $\Delta\phi^{4j}_{min}$, which is in radians. The jet p_T requirement is also applied to b-tagged jets.

Criteria common to all Gbb regions: ≥ 4 signal jets, $\geq 3b$-tagged jets				
	Variable	Signal region	Control region	Validation region
Criteria common to all regions of the same type	$N^{\text{Candidate Lepton}}$	$=0$	$\cdots$	$=0$
	$N^{\text{Signal Lepton}}$	$\cdots$	$=1$	$\cdots$
	$\Delta\phi^{4j}_{min}$	>0.4	$\cdots$	>0.4
	$m_{T,min}^{b-jets}$	$\cdots$	$\cdots$	<160
	m_T	$\cdots$	<150	$\cdots$
Region A (Large mass splitting)	$p_T{}^{jet}$	>90	>90	>90
	E_T^{miss}	>350	>250	>250
	m_{eff}^{4j}	>1600	>1200	<1400
Region B (Moderate mass splitting)	$p_T{}^{jet}$	>90	>90	>90
	E_T^{miss}	>450	>300	>300
	m_{eff}^{4j}	>1400	>1000	<1400
Region C (Small mass splitting)	$p_T{}^{jet}$	>30	>30	>30
	E_T^{miss}	>500	>400	>400
	m_{eff}^{4j}	>1400	>1200	<1400

B. Background estimation and $t\bar{t}$ control regions

The largest background in all signal regions is $t\bar{t}$ produced with additional high-p_T jets. The other relevant backgrounds are $t\bar{t}W$, $t\bar{t}Z$, $t\bar{t}t\bar{t}$, $t\bar{t}h$, single-top, $W+$jets, $Z+$jets, and diboson events. All of these smaller backgrounds are estimated with the simulated event samples normalized to the best available theory calculations described in Sec. III. The multijet background is estimated to be negligible in all regions.

For each signal region, the $t\bar{t}$ background is normalized in a dedicated control region. The $t\bar{t}$ normalization factor

TABLE III. Definitions of the Gtt 0-lepton signal, control, and validation regions. The unit of all kinematic variables is GeV except $\Delta\phi^{4j}_{min}$, which is in radians. The jet p_T requirement is also applied to b-tagged jets.

Criteria common to all Gtt 0-lepton regions: $p_T{}^{jet} > 30$ GeV					
	Variable	Signal region	Control region	VR1L	VR0L
Criteria common to all regions of the same type	$N^{\text{Signal Lepton}}$	$=0$	$=1$	$=1$	$=0$
	$\Delta\phi^{4j}_{min}$	>0.4	$\cdots$	$\cdots$	>0.4
	N^{jet}	≥ 8	≥ 7	≥ 7	≥ 8
	$m_{T,min}^{b-jets}$	>80	$\cdots$	>80	<80
	m_T	$\cdots$	<150	<150	$\cdots$
Region A (Large mass splitting)	E_T^{miss}	>400	>250	>250	>200
	m_{eff}^{incl}	>1700	>1350	>1350	>1400
	$N^{b\text{-tag}}$	≥ 3	≥ 3	≥ 3	≥ 2
	N^{top}	≥ 1	≥ 1	≥ 1	≥ 1
Region B (Moderate mass splitting)	E_T^{miss}	>350	>200	>200	>200
	m_{eff}^{incl}	>1250	>1000	>1000	>1100
	$N^{b\text{-tag}}$	≥ 4	≥ 4	≥ 4	≥ 3
	N^{top}	≥ 1	≥ 1	≥ 1	≥ 1
Region C (Small mass splitting)	E_T^{miss}	>350	>200	>200	>200
	m_{eff}^{incl}	>1250	>1000	>1000	>1250
	$N^{b\text{-tag}}$	≥ 4	≥ 4	≥ 4	≥ 3

TABLE IV. Definitions of the Gtt 1-lepton signal, control, and validation regions. The unit of all kinematic variables is GeV. The jet p_T requirement is also applied to b-tagged jets.

Criteria common to all Gtt 1-lepton regions: ≥1 signal lepton, $p_T^{jet} > 30$ GeV					
	Variable	Signal region	Control region	VR-m_T	VR-$m_{T,min}^{b-jets}$
Criteria common to all regions of the same type	m_T	>150	<150	>150	<150
	N^{jet}	≥ 6	$=6$	≥ 5	≥ 6
	$N^{b\text{-tag}}$	≥ 3	≥ 3	$=3$	$=3$
Region A (Large mass splitting)	E_T^{miss}	>200	>200	>200	>200
	m_{eff}^{incl}	>1100	>1100	>600	>600
	$m_{T,min}^{b-jets}$	>160	⋯	<160	>140
	N^{top}	≥ 1	≥ 1	≥ 1	≥ 1
Region B (Moderate to small mass splitting)	E_T^{miss}	>300	>300	>200	>200
	m_{eff}^{incl}	>900	>900	>600	>600
	$m_{T,min}^{b-jets}$	>160	⋯	<160	>160

required for the total predicted yield to match the data in the control region is used to normalize the $t\bar{t}$ background in the signal region. The control regions are designed to be dominated by $t\bar{t}$ events and to have negligible signal contamination, while being kinematically as close as possible to the corresponding signal region. The latter requirement minimizes the systematic uncertainties associated with extrapolating the normalization factors from the control to the signal regions.

The definitions of the control regions are shown next to the signal regions in Tables II, III, and IV for the Gbb, Gtt 0-lepton, and Gtt 1-lepton channels, respectively. In both the Gbb and Gtt 0-lepton channels, exactly one signal lepton is required. This is motivated by background composition studies using simulated events which show that semileptonic $t\bar{t}$ events, for which the lepton is outside the acceptance or is a hadronically decaying τ lepton, dominate the $t\bar{t}$ yield in the signal regions. An upper cut on m_T is then applied to ensure orthogonality with the Gtt 1-lepton signal regions and to suppress signal contamination. The jet multiplicity requirement is reduced to seven jets in the Gtt 0-lepton control regions (from eight jets in the signal regions), to accept more events and to obtain a number of jets from top quark decay and parton shower similar to that in the signal region. Approximately 40%–60% of the signal region events contain a hadronically decaying τ lepton that is counted as a jet. Orthogonality between Gtt 0-lepton and Gtt 1-lepton control regions is ensured by requiring exactly six jets in the Gtt 1-lepton control regions (as opposed to the requirement of *at least* six jets in the signal regions). For all Gbb and Gtt 0-lepton control regions, the number of b-tagged jets and top-tagged large-R jets is consistent with the signal region. The requirements on E_T^{miss} and m_{eff} are, however, relaxed in the control regions to achieve a sufficiently large $t\bar{t}$ yield and small signal contamination ($\lesssim 15\%$). The Gtt 1-lepton control regions are defined by inverting the m_T cut and removing the $m_{T,min}^{b-jets}$ requirement. All other requirements are exactly the same as for the signal regions.

C. Validation regions

Validation regions are defined to cross-check the background prediction in regions that are kinematically close to the signal regions but yet have a small signal contamination. They are designed primarily to cross-check the assumption that the $t\bar{t}$ normalization extracted from the control regions can be accurately extrapolated to the signal regions. Their requirements are shown in the rightmost column(s) of Tables II, III, and IV for the Gbb, Gtt 0-lepton, and Gtt 1-lepton channels, respectively. Their signal contamination is less than approximately 30% for the majority of Gbb and Gtt model points not excluded in Run 1.

One validation region per signal region is defined for the Gbb model. They feature the same requirements as their corresponding signal region except that upper cuts are applied on $m_{T,min}^{b-jets}$ and m_{eff}^{4j} to reduce signal contamination and ensure orthogonality with the signal regions. In addition, the requirement on E_T^{miss} is relaxed to obtain a sufficient $t\bar{t}$ yield.

For the Gtt 0-lepton channel, two validation regions per signal region are defined, one requiring exactly one signal lepton (VR1L) and one with a signal lepton veto (VR0L). The regions VR1L have exactly the same criteria as their corresponding control regions except that they require $m_{T,min}^{b-jets} > 80$ GeV, similar to the signal regions, in order to test the extrapolation over $m_{T,min}^{b-jets}$ between the control and the signal regions. Simulation studies show that the heavy-flavor fraction of the additional jets in the $t\bar{t}+$jets events (i.e., $t\bar{t}+b\bar{b}$ and $t\bar{t}+c\bar{c}$), which suffers from large theoretical uncertainties, is similar in the signal, control, and VR1L regions. This is achieved by requiring the same number of b-tagged jets for all three types of regions.

While the theoretical uncertainties in the heavy-flavor fraction of the additional jets in the $t\bar{t}+$jets events (i.e., $t\bar{t}+b\bar{b}$ and $t\bar{t}+c\bar{c}$) are large, they affect signal, control, and the 1-lepton validation regions in a similar way, and are thus largely canceled in the semi-data-driven $t\bar{t}$ normalization based on the observed control region yields.

The VR0L regions have similar requirements on their corresponding signal regions except that the requirements on E_T^{miss}, m_{eff}^{incl}, and the number of b-tagged jets are loosened to achieve sufficient event yields. Furthermore, the criterion $m_{T,min}^{b-jets} < 80$ GeV is applied to all VR0L regions to ensure orthogonality with the signal regions. The regions VR0L test the extrapolation of the $t\bar{t}$ normalization from a 1-lepton to a 0-lepton region. Simulation studies show that the VR0L regions have a composition of semileptonic $t\bar{t}$ events (in particular of hadronically decaying τ leptons) similar to that in the signal regions, while the control and VR1L regions are by construction dominated by semileptonic $t\bar{t}$ events with a muon or an electron.

Two requirements are different between Gtt 1-lepton control regions and their corresponding signal regions: the requirement on $m_{T,min}^{b-jets}$ (absent in the control regions) and the requirement on m_T (inverted in the control regions). Therefore, two validation regions per signal region are defined for the Gtt 1-lepton channel, VR-m_T and VR-$m_{T,min}^{b-jets}$, which respectively test, one at a time, the extrapolations over m_T and $m_{T,min}^{b-jets}$. Exactly three b-tagged jets are required for all 1-lepton validation regions to limit the signal contamination and to be close to the signal regions. For the VR-m_T regions, the same requirement $m_T > 150$ GeV as in the signal region is applied but the criterion on $m_{T,min}^{b-jets}$ is inverted. Other requirements are relaxed to achieve sufficiently large background yields and small signal contamination. For the VR-$m_{T,min}^{b-jets}$ regions, the signal region requirement on $m_{T,min}^{b-jets}$ is applied (slightly loosened to 140 GeV instead of 160 GeV in region A) and the criterion on m_T is inverted. Again, other requirements are generally relaxed. Simulation studies show that $t\bar{t}$ dilepton events dominate in the signal regions, in particular due to the requirement on m_T, while semileptonic $t\bar{t}$ events dominate in the control regions. This extrapolation is cross-checked by the VR-m_T regions, which have a $t\bar{t}$ dileptonic fraction similar to that in the signal regions.

VI. SYSTEMATIC UNCERTAINTIES

The largest sources of detector-related systematic uncertainties in this analysis relate to the JES, jet energy resolution (JER), and the b-tagging efficiencies and mistagging rates. The JES uncertainties are obtained by extrapolating the uncertainties derived from $\sqrt{s}=8$ TeV data and simulations to $\sqrt{s}=13$ TeV [77]. The uncertainties in the energy scale of the small-R jets are propagated to the reclustered large-R jets, which use them as inputs. The JES uncertainties are especially important in the Gtt signal regions, since these regions require high jet multiplicities. The impact of these uncertainties on the expected background yields in these regions is between 10% and 25%. Uncertainties in the JER are similarly derived from dijet asymmetry measurements in Run 1 data and extrapolated to $\sqrt{s}=13$ TeV. The impact of the JER uncertainties on the background yields are in the range of 1%–10%.

Uncertainties in the measured b-tagging efficiencies and mistagging rates are the subleading sources of experimental uncertainties in the Gtt 1-lepton signal regions and the leading source in the Gtt 0-lepton and Gbb regions. Uncertainties measured in $\sqrt{s}=8$ TeV data are extrapolated to $\sqrt{s}=13$ TeV, with the addition of the new IBL system in Run 2 taken into account. Uncertainties for jet p_T above 300 GeV are estimated using simulated events. The impact of the b-tagging uncertainties on the expected background yields in the Gbb and Gtt 0-lepton signal regions is around 22%–30%, and around 15% in the Gtt 1-lepton signal regions.

The uncertainties associated with lepton reconstruction and energy measurements have very small impact on the final results. All lepton and jet measurement uncertainties are propagated to the calculation of E_T^{miss}, and additional uncertainties are included in the scale and resolution of the soft term. The overall impact of the E_T^{miss} soft term uncertainties on the expected background yields is 5% or less.

Uncertainties in the modeling of the $t\bar{t}$ background are evaluated using additional samples varied by each systematic uncertainty. Hadronization and parton showering uncertainties are estimated using a sample generated with POWHEG and showered by HERWIG++ v2.7.1 [49] with the UEEE5 underlying-event tune [60]. Systematic uncertainties in the modeling of initial- and final-state radiation are explored with two alternative settings of POWHEG, both of which are showered by PYTHIA v6.428 as for the nominal sample. The first of these uses the PERUGIA2012 radHi tune and has the renormalization and factorization scales set to twice the nominal value, resulting in more radiation in the final state. It also has h_{damp} set to $2m_{top}$. The second sample, using the PERUGIA2012 radLo tune, has $h_{damp}=m_{top}$, and the renormalization and factorization scales are set to half of their nominal values, resulting in less radiation in the event. In each case, the uncertainty is taken as the deviation in the expected yield of $t\bar{t}$ background with respect to the nominal sample. The uncertainty due to the choice of generator is estimated by comparing the expected yields obtained using a $t\bar{t}$ sample generated with MADGRAPH5_aMC@NLO, and one that is generated with POWHEG. Both of these samples are showered with HERWIG++ v2.7.1. Finally, a 30% uncertainty is assigned to the cross section of $t\bar{t}$ events with additional heavy-flavor jets in the final state, in accordance with the results of the ATLAS measurement of this cross section at $\sqrt{s} = 8$ TeV [93]. Uncertainties in single-top and $W/Z + \text{jets}$ background processes are similarly estimated by comparisons between the nominal sample and samples with different generators, showering models, and radiation tunes. An additional 5% uncertainty is included in the cross section of single-top processes [94]. A 50% constant uncertainty is assigned to each of the remaining small backgrounds. The variations in the expected background yields due to $t\bar{t}$ modeling uncertainties range between 10% and 30% for the Gbb signal regions, and between 47% and 57% in most Gtt signal regions. The impact of the modeling uncertainties for the smaller backgrounds on these yields is consistently below 10% in all signal regions. The uncertainties in the cross sections of signal processes are determined from an envelope of different cross-section predictions, as described in Sec. III.

The cumulative impact of the systematic uncertainties listed above on the background yields ranges between 23% and 63%, depending on the signal region. The typical impact on the signal yields is in the range 10%–30%.

VII. RESULTS

The SM background expectation is determined separately in each signal region with a profile likelihood fit [95], referred to as a background-only fit. The fit uses as a constraint the observed event yield in the associated control region to adjust the $t\bar{t}$ normalization, assuming that a signal does not contribute to this yield, and applies that normalization factor to the number $t\bar{t}$ events predicted by simulation in the signal region. The numbers of observed and predicted events in each control region are described by Poisson probability density functions. The systematic uncertainties in the expected values are included in the fit as nuisance parameters. They are constrained by Gaussian distributions with widths corresponding to the sizes of the uncertainties and are treated as correlated, when appropriate, between the various regions. The product of the various probability density functions forms the likelihood, which the fit maximizes by adjusting the $t\bar{t}$ normalization and the nuisance parameters within their constraints. The inputs to the fit for each signal region are the number of events observed in its associated control region and the number of events predicted by simulation in each region for all background processes.

Figure 4 shows the results of the background-only fit to the control regions, extrapolated to the validation regions. The number of events predicted by the background-only fit is compared to the data in the upper panel. The pull, defined by the difference between the observed number of events (n_{obs}) and the predicted background yield (n_{pred}) divided by the total uncertainty (σ_{tot}), is shown for each region in the lower panel. No evidence of significant background mismodeling is observed in the validation regions. There is a certain tendency for the predicted background to be above the data, in particular for the Gtt-0L validation regions, but the results in the validation regions of a given channel are not independent. The validation and control regions of different mass splittings can overlap, with the overlap fraction ranging from approximately 30% to 70% for Gtt-0L. Furthermore, the uncertainties in the predicted

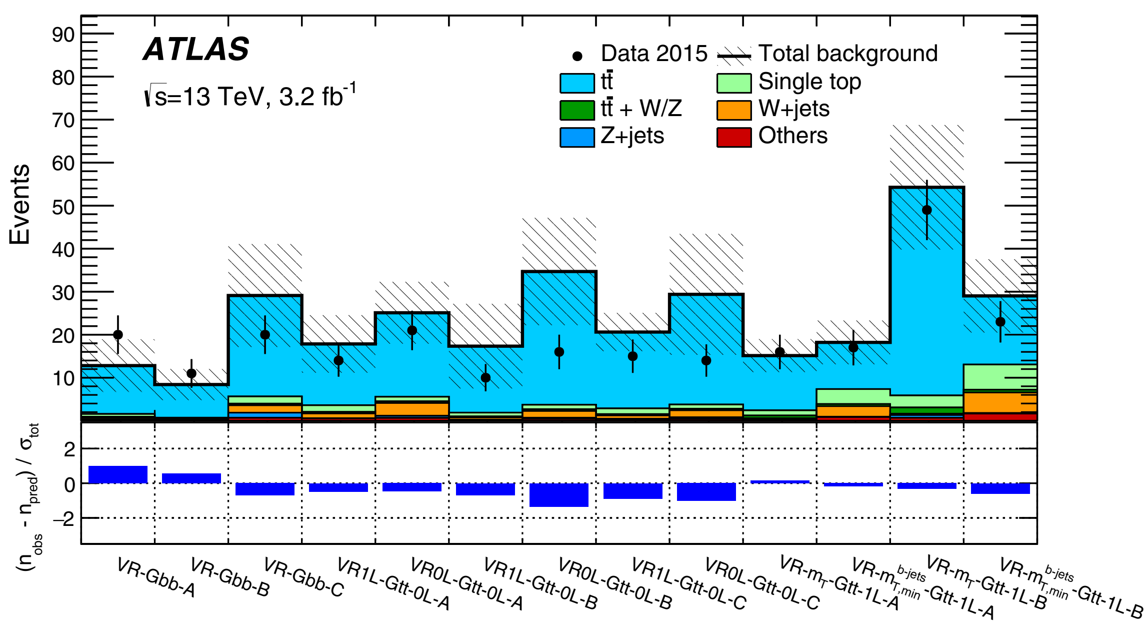

FIG. 4. Results of the likelihood fit extrapolated to the validation regions. The $t\bar{t}$ normalization is obtained from the fit to the control regions. The upper panel shows the observed number of events and the predicted background yield. The background category "Others" includes $t\bar{t}h$, $t\bar{t}t\bar{t}$, and diboson events. The lower panel shows the pulls in each validation region.

TABLE V. Results of the likelihood fit extrapolated to the Gbb signal regions. The uncertainties shown include all systematic uncertainties. The data in the signal regions are not included in the fit. The row "MC-only background prediction" provides the total background prediction when the $t\bar{t}$ normalization is obtained from a theoretical calculation [61]. The $t\bar{t}$ normalization factor $\mu_{t\bar{t}}$ obtained from the corresponding $t\bar{t}$ control region is also provided. The background category "Others" includes $t\bar{t}h$, $t\bar{t}t\bar{t}$, and diboson events. Expected yields for two example Gbb models are also shown.

	SR-Gbb-A	SR-Gbb-B	SR-Gbb-C
Observed events	0	0	5
Fitted background events	1.3 ± 0.4	1.5 ± 0.6	7.6 ± 1.7
$t\bar{t}$	0.63 ± 0.30	0.9 ± 0.5	4.3 ± 1.5
$Z + \text{jets}$	0.23 ± 0.08	0.23 ± 0.09	1.2 ± 0.5
$W + \text{jets}$	0.17 ± 0.06	0.13 ± 0.05	0.82 ± 0.28
Single-top	0.25 ± 0.14	0.15 ± 0.14	0.65 ± 0.33
$t\bar{t}W/Z$	<0.1	<0.1	0.22 ± 0.12
Others	<0.1	<0.1	0.39 ± 0.22
MC-only background prediction	1.7	1.5	6.7
$\mu_{t\bar{t}}$	0.64 ± 0.33	1.0 ± 0.4	1.2 ± 0.4
Gbb ($m_{\tilde{g}} = 1700$ GeV, $m_{\tilde{\chi}_1^0} = 200$ GeV)	3.8	3.5	4.2
Gbb ($m_{\tilde{g}} = 1400$ GeV, $m_{\tilde{\chi}_1^0} = 800$ GeV)	5.3	7.2	10.5

yield are dominated by the same (correlated) systematic uncertainties.

Tables V, VI, and VII show the observed number of events and predicted number of background events from the background-only fit in the Gbb, Gtt 0-lepton, and Gtt 1-lepton signal regions, respectively. In addition, the tables show the numbers of signal events expected for some example values of gluino and LSP masses in the Gtt and Gbb models. The event yields in the signal regions are also shown in Fig. 5, where the pull is shown for each region in the lower panel. No excess is found above the predicted background. The background is dominated by $t\bar{t}$ events in all Gbb and Gtt signal regions. The subdominant contributions in the Gbb and Gtt 0-lepton signal regions are $Z(\to \nu\nu) + \text{jets}$ and $W(\to \ell\nu) + \text{jets}$ events, where for $W + \text{jets}$ events the lepton is a nonidentified electron or muon or is a hadronically decaying τ lepton. In the Gtt 1-lepton signal regions, the subdominant backgrounds are single-top, $t\bar{t}W$ and $t\bar{t}Z$.

Figure 6 shows the $E_{\mathrm{T}}^{\mathrm{miss}}$ distributions in data and simulated samples for SR-Gbb-B, SR-Gtt-0L-C, and SR-Gtt-1L-A, after relaxing the $E_{\mathrm{T}}^{\mathrm{miss}}$ threshold to 200 GeV.

TABLE VI. Results of the likelihood fit extrapolated to the Gtt 0-lepton signal regions. The uncertainties shown include all systematic uncertainties. The data in the signal regions are not included in the fit. The row "MC-only background prediction" provides the total background prediction when the $t\bar{t}$ normalization is obtained from a theoretical calculation [61]. The $t\bar{t}$ normalization factor $\mu_{t\bar{t}}$ obtained from the corresponding $t\bar{t}$ control region is also provided. The category "Others" includes $t\bar{t}h$, $t\bar{t}t\bar{t}$, and diboson events. Expected yields for two example Gtt models are also shown.

	SR-Gtt-0L-A	SR-Gtt-0L-B	SR-Gtt-0L-C
Observed events	1	1	1
Fitted background events	2.1 ± 0.5	2.9 ± 1.8	3.4 ± 1.8
$t\bar{t}$	1.4 ± 0.4	2.4 ± 1.7	2.6 ± 1.8
$Z + \text{jets}$	0.22 ± 0.09	0.11 ± 0.06	0.14 ± 0.07
$W + \text{jets}$	0.19 ± 0.08	0.14 ± 0.06	0.18 ± 0.08
Single-top	0.17 ± 0.17	0.14 ± 0.13	0.17 ± 0.15
$t\bar{t}W/Z$	<0.1	<0.1	0.10 ± 0.07
Others	<0.1	<0.1	0.20 ± 0.17
MC-only background prediction	1.8	1.9	2.5
$\mu_{t\bar{t}}$	1.3 ± 0.4	1.8 ± 0.8	1.5 ± 0.7
Gtt ($m_{\tilde{g}} = 1600$ GeV, $m_{\tilde{\chi}_1^0} = 200$ GeV)	3.8	2.8	2.9
Gtt ($m_{\tilde{g}} = 1400$ GeV, $m_{\tilde{\chi}_1^0} = 800$ GeV)	2.0	3.7	4.1

TABLE VII. Results of the likelihood fit extrapolated to the Gtt 1-lepton signal regions. The uncertainties shown include all systematic uncertainties. The data in the signal regions are not included in the fit. The row "MC-only background prediction" provides the total background prediction when the $t\bar{t}$ normalization is obtained from a theoretical calculation [61]. The $t\bar{t}$ normalization factor $\mu_{t\bar{t}}$ obtained from the corresponding $t\bar{t}$ control region is also provided. The category "Others" includes $t\bar{t}h$, $t\bar{t}t\bar{t}$, and diboson events. Expected yields for two example Gtt models are also shown.

	SR-Gtt-1L-A	SR-Gtt-1L-B
Observed events	2	0
Fitted background events	1.2 ± 0.6	1.2 ± 0.8
$t\bar{t}$	0.8 ± 0.6	0.8 ± 0.7
$Z +$ jets	⋯	<0.1
$W +$ jets	<0.1	<0.1
Single-top	0.18 ± 0.14	0.14 ± 0.12
$t\bar{t}W/Z$	0.14 ± 0.08	0.15 ± 0.09
Others	<0.1	<0.1
MC-only background prediction	1.3	1.2
$\mu_{t\bar{t}}$	0.86 ± 0.28	1.0 ± 0.4
Gtt ($m_{\tilde{g}} = 1600$ GeV, $m_{\tilde{\chi}_1^0} = 200$ GeV)	3.4	3.3
Gtt ($m_{\tilde{g}} = 1400$ GeV, $m_{\tilde{\chi}_1^0} = 800$ GeV)	3.8	4.6

VIII. INTERPRETATION

Since no significant excess over the expected background from SM processes is observed, the data are used to derive one-sided upper limits at 95% C.L. Model-independent limits on the number of beyond-the-SM (BSM) events for each signal region are derived with pseudoexperiments using the CL_s prescription [96]. They can be translated into upper limits on the visible BSM cross section (σ_{vis}), where σ_{vis} is defined as the product of acceptance, reconstruction efficiency, and production cross section. The results are given in Table VIII, where the observed (S^{95}_{obs}) and expected (S^{95}_{exp}) 95% C.L. upper limits on the number of BSM events are also provided.

The measurement is used to place exclusion limits on gluino and LSP masses in the Gbb and Gtt simplified models. The results are obtained using the CL_s prescription in the asymptotic approximation [97]. The signal contamination in the control regions and the experimental

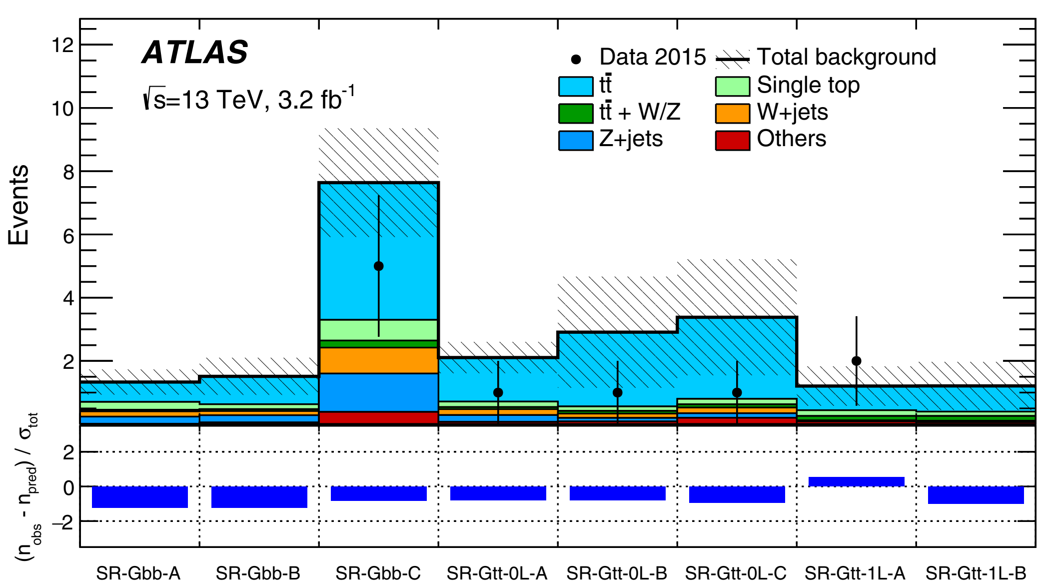

FIG. 5. Results of the likelihood fit extrapolated to the signal regions. The data in the signal regions are not included in the fit. The upper panel shows the observed number of events and the predicted background yield. The signal regions SR-Gbb-A, SR-Gbb-B, and SR-Gtt-1L-B have no observed events. The background category "Others" includes $t\bar{t}h$, $t\bar{t}t\bar{t}$, and diboson events. The lower panel shows the pulls in each signal region.

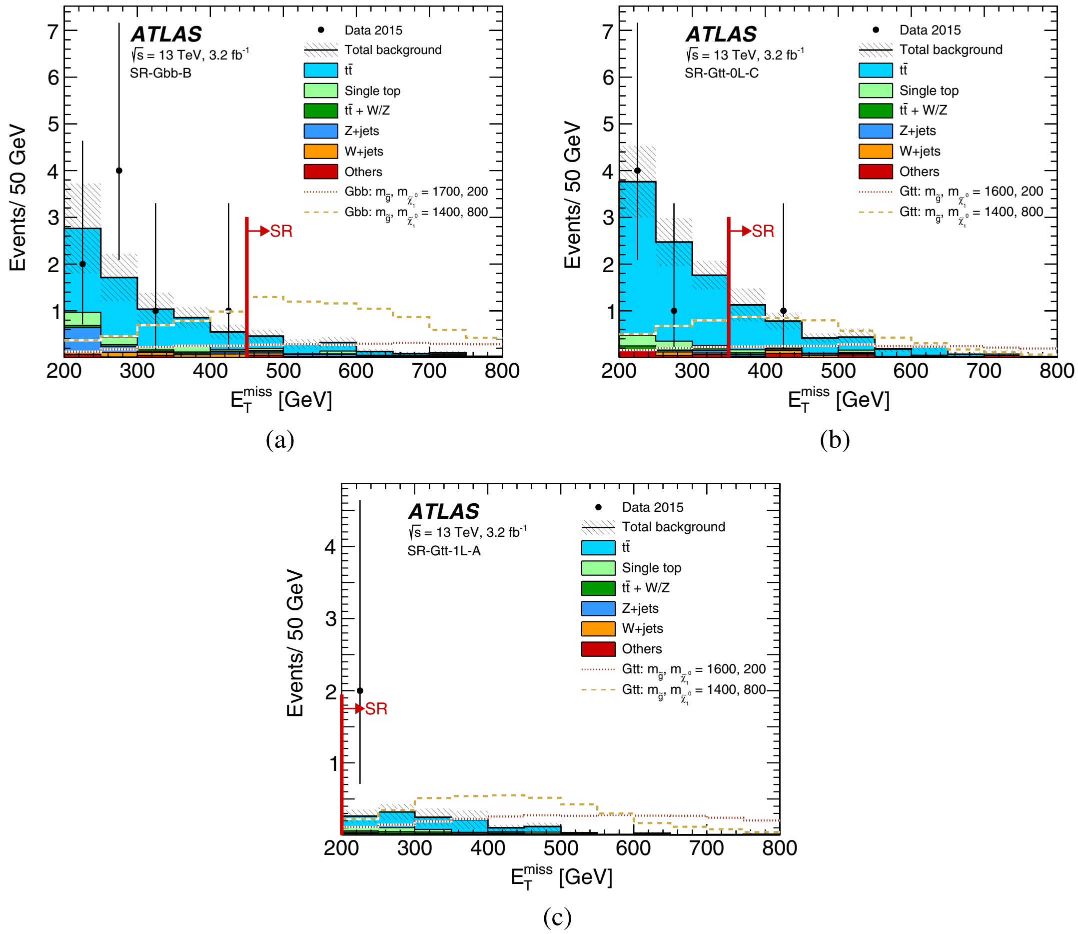

FIG. 6. Distributions of $E_{\mathrm{T}}^{\mathrm{miss}}$ for (a) SR-Gbb-B, (b) SR-Gtt-0L-C, and (c) SR-Gtt-1L-A. The $E_{\mathrm{T}}^{\mathrm{miss}}$ threshold is set to 200 GeV for these plots, with the red lines indicating the threshold values in the actual signal regions for SR-Gbb-B and SR-Gtt-0L-C (the $E_{\mathrm{T}}^{\mathrm{miss}}$ threshold in SR-Gtt-1L-A is 200 GeV). The statistical and experimental systematic uncertainties are included in the uncertainty band. Two example signal models are overlaid.

systematic uncertainties in the signal are taken into account for this calculation. For the Gbb models, the results are obtained from the Gbb signal region with the best expected sensitivity at each point of the parameter space of each model. For the Gtt models, the 0- and 1-lepton channels both contribute to the sensitivity, and they are combined in a simultaneous fit to enhance the sensitivity of the analysis. This is performed by considering all possible permutations between the three Gtt 0-lepton and the two Gtt 1-lepton signal regions for each point of the parameter space, and the best expected combination is used. The 95% C.L. observed and expected exclusion limits for the Gbb and Gtt models are shown in the LSP and gluino mass plane in Figs. 7(a) and 7(b), respectively. The $\pm 1\sigma_{\mathrm{theory}}^{\mathrm{SUSY}}$ lines around the observed limits are obtained by changing the SUSY cross section by 1 standard deviation ($\pm 1\sigma$), as described in Sec. III. The yellow band around the expected limit shows the $\pm 1\sigma$ uncertainty, including all statistical and systematic uncertainties except the theoretical uncertainties in the SUSY cross section. It has been checked that the observed exclusion limits obtained from pseudoexperiments differ by less than 25 GeV from the asymptotic approximation in gluino or LSP mass in the combined limits in Fig. 7, although the difference can be up to 50 GeV when using

TABLE VIII. The 95% C.L. upper limits on the visible cross section (σ_{vis}), defined as the product of acceptance, reconstruction efficiency, and production cross section, and the observed and expected 95% C.L. upper limits on the number of BSM events (S_{obs}^{95} and S_{exp}^{95}).

Signal channel	σ_{vis} [fb]	S_{obs}^{95}	S_{exp}^{95}
SR-Gbb-A	0.94	3.0	$3.9_{-0.7}^{+1.3}$
SR-Gbb-B	0.94	3.0	$3.8_{-0.8}^{+1.4}$
SR-Gbb-C	1.74	5.6	$7.2_{-1.8}^{+2.6}$
SR-Gtt-1L-A	1.49	4.8	$3.9_{-0.5}^{+1.4}$
SR-Gtt-1L-B	0.91	3.0	$3.0_{-0.0}^{+1.4}$
SR-Gtt-0L-A	1.13	3.6	$4.4_{-1.0}^{+1.7}$
SR-Gtt-0L-B	1.16	3.7	$4.4_{-0.9}^{+1.9}$
SR-Gtt-0L-C	1.10	3.5	$4.5_{-1.2}^{+2.0}$

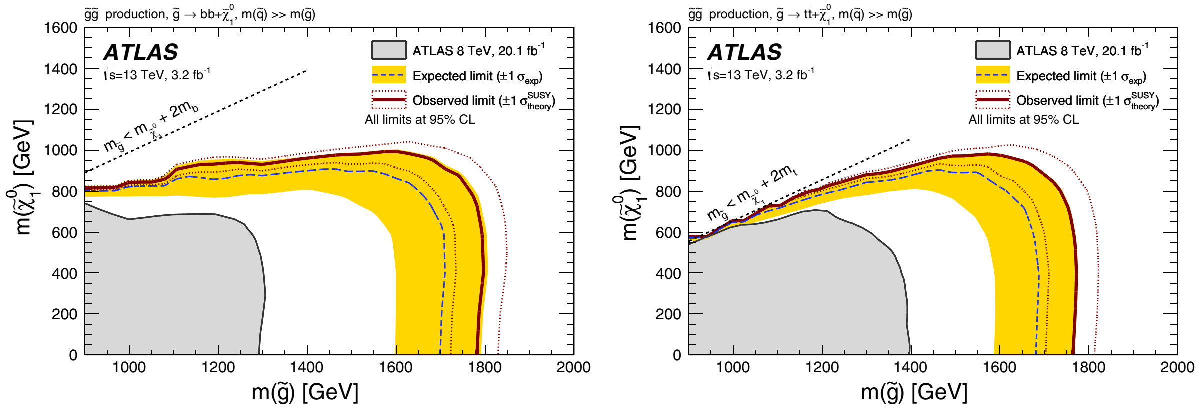

(a) (b)

FIG. 7. Exclusion limits in the $\tilde{\chi}_1^0$ and $\tilde{g}$ mass plane for the (a) Gbb and (b) Gtt models. The dashed and solid bold lines show the 95% C.L. expected and observed limits, respectively. The shaded bands around the expected limits show the impact of the experimental and background theoretical uncertainties. The dotted lines show the impact on the observed limit of the variation of the nominal signal cross section by $\pm 1\sigma$ of its theoretical uncertainty. The 95% C.L. observed limits from the $\sqrt{s} = 8$ TeV ATLAS search requiring at least three b-tagged jets [17] are also shown.

single analysis regions. The two methods of computation produce equivalent expected limits.

For the Gbb models, gluinos with masses below 1.78 TeV are excluded at 95% C.L. for LSP masses below 800 GeV. At high gluino masses, the exclusion limits are driven by the SR-Gbb-A and SR-Gbb-B signal regions. The best exclusion limit on the LSP mass is approximately 1.0 TeV, which is reached for a gluino mass of approximately 1.6 TeV. The exclusion limit is dominated by SR-Gbb-C for high LSP masses. For the Gtt models, gluino masses up to 1.8 TeV are excluded for massless LSP. For LSP masses below 700 GeV, gluino masses below 1.76 TeV are excluded. For large gluino masses, the exclusion limits are driven by the combination of SR-Gtt-1L-B and SR-Gtt-0L-A. The LSP exclusion extends up to approximately 975 GeV, corresponding to a gluino mass of approximately 1.5 TeV–1.6 TeV. The best exclusion limits are obtained by the combination of SR-Gtt-1L-B and SR-Gtt-0L-C for high LSP masses. The ATLAS exclusion limits obtained with the full $\sqrt{s} = 8$ TeV data set are also shown in Fig. 7. The current results largely improve on the $\sqrt{s} = 8$ TeV limits despite the lower integrated luminosity. The exclusion limit on the gluino mass is extended by approximately 500 GeV and 400 GeV for the Gbb and Gtt models for massless LSP, respectively. This improvement is primarily attributable to the increased center-of-mass energy of the LHC. The addition of the IBL pixel layer in Run 2, which improves the capability to tag b jets [35], also particularly benefits this analysis that employs a data set requiring at least three b-tagged jets. The sensitivity of the data analysis is also improved with respect to the $\sqrt{s} = 8$ TeV analysis [17] by using top-tagged large-R jets, lepton isolation adapted to a busy environment, and the $m_{\mathrm{T,min}}^{b\text{-jets}}$ variable.

IX. CONCLUSION

A search for pair-produced gluinos decaying via sbottom or stop is presented. LHC proton-proton collision data from the full 2015 data-taking period were analyzed, corresponding to an integrated luminosity of 3.2 fb^{-1} collected at $\sqrt{s} = 13$ TeV by the ATLAS detector. Several signal regions are designed for different scenarios of gluino and LSP masses. They require several high-p_{T} jets, of which at least three must be b tagged, large $E_{\mathrm{T}}^{\mathrm{miss}}$, and either zero or at least one charged lepton. For the gluino models with stop-mediated decays in which there is a large mass difference between the gluino and the LSP, large-R jets identified as originating from highly boosted top quarks are employed. The background is dominated by $t\bar{t}$ + jets, which is normalized in dedicated control regions. No excess is found above the predicted background of each signal region. Model-independent limits are set on the visible cross section for new physics processes. Exclusion limits are set on gluino and LSP masses in the simplified gluino models with stop-mediated and sbottom-mediated decays. For LSP masses below approximately 700 GeV, gluino masses of less than 1.78 TeV and 1.76 TeV are excluded at the 95% C.L. for the gluino models with sbottom-mediated and stop-mediated decays, respectively. These results significantly extend the exclusion limits obtained with the $\sqrt{s} = 8$ TeV data set.

ACKNOWLEDGMENTS

We thank CERN for the very successful operation of the LHC, as well as the support staff from our institutions without whom ATLAS could not be operated efficiently. We acknowledge the support of ANPCyT, Argentina; YerPhI, Armenia; ARC, Australia; BMWFW and FWF, Austria; ANAS, Azerbaijan; SSTC, Belarus; CNPq and FAPESP, Brazil; NSERC, NRC, and CFI, Canada; CERN; CONICYT, Chile; CAS, MOST, and NSFC, China; COLCIENCIAS, Colombia; MSMT CR, MPO CR, and VSC CR, Czech Republic; DNRF and DNSRC, Denmark; IN2P3-CNRS, CEA-DSM/IRFU, France; GNSF, Georgia; BMBF, HGF, and MPG, Germany; GSRT, Greece; RGC, Hong Kong SAR, China; ISF, I-CORE, and Benoziyo Center, Israel; INFN, Italy; MEXT and JSPS, Japan; CNRST, Morocco; FOM and NWO, Netherlands; RCN, Norway; MNiSW and NCN, Poland; FCT, Portugal; MNE/IFA, Romania; MES of Russia and NRC KI, Russian Federation; JINR; MESTD, Serbia; MSSR, Slovakia; ARRS and MIZŠ, Slovenia; DST/NRF, South Africa; MINECO, Spain; SRC and Wallenberg Foundation, Sweden; SERI, SNSF, and Cantons of Bern and Geneva, Switzerland; MOST, Taiwan; TAEK, Turkey; STFC, United Kingdom; DOE and NSF, United States of America. In addition, individual groups and members have received support from BCKDF, the Canada Council, CANARIE, CRC, Compute Canada, FQRNT, and the Ontario Innovation Trust, Canada; EPLANET, ERC, FP7, Horizon 2020, and Marie Skłodowska-Curie Actions, European Union; Investissements d'Avenir Labex and Idex, ANR, Région Auvergne and Fondation Partager le Savoir, France; DFG and AvH Foundation, Germany; Herakleitos, Thales, and Aristeia programmes cofinanced by EU-ESF and the Greek NSRF; BSF, GIF, and Minerva, Israel; BRF, Norway; Generalitat de Catalunya, Generalitat Valenciana, Spain; the Royal Society and Leverhulme Trust, United Kingdom. The crucial computing support from all WLCG partners is acknowledged gratefully, in particular from CERN and the ATLAS Tier-1 facilities at TRIUMF (Canada), NDGF (Denmark, Norway, Sweden), CC-IN2P3 (France), KIT/GridKA (Germany), INFN-CNAF (Italy), NL-T1 (Netherlands), PIC (Spain), ASGC (Taiwan), RAL (UK), and BNL (USA) and in the Tier-2 facilities worldwide.

---

[1] Yu. A. Golfand and E. P. Likhtman, Extension of the algebra of Poincare group generators and violation of p invariance, Pis'ma Zh. Eksp. Teor. Fiz. **13**, 452 (1971) [JETP Lett. **13**, 323 (1971)].

[2] D. V. Volkov and V. P. Akulov, Is the neutrino a Goldstone particle?, Phys. Lett. **46B**, 109 (1973).

[3] J. Wess and B. Zumino, Supergauge transformations in four-dimensions, Nucl. Phys. **B70**, 39 (1974).

[4] J. Wess and B. Zumino, Supergauge invariant extension of quantum electrodynamics, Nucl. Phys. **B78**, 1 (1974).

[5] S. Ferrara and B. Zumino, Supergauge invariant Yang-Mills theories, Nucl. Phys. **B79**, 413 (1974).

[6] A. Salam and J. A. Strathdee, Supersymmetry and non-abelian gauges, Phys. Lett. **51B**, 353 (1974).

[7] G. R. Farrar and P. Fayet, Phenomenology of the production, decay, and detection of new hadronic states associated with supersymmetry, Phys. Lett. **76B**, 575 (1978).

[8] N. Sakai, Naturalness in supersymmetric GUTs, Z. Phys. C **11**, 153 (1981).

[9] S. Dimopoulos, S. Raby, and F. Wilczek, Supersymmetry and the scale of unification, Phys. Rev. D **24**, 1681 (1981).

[10] L. E. Ibanez and G. G. Ross, Low-energy predictions in supersymmetric grand unified theories, Phys. Lett. **105B**, 439 (1981).

[11] S. Dimopoulos and H. Georgi, Softly broken supersymmetry and SU(5), Nucl. Phys. **B193**, 150 (1981).

[12] R. Barbieri and G. F. Giudice, Upper bounds on supersymmetric particle masses, Nucl. Phys. **B306**, 63 (1988).

[13] B. de Carlos and J. A. Casas, One loop analysis of the electroweak breaking in supersymmetric models and the fine tuning problem, Phys. Lett. B **309**, 320 (1993).

[14] ATLAS Collaboration, The ATLAS experiment at the CERN Large Hadron Collider, J. Instrum. **3**, S08003 (2008).

[15] J. Alwall, P. Schuster, and N. Toro, Simplified models for a first characterization of new physics at the LHC, Phys. Rev. D **79**, 075020 (2009).

[16] D. Alves *et al.*, Simplified models for LHC new physics searches, J. Phys. G **39**, 105005 (2012).

[17] ATLAS Collaboration, Search for strong production of supersymmetric particles in final states with missing transverse momentum and at least three b-jets at $\sqrt{s} = 8$ TeV proton-proton collisions with the ATLAS detector, J. High Energy Phys. 10 (2014) 24.

[18] D. Krohn, J. Thaler, and L.-T. Wang, Jet trimming, J. High Energy Phys. 02 (2010) 084.

[19] B. Nachman, P. Nef, A. Schwartzman, M. Swiatlowski, and C. Wanotayaroj, Jets from jets: Re-clustering as a tool for large radius jet reconstruction and grooming at the LHC, J. High Energy Phys. 02 (2015) 075.

[20] ATLAS Collaboration, Summary of the searches for squarks and gluinos using $\sqrt{s} = 8$ TeV pp collisions with the ATLAS experiment at the LHC, J. High Energy Phys. 10 (2015) 054.

[21] ATLAS Collaboration, Search for new phenomena in final states with large jet multiplicities and missing transverse momentum at $\sqrt{s} = 8$ TeV proton-proton collisions using the ATLAS experiment, J. High Energy Phys. 10 (2013) 130.

[22] ATLAS Collaboration, Search for squarks and gluinos in events with isolated leptons, jets and missing transverse momentum at $\sqrt{s} = 8$ TeV with the ATLAS detector, J. High Energy Phys. 04 (2015) 116.

[23] ATLAS Collaboration, Search for supersymmetry at $\sqrt{s} =$ 8 TeV in final states with jets and two same-sign leptons or three leptons with the ATLAS detector, J. High Energy Phys. 06 (2014) 035.
[24] ATLAS Collaboration, Search for supersymmetry at $\sqrt{s} =$ 13 TeV in final states with jets and two same-sign leptons or three leptons with the ATLAS detector, Eur. Phys. J. C **76**, 259 (2016).
[25] CMS Collaboration, Search for gluino mediated bottom- and top-squark production in multijet final states in pp collisions at 8 TeV, Phys. Lett. B **725**, 243 (2013).
[26] CMS Collaboration, Search for supersymmetry in pp collisions at $\sqrt{s} = 8$ TeV in events with a single lepton, large jet multiplicity, and multiple b jets, Phys. Lett. B **733**, 328 (2014).
[27] CMS Collaboration, Search for supersymmetry using razor variables in events with b-tagged jets in pp collisions at $\sqrt{s} = 8$ TeV, Phys. Rev. D **91**, 052018 (2015).
[28] CMS Collaboration, Search for new physics in the multijet and missing transverse momentum final state in proton-proton collisions at $\sqrt{s} = 8$ TeV, J. High Energy Phys. 06 (2014) 055.
[29] CMS Collaboration, Search for new physics in events with same-sign dileptons and jets in pp collisions at $\sqrt{s} = 8$ TeV, J. High Energy Phys. 01 (2014) 163.
[30] CMS Collaboration, Searches for supersymmetry based on events with b jets and four W bosons in pp collisions at 8 TeV, Phys. Lett. B **745**, 5 (2015).
[31] CMS Collaboration, Search for supersymmetry in the multijet and missing transverse momentum final state in pp collisions at 13 TeV, Phys. Lett. B **758**, 152 (2016).
[32] CMS Collaboration, Search for new physics with the MT2 variable in all-jets final states produced in pp collisions at $\sqrt{s} = 13$ TeV (to be published).
[33] CMS Collaboration, Search for supersymmetry in pp collisions at $\sqrt{s} = 13$ TeV in the single-lepton final state using the sum of masses of large-radius jets (to be published).
[34] CMS Collaboration, Search for new physics in same-sign dilepton events in proton-proton collisions at $\sqrt{s} = 13$ TeV (to be published).
[35] ATLAS Collaboration, ATLAS Insertable B-Layer Technical Design Report No. CERN-LHCC-2010-013, ATLAS-TDR-19, 2010, https://cds.cern.ch/record/1291633.
[36] ATLAS Collaboration, Performance of the ATLAS trigger system in 2010, Eur. Phys. J. C **72**, 1849 (2012).
[37] ATLAS Collaboration, Improved luminosity determination in pp collisions at $\sqrt{s} = 7$ TeV using the ATLAS detector at the LHC, Eur. Phys. J. C **73**, 2518 (2013).
[38] J. Alwall, R. Frederix, S. Frixione, V. Hirschi, F. Maltoni, O. Mattelaer, H.-S. Shao, T. Stelzer, P. Torrielli, and M. Zaro, The automated computation of tree-level and next-to-leading order differential cross sections, and their matching to parton shower simulations, J. High Energy Phys. 07 (2014) 079.
[39] P. M. Nadolsky, H.-L. Lai, Q.-H. Cao, J. Huston, J. Pumplin, D. Stump, W.-K. Tung, and C.-P. Yuan, Implications of CTEQ global analysis for collider observation, Phys. Rev. D **78**, 013004 (2008).
[40] T. Sjostrand, S. Mrenna, and P. Z. Skands, A brief introduction to PYTHIA 8.1, Comput. Phys. Commun. **178**, 852 (2008).
[41] S. Alioli, P. Nason, C. Oleari, and E. Re, A general framework for implementing NLO calculations in shower Monte Carlo programs: The POWHEG BOX, J. High Energy Phys. 06 (2010) 043.
[42] S. Frixione, P. Nason, and C. Oleari, Matching NLO QCD computations with parton shower simulations: The POWHEG method, J. High Energy Phys. 11 (2007) 070.
[43] H.-L. Lai, M. Guzzi, J. Huston, Z. Li, P. M. Nadolsky, J. Pumplin, and C.-P. Yuan, New parton distributions for collider physics, Phys. Rev. D **82**, 074024 (2010).
[44] T. Sjöstrand, S. Mrenna, and P. Z. Skands, PYTHIA 6.4 physics and manual, J. High Energy Phys. 05 (2006) 026.
[45] D. J. Lange, The EvtGen particle decay simulation package, Nucl. Instrum. Methods Phys. Res., Sect. A **462**, 152 (2001).
[46] ATLAS Collaboration, Comparison of Monte Carlo generator predictions to ATLAS measurements of top pair production at $\sqrt{s} = 7$ TeV, Report No. ATLAS-PHYS-PUB-2015-002, 2015, http://cdsweb.cern.ch/record/1981319.
[47] ATLAS Collaboration, Measurement of the differential cross-section of highly boosted top quarks as a function of their transverse momentum in $\sqrt{s} = 8$ TeV proton-proton collisions using the ATLAS detector, Phys. Rev. D **93**, 032009 (2016).
[48] J. Alwall, M. Herquet, F. Maltoni, O. Mattelaer, and T. Stelzer, MadGraph 5: Going beyond, J. High Energy Phys. 06 (2011) 128.
[49] M. Bähr *et al.*, Herwig++ physics and manual, Eur. Phys. J. C **58**, 639 (2008).
[50] T. Gleisberg, S. Höche, F. Krauss, M. Schönherr, S. Schumann, F. Siegert, and J. Winter, Event generation with SHERPA 1.1, J. High Energy Phys. 02 (2009) 007.
[51] T. Gleisberg and S. Höche, Comix, a new matrix element generator, J. High Energy Phys. 12 (2008) 039.
[52] F. Cascioli, P. Maierhofer, and S. Pozzorini, Scattering amplitudes with open loops, Phys. Rev. Lett. **108**, 111601 (2012).
[53] S. Schumann and F. Krauss, A Parton shower algorithm based on Catani-Seymour dipole factorisation, J. High Energy Phys. 03 (2008) 038.
[54] S. Höche, F. Krauss, M. Schönherr, and F. Siegert, QCD matrix elements + parton showers: The NLO case, J. High Energy Phys. 04 (2013) 027.
[55] S. Agostinelli *et al.*, Geant4: A simulation toolkit, Nucl. Instrum. Methods Phys. Res., Sect. A **506**, 250 (2003).
[56] ATLAS Collaboration, The ATLAS simulation infrastructure, Eur. Phys. J. C **70**, 823 (2010).
[57] ATLAS Collaboration, The simulation principle and performance of the ATLAS fast calorimeter simulation fastcalosim, Report No. ATL-PHYS-PUB-2010-013, 2010, https://cds.cern.ch/record/1300517.
[58] P. Z. Skands, Tuning Monte Carlo generators: The Perugia tunes, Phys. Rev. D **82**, 074018 (2010).
[59] ATLAS Collaboration, ATLAS Run-1 Pythia8 tunes, Report No. ATLAS-PHYS-PUB-2014-021, 2014, http://cdsweb.cern.ch/record/1966419.

[60] S. Gieseke, C. Rohr, and A. Siodmok, Colour reconnections in Herwig++, Eur. Phys. J. C **72**, 2225 (2012).
[61] M. Czakon and A. Mitov, Top++: A program for the calculation of the top-pair cross-section at hadron colliders, Comput. Phys. Commun. **185**, 2930 (2014).
[62] N. Kidonakis, Next-to-next-to-leading-order collinear and soft gluon corrections for t-channel single top quark production, Phys. Rev. D **83**, 091503 (2011).
[63] N. Kidonakis, Two-loop soft anomalous dimensions for single top quark associated production with a W- or H-, Phys. Rev. D **82**, 054018 (2010).
[64] N. Kidonakis, NNLL resummation for s-channel single top quark production, Phys. Rev. D **81**, 054028 (2010).
[65] R. D. Ball *et al.*, Parton distributions with LHC data, Nucl. Phys. **B867**, 244 (2013).
[66] S. Heinemeyer *et al.*, Handbook of LHC Higgs cross sections: 3. Higgs properties: Report of the LHC Higgs Cross Section Working Group, 2013, https://cds.cern.ch/record/1559921.
[67] S. Catani, L. Cieri, G. Ferrera, D. de Florian, and M. Grazzini, Vector boson production at hadron colliders: A fully exclusive QCD calculation at NNLO, Phys. Rev. Lett. **103**, 082001 (2009).
[68] W. Beenakker, R. Höpker, M. Spira, and P. M. Zerwas, Squark and gluino production at hadron colliders, Nucl. Phys. **B492**, 51 (1997).
[69] A. Kulesza and L. Motyka, Threshold resummation for squark-antisquark and gluino-pair production at the LHC, Phys. Rev. Lett. **102**, 111802 (2009).
[70] A. Kulesza and L. Motyka, Soft gluon resummation for the production of gluino-gluino and squark-antisquark pairs at the LHC, Phys. Rev. D **80**, 095004 (2009).
[71] W. Beenakker, S. Brensing, M. Krämer, A. Kulesza, E. Laenen, and I. Niessen, Soft-gluon resummation for squark and gluino hadroproduction, J. High Energy Phys. 12 (2009) 041.
[72] W. Beenakker, S. Brensing, M. Krämer, A. Kulesza, E. Laenen, L. Motyka, and I. Niessen, Squark and gluino hadroproduction, Int. J. Mod. Phys. A **26**, 2637 (2011).
[73] M. Kramer *et al.*, Supersymmetry production cross sections in pp collisions at $\sqrt{s} = 7$ TeV, Report No. CERN-PH-TH-2012-163, 2012, https://cds.cern.ch/record/1456029.
[74] ATLAS Collaboration, Vertex reconstruction performance of the ATLAS detector at $\sqrt{s} = 13$ TeV, Report No. ATL-PHYS-PUB-2015-026, 2015, http://cdsweb.cern.ch/record/2037717.
[75] W. Lampl *et al.*, Calorimeter clustering algorithms: Description and performance, 2008, https://cds.cern.ch/record/1099735.
[76] M. Cacciari, G. Salam, and G. Soyez, The anti-k_t jet clustering algorithm, J. High Energy Phys. 04 (2008) 063.
[77] ATLAS Collaboration, Jet calibration and systematic uncertainties for jets reconstructed in the ATLAS detector at $\sqrt{s} = 13$ TeV, Report No. ATLAS-PHYS-PUB-2015-015 (2015), http://cdsweb.cern.ch/record/2037613.
[78] ATLAS Collaboration, Monte Carlo calibration and combination of in-situ measurements of jet energy scale, jet energy resolution and jet mass in ATLAS, Report No. ATLAS-CONF-2015-037, 2015, http://cdsweb.cern.ch/record/2044941.
[79] ATLAS Collaboration, Selection of jets produced in 13 TeV proton-proton collisions with the ATLAS detector, Report No. ATLAS-CONF-2015-029, 2015, http://cdsweb.cern.ch/record/2037702.
[80] ATLAS Collaboration, Performance of pile-up mitigation techniques for jets in pp collisions at $\sqrt{s} = 8$ TeV using the ATLAS detector, Report No. CERN-PH-EP-2015-206, 2015, https://cds.cern.ch/record/2058295.
[81] ATLAS Collaboration, Commissioning of the ATLAS b-tagging algorithms using $t\bar{t}$ events in early Run-2 data, Report No. ATLAS-PHYS-PUB-2015-039, 2015, http://cdsweb.cern.ch/record/2047871.
[82] ATLAS Collaboration, Calibration of b-tagging using dileptonic top pair events in a combinatorial likelihood approach with the ATLAS experiment, Report No. ATLAS-CONF-2014-004, 2014, http://cdsweb.cern.ch/record/1664335.
[83] ATLAS Collaboration, Calibration of the performance of b-tagging for c and light-flavour jets in the 2012 ATLAS data, Report No. ATLAS-CONF-2012-046, 2014, http://cdsweb.cern.ch/record/1741020.
[84] ATLAS Collaboration, Electron reconstruction and identification efficiency measurements with the ATLAS detector using the 2011 LHC proton-proton collision data, Eur. Phys. J. C **74**, 2941 (2014).
[85] ATLAS Collaboration, Electron and photon energy calibration with the ATLAS detector using LHC Run 1 data, Eur. Phys. J. C **74**, 3071 (2014).
[86] ATLAS Collaboration, Electron identification measurements in ATLAS using $\sqrt{s} = 13$ TeV data with 50 ns bunch spacing, Report No. ATLAS-PHYS-PUB-2015-041, 2015, http://cdsweb.cern.ch/record/2048202.
[87] ATLAS Collaboration, Muon reconstruction performance of the ATLAS detector in proton-proton collision data at $\sqrt{s} = 13$ TeV, Eur. Phys. J. C **76**, 292 (2016).
[88] ATLAS Collaboration, Measurement of the muon reconstruction performance of the ATLAS detector using 2011 and 2012 LHC proton-proton collision data, Eur. Phys. J. C **74**, 3130 (2014).
[89] ATLAS Collaboration, A search for $t\bar{t}$ resonances using lepton-plus-jets events in proton-proton collisions at $\sqrt{s} = 8$ TeV with the ATLAS detector, J. High Energy Phys. 08 (2015) 148.
[90] ATLAS Collaboration, Performance of missing transverse momentum reconstruction for the ATLAS detector in the first proton-proton collisions at $\sqrt{s} = 13$ TeV, Report No. ATLAS-CONF-2013-082, 2013, https://cds.cern.ch/record/1570993.
[91] ATLAS Collaboration, Performance of missing transverse momentum reconstruction in proton-proton collisions at 7 TeV with ATLAS, Eur. Phys. J. C **72**, 1844 (2012).
[92] ATLAS Collaboration, Preliminary results on the muon reconstruction efficiency, momentum resolution, and momentum scale in ATLAS 2012 pp collision data, Report No. ATLAS-CONF-2013-088, 2013, http://cdsweb.cern.ch/record/1580207.
[93] ATLAS Collaboration, Measurements of fiducial cross-sections for $t\bar{t}$ production with one or two additional b-jets in pp collisions at $\sqrt{s} = 8$ TeV using the ATLAS detector, Eur. Phys. J. C **76**, 11 (2016).
[94] P. Kant, O. M. Kind, T. Kintscher, T. Lohse, T. Martini, S. Mölbitz, P. Rieck, and P. Uwer, HatHor for single top-quark

production: Updated predictions and uncertainty estimates for single top-quark production in hadronic collisions, Comput. Phys. Commun. **191**, 74 (2015).
[95] M. Baak, G. J. Besjes, D. Côté, A. Koutsman, J. Lorenz, and D. Short, HistFitter software framework for statistical data analysis, Eur. Phys. J. C **75**, 153 (2015).
[96] A. L. Read, Presentation of search results: The CL(s) technique, J. Phys. G **28**, 2693 (2002).
[97] G. Cowan, K. Cranmer, E. Gross, and O. Vitells, Asymptotic formulae for likelihood-based tests of new physics, Eur. Phys. J. C **71**, 1554 (2011).

G. Aad,[87] B. Abbott,[114] J. Abdallah,[65] O. Abdinov,[12] B. Abeloos,[118] R. Aben,[108] O. S. AbouZeid,[138] N. L. Abraham,[150] H. Abramowicz,[154] H. Abreu,[153] R. Abreu,[117] Y. Abulaiti,[147a,147b] B. S. Acharya,[164a,164b,b] L. Adamczyk,[40a] D. L. Adams,[27] J. Adelman,[109] S. Adomeit,[101] T. Adye,[132] A. A. Affolder,[76] T. Agatonovic-Jovin,[14] J. Agricola,[56] J. A. Aguilar-Saavedra,[127a,127f] S. P. Ahlen,[24] F. Ahmadov,[67,c] G. Aielli,[134a,134b] H. Akerstedt,[147a,147b] T. P. A. Åkesson,[83] A. V. Akimov,[97] G. L. Alberghi,[22a,22b] J. Albert,[169] S. Albrand,[57] M. J. Alconada Verzini,[73] M. Aleksa,[32] I. N. Aleksandrov,[67] C. Alexa,[28b] G. Alexander,[154] T. Alexopoulos,[10] M. Alhroob,[114] M. Aliev,[75a,75b] G. Alimonti,[93a] J. Alison,[33] S. P. Alkire,[37] B. M. M. Allbrooke,[150] B. W. Allen,[117] P. P. Allport,[19] A. Aloisio,[105a,105b] A. Alonso,[38] F. Alonso,[73] C. Alpigiani,[139] M. Alstaty,[87] B. Alvarez Gonzalez,[32] D. Álvarez Piqueras,[167] M. G. Alviggi,[105a,105b] B. T. Amadio,[16] K. Amako,[68] Y. Amaral Coutinho,[26a] C. Amelung,[25] D. Amidei,[91] S. P. Amor Dos Santos,[127a,127c] A. Amorim,[127a,127b] S. Amoroso,[32] G. Amundsen,[25] C. Anastopoulos,[140] L. S. Ancu,[51] N. Andari,[109] T. Andeen,[11] C. F. Anders,[60b] G. Anders,[32] J. K. Anders,[76] K. J. Anderson,[33] A. Andreazza,[93a,93b] V. Andrei,[60a] S. Angelidakis,[9] I. Angelozzi,[108] P. Anger,[46] A. Angerami,[37] F. Anghinolfi,[32] A. V. Anisenkov,[110,d] N. Anjos,[13] A. Annovi,[125a,125b] M. Antonelli,[49] A. Antonov,[99] F. Anulli,[133a] M. Aoki,[68] L. Aperio Bella,[19] G. Arabidze,[92] Y. Arai,[68] J. P. Araque,[127a] A. T. H. Arce,[47] F. A. Arduh,[73] J-F. Arguin,[96] S. Argyropoulos,[65] M. Arik,[20a] A. J. Armbruster,[144] L. J. Armitage,[78] O. Arnaez,[32] H. Arnold,[50] M. Arratia,[30] O. Arslan,[23] A. Artamonov,[98] G. Artoni,[121] S. Artz,[85] S. Asai,[156] N. Asbah,[44] A. Ashkenazi,[154] B. Åsman,[147a,147b] L. Asquith,[150] K. Assamagan,[27] R. Astalos,[145a] M. Atkinson,[166] N. B. Atlay,[142] K. Augsten,[129] G. Avolio,[32] B. Axen,[16] M. K. Ayoub,[118] G. Azuelos,[96,e] M. A. Baak,[32] A. E. Baas,[60a] M. J. Baca,[19] H. Bachacou,[137] K. Bachas,[75a,75b] M. Backes,[32] M. Backhaus,[32] P. Bagiacchi,[133a,133b] P. Bagnaia,[133a,133b] Y. Bai,[35a] J. T. Baines,[132] O. K. Baker,[176] E. M. Baldin,[110,d] P. Balek,[130] T. Balestri,[149] F. Balli,[137] W. K. Balunas,[123] E. Banas,[41] Sw. Banerjee,[173,f] A. A. E. Bannoura,[175] L. Barak,[32] E. L. Barberio,[90] D. Barberis,[52a,52b] M. Barbero,[87] T. Barillari,[102] T. Barklow,[144] N. Barlow,[30] S. L. Barnes,[86] B. M. Barnett,[132] R. M. Barnett,[16] Z. Barnovska,[5] A. Baroncelli,[135a] G. Barone,[25] A. J. Barr,[121] L. Barranco Navarro,[167] F. Barreiro,[84] J. Barreiro Guimarães da Costa,[35a] R. Bartoldus,[144] A. E. Barton,[74] P. Bartos,[145a] A. Basalaev,[124] A. Bassalat,[118] R. L. Bates,[55] S. J. Batista,[159] J. R. Batley,[30] M. Battaglia,[138] M. Bauce,[133a,133b] F. Bauer,[137] H. S. Bawa,[144,g] J. B. Beacham,[112] M. D. Beattie,[74] T. Beau,[82] P. H. Beauchemin,[162] P. Bechtle,[23] H. P. Beck,[18,h] K. Becker,[121] M. Becker,[85] M. Beckingham,[170] C. Becot,[111] A. J. Beddall,[20e] A. Beddall,[20b] V. A. Bednyakov,[67] M. Bedognetti,[108] C. P. Bee,[149] L. J. Beemster,[108] T. A. Beermann,[32] M. Begel,[27] J. K. Behr,[44] C. Belanger-Champagne,[89] A. S. Bell,[80] G. Bella,[154] L. Bellagamba,[22a] A. Bellerive,[31] M. Bellomo,[88] K. Belotskiy,[99] O. Beltramello,[32] N. L. Belyaev,[99] O. Benary,[154] D. Benchekroun,[136a] M. Bender,[101] K. Bendtz,[147a,147b] N. Benekos,[10] Y. Benhammou,[154] E. Benhar Noccioli,[176] J. Benitez,[65] D. P. Benjamin,[47] J. R. Bensinger,[25] S. Bentvelsen,[108] L. Beresford,[121] M. Beretta,[49] D. Berge,[108] E. Bergeaas Kuutmann,[165] N. Berger,[5] J. Beringer,[16] S. Berlendis,[57] N. R. Bernard,[88] C. Bernius,[111] F. U. Bernlochner,[23] T. Berry,[79] P. Berta,[130] C. Bertella,[85] G. Bertoli,[147a,147b] F. Bertolucci,[125a,125b] I. A. Bertram,[74] C. Bertsche,[44] D. Bertsche,[114] G. J. Besjes,[38] O. Bessidskaia Bylund,[147a,147b] M. Bessner,[44] N. Besson,[137] C. Betancourt,[50] S. Bethke,[102] A. J. Bevan,[78] W. Bhimji,[16] R. M. Bianchi,[126] L. Bianchini,[25] M. Bianco,[32] O. Biebel,[101] D. Biedermann,[17] R. Bielski,[86] N. V. Biesuz,[125a,125b] M. Biglietti,[135a] J. Bilbao De Mendizabal,[51] H. Bilokon,[49] M. Bindi,[56] S. Binet,[118] A. Bingul,[20b] C. Bini,[133a,133b] S. Biondi,[22a,22b] D. M. Bjergaard,[47] C. W. Black,[151] J. E. Black,[144] K. M. Black,[24] D. Blackburn,[139] R. E. Blair,[6] J.-B. Blanchard,[137] J. E. Blanco,[79] T. Blazek,[145a] I. Bloch,[44] C. Blocker,[25] W. Blum,[85,a] U. Blumenschein,[56] S. Blunier,[34a] G. J. Bobbink,[108] V. S. Bobrovnikov,[110,d] S. S. Bocchetta,[83] A. Bocci,[47] C. Bock,[101] M. Boehler,[50] D. Boerner,[175] J. A. Bogaerts,[32] D. Bogavac,[14] A. G. Bogdanchikov,[110] C. Bohm,[147a] V. Boisvert,[79] P. Bokan,[14] T. Bold,[40a] A. S. Boldyrev,[164a,164c] M. Bomben,[82] M. Bona,[78] M. Boonekamp,[137] A. Borisov,[131] G. Borissov,[74] J. Bortfeldt,[101] D. Bortoletto,[121] V. Bortolotto,[62a,62b,62c] K. Bos,[108] D. Boscherini,[22a] M. Bosman,[13] J. D. Bossio Sola,[29] J. Boudreau,[126] J. Bouffard,[2] E. V. Bouhova-Thacker,[74] D. Boumediene,[36] C. Bourdarios,[118] S. K. Boutle,[55] A. Boveia,[32] J. Boyd,[32]

I. R. Boyko,[67] J. Bracinik,[19] A. Brandt,[8] G. Brandt,[56] O. Brandt,[60a] U. Bratzler,[157] B. Brau,[88] J. E. Brau,[117] H. M. Braun,[175,a] W. D. Breaden Madden,[55] K. Brendlinger,[123] A. J. Brennan,[90] L. Brenner,[108] R. Brenner,[165] S. Bressler,[172] T. M. Bristow,[48] D. Britton,[55] D. Britzger,[44] F. M. Brochu,[30] I. Brock,[23] R. Brock,[92] G. Brooijmans,[37] T. Brooks,[79] W. K. Brooks,[34b] J. Brosamer,[16] E. Brost,[117] J. H Broughton,[19] P. A. Bruckman de Renstrom,[41] D. Bruncko,[145b] R. Bruneliere,[50] A. Bruni,[22a] G. Bruni,[22a] BH Brunt,[30] M. Bruschi,[22a] N. Bruscino,[23] P. Bryant,[33] L. Bryngemark,[83] T. Buanes,[15] Q. Buat,[143] P. Buchholz,[142] A. G. Buckley,[55] I. A. Budagov,[67] F. Buehrer,[50] M. K. Bugge,[120] O. Bulekov,[99] D. Bullock,[8] H. Burckhart,[32] S. Burdin,[76] C. D. Burgard,[50] B. Burghgrave,[109] K. Burka,[41] S. Burke,[132] I. Burmeister,[45] E. Busato,[36] D. Büscher,[50] V. Büscher,[85] P. Bussey,[55] J. M. Butler,[24] C. M. Buttar,[55] J. M. Butterworth,[80] P. Butti,[108] W. Buttinger,[27] A. Buzatu,[55] A. R. Buzykaev,[110,d] S. Cabrera Urbán,[167] D. Caforio,[129] V. M. Cairo,[39a,39b] O. Cakir,[4a] N. Calace,[51] P. Calafiura,[16] A. Calandri,[87] G. Calderini,[82] P. Calfayan,[101] L. P. Caloba,[26a] D. Calvet,[36] S. Calvet,[36] T. P. Calvet,[87] R. Camacho Toro,[33] S. Camarda,[32] P. Camarri,[134a,134b] D. Cameron,[120] R. Caminal Armadans,[166] C. Camincher,[57] S. Campana,[32] M. Campanelli,[80] A. Camplani,[93a,93b] A. Campoverde,[149] V. Canale,[105a,105b] A. Canepa,[160a] M. Cano Bret,[35e] J. Cantero,[115] R. Cantrill,[127a] T. Cao,[42] M. D. M. Capeans Garrido,[32] I. Caprini,[28b] M. Caprini,[28b] M. Capua,[39a,39b] R. Caputo,[85] R. M. Carbone,[37] R. Cardarelli,[134a] F. Cardillo,[50] I. Carli,[130] T. Carli,[32] G. Carlino,[105a] L. Carminati,[93a,93b] S. Caron,[107] E. Carquin,[34b] G. D. Carrillo-Montoya,[32] J. R. Carter,[30] J. Carvalho,[127a,127c] D. Casadei,[19] M. P. Casado,[13,i] M. Casolino,[13] D. W. Casper,[163] E. Castaneda-Miranda,[146a] R. Castelijn,[108] A. Castelli,[108] V. Castillo Gimenez,[167] N. F. Castro,[127a,j] A. Catinaccio,[32] J. R. Catmore,[120] A. Cattai,[32] J. Caudron,[85] V. Cavaliere,[166] E. Cavallaro,[13] D. Cavalli,[93a] M. Cavalli-Sforza,[13] V. Cavasinni,[125a,125b] F. Ceradini,[135a,135b] L. Cerda Alberich,[167] B. C. Cerio,[47] A. S. Cerqueira,[26b] A. Cerri,[150] L. Cerrito,[78] F. Cerutti,[16] M. Cerv,[32] A. Cervelli,[18] S. A. Cetin,[20d] A. Chafaq,[136a] D. Chakraborty,[109] S. K. Chan,[59] Y. L. Chan,[62a] P. Chang,[166] J. D. Chapman,[30] D. G. Charlton,[19] A. Chatterjee,[51] C. C. Chau,[159] C. A. Chavez Barajas,[150] S. Che,[112] S. Cheatham,[74] A. Chegwidden,[92] S. Chekanov,[6] S. V. Chekulaev,[160a] G. A. Chelkov,[67,k] M. A. Chelstowska,[91] C. Chen,[66] H. Chen,[27] K. Chen,[149] S. Chen,[35c] S. Chen,[156] X. Chen,[35f] Y. Chen,[69] H. C. Cheng,[91] H. J Cheng,[35a] Y. Cheng,[33] A. Cheplakov,[67] E. Cheremushkina,[131] R. Cherkaoui El Moursli,[136e] V. Chernyatin,[27,a] E. Cheu,[7] L. Chevalier,[137] V. Chiarella,[49] G. Chiarelli,[125a,125b] G. Chiodini,[75a] A. S. Chisholm,[19] A. Chitan,[28b] M. V. Chizhov,[67] K. Choi,[63] A. R. Chomont,[36] S. Chouridou,[9] B. K. B. Chow,[101] V. Christodoulou,[80] D. Chromek-Burckhart,[32] J. Chudoba,[128] A. J. Chuinard,[89] J. J. Chwastowski,[41] L. Chytka,[116] G. Ciapetti,[133a,133b] A. K. Ciftci,[4a] D. Cinca,[55] V. Cindro,[77] I. A. Cioara,[23] A. Ciocio,[16] F. Cirotto,[105a,105b] Z. H. Citron,[172] M. Citterio,[93a] M. Ciubancan,[28b] A. Clark,[51] B. L. Clark,[59] M. R. Clark,[37] P. J. Clark,[48] R. N. Clarke,[16] C. Clement,[147a,147b] Y. Coadou,[87] M. Cobal,[164a,164c] A. Coccaro,[51] J. Cochran,[66] L. Coffey,[25] L. Colasurdo,[107] B. Cole,[37] A. P. Colijn,[108] J. Collot,[57] T. Colombo,[32] G. Compostella,[102] P. Conde Muiño,[127a,127b] E. Coniavitis,[50] S. H. Connell,[146b] I. A. Connelly,[79] V. Consorti,[50] S. Constantinescu,[28b] G. Conti,[32] F. Conventi,[105a,l] M. Cooke,[16] B. D. Cooper,[80] A. M. Cooper-Sarkar,[121] K. J. R. Cormier,[159] T. Cornelissen,[175] M. Corradi,[133a,133b] F. Corriveau,[89,m] A. Corso-Radu,[163] A. Cortes-Gonzalez,[13] G. Cortiana,[102] G. Costa,[93a] M. J. Costa,[167] D. Costanzo,[140] G. Cottin,[30] G. Cowan,[79] B. E. Cox,[86] K. Cranmer,[111] S. J. Crawley,[55] G. Cree,[31] S. Crépé-Renaudin,[57] F. Crescioli,[82] W. A. Cribbs,[147a,147b] M. Crispin Ortuzar,[121] M. Cristinziani,[23] V. Croft,[107] G. Crosetti,[39a,39b] T. Cuhadar Donszelmann,[140] J. Cummings,[176] M. Curatolo,[49] J. Cúth,[85] C. Cuthbert,[151] H. Czirr,[142] P. Czodrowski,[3] G. D'amen,[22a,22b] S. D'Auria,[55] M. D'Onofrio,[76] M. J. Da Cunha Sargedas De Sousa,[127a,127b] C. Da Via,[86] W. Dabrowski,[40a] T. Dado,[145a] T. Dai,[91] O. Dale,[15] F. Dallaire,[96] C. Dallapiccola,[88] M. Dam,[38] J. R. Dandoy,[33] N. P. Dang,[50] A. C. Daniells,[19] N. S. Dann,[86] M. Danninger,[168] M. Dano Hoffmann,[137] V. Dao,[50] G. Darbo,[52a] S. Darmora,[8] J. Dassoulas,[3] A. Dattagupta,[63] W. Davey,[23] C. David,[169] T. Davidek,[130] M. Davies,[154] P. Davison,[80] E. Dawe,[90] I. Dawson,[140] R. K. Daya-Ishmukhametova,[88] K. De,[8] R. de Asmundis,[105a] A. De Benedetti,[114] S. De Castro,[22a,22b] S. De Cecco,[82] N. De Groot,[107] P. de Jong,[108] H. De la Torre,[84] F. De Lorenzi,[66] A. De Maria,[56] D. De Pedis,[133a] A. De Salvo,[133a] U. De Sanctis,[150] A. De Santo,[150] J. B. De Vivie De Regie,[118] W. J. Dearnaley,[74] R. Debbe,[27] C. Debenedetti,[138] D. V. Dedovich,[67] N. Dehghanian,[3] I. Deigaard,[108] M. Del Gaudio,[39a,39b] J. Del Peso,[84] T. Del Prete,[125a,125b] D. Delgove,[118] F. Deliot,[137] C. M. Delitzsch,[51] M. Deliyergiyev,[77] A. Dell'Acqua,[32] L. Dell'Asta,[24] M. Dell'Orso,[125a,125b] M. Della Pietra,[105a,l] D. della Volpe,[51] M. Delmastro,[5] P. A. Delsart,[57] C. Deluca,[108] D. A. DeMarco,[159] S. Demers,[176] M. Demichev,[67] A. Demilly,[82] S. P. Denisov,[131] D. Denysiuk,[137] D. Derendarz,[41] J. E. Derkaoui,[136d] F. Derue,[82] P. Dervan,[76] K. Desch,[23] C. Deterre,[44] K. Dette,[45] P. O. Deviveiros,[32] A. Dewhurst,[132] S. Dhaliwal,[25] A. Di Ciaccio,[134a,134b] L. Di Ciaccio,[5] W. K. Di Clemente,[123] C. Di Donato,[133a,133b] A. Di Girolamo,[32] B. Di Girolamo,[32] B. Di Micco,[135a,135b] R. Di Nardo,[32] A. Di Simone,[50] R. Di Sipio,[159] D. Di Valentino,[31] C. Diaconu,[87] M. Diamond,[159] F. A. Dias,[48] M. A. Diaz,[34a]

E. B. Diehl,[91] J. Dietrich,[17] S. Diglio,[87] A. Dimitrievska,[14] J. Dingfelder,[23] P. Dita,[28b] S. Dita,[28b] F. Dittus,[32] F. Djama,[87] T. Djobava,[53b] J. I. Djuvsland,[60a] M. A. B. do Vale,[26c] D. Dobos,[32] M. Dobre,[28b] C. Doglioni,[83] T. Dohmae,[156] J. Dolejsi,[130] Z. Dolezal,[130] B. A. Dolgoshein,[99,a] M. Donadelli,[26d] S. Donati,[125a,125b] P. Dondero,[122a,122b] J. Donini,[36] J. Dopke,[132] A. Doria,[105a] M. T. Dova,[73] A. T. Doyle,[55] E. Drechsler,[56] M. Dris,[10] Y. Du,[35d] J. Duarte-Campderros,[154] E. Duchovni,[172] G. Duckeck,[101] O. A. Ducu,[96,n] D. Duda,[108] A. Dudarev,[32] E. M. Duffield,[16] L. Duflot,[118] L. Duguid,[79] M. Dührssen,[32] M. Dumancic,[172] M. Dunford,[60a] H. Duran Yildiz,[4a] M. Düren,[54] A. Durglishvili,[53b] D. Duschinger,[46] B. Dutta,[44] M. Dyndal,[44] C. Eckardt,[44] K. M. Ecker,[102] R. C. Edgar,[91] N. C. Edwards,[48] T. Eifert,[32] G. Eigen,[15] K. Einsweiler,[16] T. Ekelof,[165] M. El Kacimi,[136c] V. Ellajosyula,[87] M. Ellert,[165] S. Elles,[5] F. Ellinghaus,[175] A. A. Elliot,[169] N. Ellis,[32] J. Elmsheuser,[27] M. Elsing,[32] D. Emeliyanov,[132] Y. Enari,[156] O. C. Endner,[85] M. Endo,[119] J. S. Ennis,[170] J. Erdmann,[45] A. Ereditato,[18] G. Ernis,[175] J. Ernst,[2] M. Ernst,[27] S. Errede,[166] E. Ertel,[85] M. Escalier,[118] H. Esch,[45] C. Escobar,[126] B. Esposito,[49] A. I. Etienvre,[137] E. Etzion,[154] H. Evans,[63] A. Ezhilov,[124] F. Fabbri,[22a,22b] L. Fabbri,[22a,22b] G. Facini,[33] R. M. Fakhrutdinov,[131] S. Falciano,[133a] R. J. Falla,[80] J. Faltova,[130] Y. Fang,[35a] M. Fanti,[93a,93b] A. Farbin,[8] A. Farilla,[135a] C. Farina,[126] T. Farooque,[13] S. Farrell,[16] S. M. Farrington,[170] P. Farthouat,[32] F. Fassi,[136e] P. Fassnacht,[32] D. Fassouliotis,[9] M. Faucci Giannelli,[79] A. Favareto,[52a,52b] W. J. Fawcett,[121] L. Fayard,[118] O. L. Fedin,[124,o] W. Fedorko,[168] S. Feigl,[120] L. Feligioni,[87] C. Feng,[35d] E. J. Feng,[32] H. Feng,[91] A. B. Fenyuk,[131] L. Feremenga,[8] P. Fernandez Martinez,[167] S. Fernandez Perez,[13] J. Ferrando,[55] A. Ferrari,[165] P. Ferrari,[108] R. Ferrari,[122a] D. E. Ferreira de Lima,[60b] A. Ferrer,[167] D. Ferrere,[51] C. Ferretti,[91] A. Ferretto Parodi,[52a,52b] F. Fiedler,[85] A. Filipčič,[77] M. Filipuzzi,[44] F. Filthaut,[107] M. Fincke-Keeler,[169] K. D. Finelli,[151] M. C. N. Fiolhais,[127a,127c] L. Fiorini,[167] A. Firan,[42] A. Fischer,[2] C. Fischer,[13] J. Fischer,[175] W. C. Fisher,[92] N. Flaschel,[44] I. Fleck,[142] P. Fleischmann,[91] G. T. Fletcher,[140] R. R. M. Fletcher,[123] T. Flick,[175] A. Floderus,[83] L. R. Flores Castillo,[62a] M. J. Flowerdew,[102] G. T. Forcolin,[86] A. Formica,[137] A. Forti,[86] A. G. Foster,[19] D. Fournier,[118] H. Fox,[74] S. Fracchia,[13] P. Francavilla,[82] M. Franchini,[22a,22b] D. Francis,[32] L. Franconi,[120] M. Franklin,[59] M. Frate,[163] M. Fraternali,[122a,122b] D. Freeborn,[80] S. M. Fressard-Batraneanu,[32] F. Friedrich,[46] D. Froidevaux,[32] J. A. Frost,[121] C. Fukunaga,[157] E. Fullana Torregrosa,[85] T. Fusayasu,[103] J. Fuster,[167] C. Gabaldon,[57] O. Gabizon,[175] A. Gabrielli,[22a,22b] A. Gabrielli,[16] G. P. Gach,[40a] S. Gadatsch,[32] S. Gadomski,[51] G. Gagliardi,[52a,52b] L. G. Gagnon,[96] P. Gagnon,[63] C. Galea,[107] B. Galhardo,[127a,127c] E. J. Gallas,[121] B. J. Gallop,[132] P. Gallus,[129] G. Galster,[38] K. K. Gan,[112] J. Gao,[35b,87] Y. Gao,[48] Y. S. Gao,[144,g] F. M. Garay Walls,[48] C. García,[167] J. E. García Navarro,[167] M. Garcia-Sciveres,[16] R. W. Gardner,[33] N. Garelli,[144] V. Garonne,[120] A. Gascon Bravo,[44] C. Gatti,[49] A. Gaudiello,[52a,52b] G. Gaudio,[122a] B. Gaur,[142] L. Gauthier,[96] I. L. Gavrilenko,[97] C. Gay,[168] G. Gaycken,[23] E. N. Gazis,[10] Z. Gecse,[168] C. N. P. Gee,[132] Ch. Geich-Gimbel,[23] M. P. Geisler,[60a] C. Gemme,[52a] M. H. Genest,[57] C. Geng,[35b,p] S. Gentile,[133a,133b] S. George,[79] D. Gerbaudo,[13] A. Gershon,[154] S. Ghasemi,[142] H. Ghazlane,[136b] M. Ghneimat,[23] B. Giacobbe,[22a] S. Giagu,[133a,133b] P. Giannetti,[125a,125b] B. Gibbard,[27] S. M. Gibson,[79] M. Gignac,[168] M. Gilchriese,[16] T. P. S. Gillam,[30] D. Gillberg,[31] G. Gilles,[175] D. M. Gingrich,[3,e] N. Giokaris,[9] M. P. Giordani,[164a,164c] F. M. Giorgi,[22a] F. M. Giorgi,[17] P. F. Giraud,[137] P. Giromini,[59] D. Giugni,[93a] F. Giuli,[121] C. Giuliani,[102] M. Giulini,[60b] B. K. Gjelsten,[120] S. Gkaitatzis,[155] I. Gkialas,[155] E. L. Gkougkousis,[118] L. K. Gladilin,[100] C. Glasman,[84] J. Glatzer,[32] P. C. F. Glaysher,[48] A. Glazov,[44] M. Goblirsch-Kolb,[102] J. Godlewski,[41] S. Goldfarb,[91] T. Golling,[51] D. Golubkov,[131] A. Gomes,[127a,127b,127d] R. Gonçalo,[127a] J. Goncalves Pinto Firmino Da Costa,[137] L. Gonella,[19] A. Gongadze,[67] S. González de la Hoz,[167] G. Gonzalez Parra,[13] S. Gonzalez-Sevilla,[51] L. Goossens,[32] P. A. Gorbounov,[98] H. A. Gordon,[27] I. Gorelov,[106] B. Gorini,[32] E. Gorini,[75a,75b] A. Gorišek,[77] E. Gornicki,[41] A. T. Goshaw,[47] C. Gössling,[45] M. I. Gostkin,[67] C. R. Goudet,[118] D. Goujdami,[136c] A. G. Goussiou,[139] N. Govender,[146b,q] E. Gozani,[153] L. Graber,[56] I. Grabowska-Bold,[40a] P. O. J. Gradin,[57] P. Grafström,[22a,22b] J. Gramling,[51] E. Gramstad,[120] S. Grancagnolo,[17] V. Gratchev,[124] P. M. Gravila,[28e] H. M. Gray,[32] E. Graziani,[135a] Z. D. Greenwood,[81,r] C. Grefe,[23] K. Gregersen,[80] I. M. Gregor,[44] P. Grenier,[144] K. Grevtsov,[5] J. Griffiths,[8] A. A. Grillo,[138] K. Grimm,[74] S. Grinstein,[13,s] Ph. Gris,[36] J.-F. Grivaz,[118] S. Groh,[85] J. P. Grohs,[46] E. Gross,[172] J. Grosse-Knetter,[56] G. C. Grossi,[81] Z. J. Grout,[150] L. Guan,[91] W. Guan,[173] J. Guenther,[129] F. Guescini,[51] D. Guest,[163] O. Gueta,[154] E. Guido,[52a,52b] T. Guillemin,[5] S. Guindon,[2] U. Gul,[55] C. Gumpert,[32] J. Guo,[35e] Y. Guo,[35b,p] S. Gupta,[121] G. Gustavino,[133a,133b] P. Gutierrez,[114] N. G. Gutierrez Ortiz,[80] C. Gutschow,[46] C. Guyot,[137] C. Gwenlan,[121] C. B. Gwilliam,[76] A. Haas,[111] C. Haber,[16] H. K. Hadavand,[8] N. Haddad,[136e] A. Hadef,[87] P. Haefner,[23] S. Hageböck,[23] Z. Hajduk,[41] H. Hakobyan,[177,a] M. Haleem,[44] J. Haley,[115] G. Halladjian,[92] G. D. Hallewell,[87] K. Hamacher,[175] P. Hamal,[116] K. Hamano,[169] A. Hamilton,[146a] G. N. Hamity,[140] P. G. Hamnett,[44] L. Han,[35b] K. Hanagaki,[68,t] K. Hanawa,[156] M. Hance,[138] B. Haney,[123] P. Hanke,[60a] R. Hanna,[137] J. B. Hansen,[38] J. D. Hansen,[38] M. C. Hansen,[23] P. H. Hansen,[38] K. Hara,[161] A. S. Hard,[173] T. Harenberg,[175] F. Hariri,[118] S. Harkusha,[94]

R. D. Harrington,[48] P. F. Harrison,[170] F. Hartjes,[108] N. M. Hartmann,[101] M. Hasegawa,[69] Y. Hasegawa,[141] A. Hasib,[114] S. Hassani,[137] S. Haug,[18] R. Hauser,[92] L. Hauswald,[46] M. Havranek,[128] C. M. Hawkes,[19] R. J. Hawkings,[32] D. Hayden,[92] C. P. Hays,[121] J. M. Hays,[78] H. S. Hayward,[76] S. J. Haywood,[132] S. J. Head,[19] T. Heck,[85] V. Hedberg,[83] L. Heelan,[8] S. Heim,[123] T. Heim,[16] B. Heinemann,[16] J. J. Heinrich,[101] L. Heinrich,[111] C. Heinz,[54] J. Hejbal,[128] L. Helary,[24] S. Hellman,[147a,147b] C. Helsens,[32] J. Henderson,[121] R. C. W. Henderson,[74] Y. Heng,[173] S. Henkelmann,[168] A. M. Henriques Correia,[32] S. Henrot-Versille,[118] G. H. Herbert,[17] Y. Hernández Jiménez,[167] G. Herten,[50] R. Hertenberger,[101] L. Hervas,[32] G. G. Hesketh,[80] N. P. Hessey,[108] J. W. Hetherly,[42] R. Hickling,[78] E. Higón-Rodriguez,[167] E. Hill,[169] J. C. Hill,[30] K. H. Hiller,[44] S. J. Hillier,[19] I. Hinchliffe,[16] E. Hines,[123] R. R. Hinman,[16] M. Hirose,[158] D. Hirschbuehl,[175] J. Hobbs,[149] N. Hod,[160a] M. C. Hodgkinson,[140] P. Hodgson,[140] A. Hoecker,[32] M. R. Hoeferkamp,[106] F. Hoenig,[101] D. Hohn,[23] T. R. Holmes,[16] M. Homann,[45] T. M. Hong,[126] B. H. Hooberman,[166] W. H. Hopkins,[117] Y. Horii,[104] A. J. Horton,[143] J-Y. Hostachy,[57] S. Hou,[152] A. Hoummada,[136a] J. Howarth,[44] M. Hrabovsky,[116] I. Hristova,[17] J. Hrivnac,[118] T. Hryn'ova,[5] A. Hrynevich,[95] C. Hsu,[146c] P. J. Hsu,[152,u] S.-C. Hsu,[139] D. Hu,[37] Q. Hu,[35b] Y. Huang,[44] Z. Hubacek,[129] F. Hubaut,[87] F. Huegging,[23] T. B. Huffman,[121] E. W. Hughes,[37] G. Hughes,[74] M. Huhtinen,[32] T. A. Hülsing,[85] P. Huo,[149] N. Huseynov,[67,c] J. Huston,[92] J. Huth,[59] G. Iacobucci,[51] G. Iakovidis,[27] I. Ibragimov,[142] L. Iconomidou-Fayard,[118] E. Ideal,[176] Z. Idrissi,[136e] P. Iengo,[32] O. Igonkina,[108,v] T. Iizawa,[171] Y. Ikegami,[68] M. Ikeno,[68] Y. Ilchenko,[11,w] D. Iliadis,[155] N. Ilic,[144] T. Ince,[102] G. Introzzi,[122a,122b] P. Ioannou,[9,a] M. Iodice,[135a] K. Iordanidou,[37] V. Ippolito,[59] M. Ishino,[70] M. Ishitsuka,[158] R. Ishmukhametov,[112] C. Issever,[121] S. Istin,[20a] F. Ito,[161] J. M. Iturbe Ponce,[86] R. Iuppa,[134a,134b] W. Iwanski,[41] H. Iwasaki,[68] J. M. Izen,[43] V. Izzo,[105a] S. Jabbar,[3] B. Jackson,[123] M. Jackson,[76] P. Jackson,[1] V. Jain,[2] K. B. Jakobi,[85] K. Jakobs,[50] S. Jakobsen,[32] T. Jakoubek,[128] D. O. Jamin,[115] D. K. Jana,[81] E. Jansen,[80] R. Jansky,[64] J. Janssen,[23] M. Janus,[56] G. Jarlskog,[83] N. Javadov,[67,c] T. Javůrek,[50] F. Jeanneau,[137] L. Jeanty,[16] J. Jejelava,[53a,x] G.-Y. Jeng,[151] D. Jennens,[90] P. Jenni,[50,y] J. Jentzsch,[45] C. Jeske,[170] S. Jézéquel,[5] H. Ji,[173] J. Jia,[149] H. Jiang,[66] Y. Jiang,[35b] S. Jiggins,[80] J. Jimenez Pena,[167] S. Jin,[35a] A. Jinaru,[28b] O. Jinnouchi,[158] P. Johansson,[140] K. A. Johns,[7] W. J. Johnson,[139] K. Jon-And,[147a,147b] G. Jones,[170] R. W. L. Jones,[74] S. Jones,[7] T. J. Jones,[76] J. Jongmanns,[60a] P. M. Jorge,[127a,127b] J. Jovicevic,[160a] X. Ju,[173] A. Juste Rozas,[13,s] M. K. Köhler,[172] A. Kaczmarska,[41] M. Kado,[118] H. Kagan,[112] M. Kagan,[144] S. J. Kahn,[87] E. Kajomovitz,[47] C. W. Kalderon,[121] A. Kaluza,[85] S. Kama,[42] A. Kamenshchikov,[131] N. Kanaya,[156] S. Kaneti,[30] L. Kanjir,[77] V. A. Kantserov,[99] J. Kanzaki,[68] B. Kaplan,[111] L. S. Kaplan,[173] A. Kapliy,[33] D. Kar,[146c] K. Karakostas,[10] A. Karamaoun,[3] N. Karastathis,[10] M. J. Kareem,[56] E. Karentzos,[10] M. Karnevskiy,[85] S. N. Karpov,[67] Z. M. Karpova,[67] K. Karthik,[111] V. Kartvelishvili,[74] A. N. Karyukhin,[131] K. Kasahara,[161] L. Kashif,[173] R. D. Kass,[112] A. Kastanas,[15] Y. Kataoka,[156] C. Kato,[156] A. Katre,[51] J. Katzy,[44] K. Kawagoe,[72] T. Kawamoto,[156] G. Kawamura,[56] S. Kazama,[156] V. F. Kazanin,[110,d] R. Keeler,[169] R. Kehoe,[42] J. S. Keller,[44] J. J. Kempster,[79] K Kentaro,[104] H. Keoshkerian,[159] O. Kepka,[128] B. P. Kerševan,[77] S. Kersten,[175] R. A. Keyes,[89] F. Khalil-zada,[12] A. Khanov,[115] A. G. Kharlamov,[110,d] T. J. Khoo,[51] V. Khovanskiy,[98] E. Khramov,[67] J. Khubua,[53b,z] S. Kido,[69] H. Y. Kim,[8] S. H. Kim,[161] Y. K. Kim,[33] N. Kimura,[155] O. M. Kind,[17] B. T. King,[76] M. King,[167] S. B. King,[168] J. Kirk,[132] A. E. Kiryunin,[102] T. Kishimoto,[69] D. Kisielewska,[40a] F. Kiss,[50] K. Kiuchi,[161] O. Kivernyk,[137] E. Kladiva,[145b] M. H. Klein,[37] M. Klein,[76] U. Klein,[76] K. Kleinknecht,[85] P. Klimek,[147a,147b] A. Klimentov,[27] R. Klingenberg,[45] J. A. Klinger,[140] T. Klioutchnikova,[32] E.-E. Kluge,[60a] P. Kluit,[108] S. Kluth,[102] J. Knapik,[41] E. Kneringer,[64] E. B. F. G. Knoops,[87] A. Knue,[55] A. Kobayashi,[156] D. Kobayashi,[158] T. Kobayashi,[156] M. Kobel,[46] M. Kocian,[144] P. Kodys,[130] T. Koffas,[31] E. Koffeman,[108] T. Koi,[144] H. Kolanoski,[17] M. Kolb,[60b] I. Koletsou,[5] A. A. Komar,[97,a] Y. Komori,[156] T. Kondo,[68] N. Kondrashova,[44] K. Köneke,[50] A. C. König,[107] T. Kono,[68,aa] R. Konoplich,[111,bb] N. Konstantinidis,[80] R. Kopeliansky,[63] S. Koperny,[40a] L. Köpke,[85] A. K. Kopp,[50] K. Korcyl,[41] K. Kordas,[155] A. Korn,[80] A. A. Korol,[110,d] I. Korolkov,[13] E. V. Korolkova,[140] O. Kortner,[102] S. Kortner,[102] T. Kosek,[130] V. V. Kostyukhin,[23] A. Kotwal,[47] A. Kourkoumeli-Charalampidi,[155] C. Kourkoumelis,[9] V. Kouskoura,[27] A. B. Kowalewska,[41] R. Kowalewski,[169] T. Z. Kowalski,[40a] C. Kozakai,[156] W. Kozanecki,[137] A. S. Kozhin,[131] V. A. Kramarenko,[100] G. Kramberger,[77] D. Krasnopevtsev,[99] M. W. Krasny,[82] A. Krasznahorkay,[32] J. K. Kraus,[23] A. Kravchenko,[27] M. Kretz,[60c] J. Kretzschmar,[76] K. Kreutzfeldt,[54] P. Krieger,[159] K. Krizka,[33] K. Kroeninger,[45] H. Kroha,[102] J. Kroll,[123] J. Kroseberg,[23] J. Krstic,[14] U. Kruchonak,[67] H. Krüger,[23] N. Krumnack,[66] A. Kruse,[173] M. C. Kruse,[47] M. Kruskal,[24] T. Kubota,[90] H. Kucuk,[80] S. Kuday,[4b] J. T. Kuechler,[175] S. Kuehn,[50] A. Kugel,[60c] F. Kuger,[174] A. Kuhl,[138] T. Kuhl,[44] V. Kukhtin,[67] R. Kukla,[137] Y. Kulchitsky,[94] S. Kuleshov,[34b] M. Kuna,[133a,133b] T. Kunigo,[70] A. Kupco,[128] H. Kurashige,[69] Y. A. Kurochkin,[94] V. Kus,[128] E. S. Kuwertz,[169] M. Kuze,[158] J. Kvita,[116] T. Kwan,[169] D. Kyriazopoulos,[140]

A. La Rosa,[102] J. L. La Rosa Navarro,[26d] L. La Rotonda,[39a,39b] C. Lacasta,[167] F. Lacava,[133a,133b] J. Lacey,[31] H. Lacker,[17] D. Lacour,[82] V. R. Lacuesta,[167] E. Ladygin,[67] R. Lafaye,[5] B. Laforge,[82] T. Lagouri,[176] S. Lai,[56] S. Lammers,[63] W. Lampl,[7] E. Lançon,[137] U. Landgraf,[50] M. P. J. Landon,[78] V. S. Lang,[60a] J. C. Lange,[13] A. J. Lankford,[163] F. Lanni,[27] K. Lantzsch,[23] A. Lanza,[122a] S. Laplace,[82] C. Lapoire,[32] J. F. Laporte,[137] T. Lari,[93a] F. Lasagni Manghi,[22a,22b] M. Lassnig,[32] P. Laurelli,[49] W. Lavrijsen,[16] A. T. Law,[138] P. Laycock,[76] T. Lazovich,[59] M. Lazzaroni,[93a,93b] B. Le,[90] O. Le Dortz,[82] E. Le Guirriec,[87] E. P. Le Quilleuc,[137] M. LeBlanc,[169] T. LeCompte,[6] F. Ledroit-Guillon,[57] C. A. Lee,[27] S. C. Lee,[152] L. Lee,[1] G. Lefebvre,[82] M. Lefebvre,[169] F. Legger,[101] C. Leggett,[16] A. Lehan,[76] G. Lehmann Miotto,[32] X. Lei,[7] W. A. Leight,[31] A. Leisos,[155,cc] A. G. Leister,[176] M. A. L. Leite,[26d] R. Leitner,[130] D. Lellouch,[172] B. Lemmer,[56] K. J. C. Leney,[80] T. Lenz,[23] B. Lenzi,[32] R. Leone,[7] S. Leone,[125a,125b] C. Leonidopoulos,[48] S. Leontsinis,[10] G. Lerner,[150] C. Leroy,[96] A. A. J. Lesage,[137] C. G. Lester,[30] M. Levchenko,[124] J. Levêque,[5] D. Levin,[91] L. J. Levinson,[172] M. Levy,[19] D. Lewis,[78] A. M. Leyko,[23] M. Leyton,[43] B. Li,[35b,p] H. Li,[149] H. L. Li,[33] L. Li,[47] L. Li,[35e] Q. Li,[35a] S. Li,[47] X. Li,[86] Y. Li,[142] Z. Liang,[35a] B. Liberti,[134a] A. Liblong,[159] P. Lichard,[32] K. Lie,[166] J. Liebal,[23] W. Liebig,[15] A. Limosani,[151] S. C. Lin,[152,dd] T. H. Lin,[85] B. E. Lindquist,[149] A. E. Lionti,[51] E. Lipeles,[123] A. Lipniacka,[15] M. Lisovyi,[60b] T. M. Liss,[166] A. Lister,[168] A. M. Litke,[138] B. Liu,[152,ee] D. Liu,[152] H. Liu,[91] H. Liu,[27] J. Liu,[87] J. B. Liu,[35b] K. Liu,[87] L. Liu,[166] M. Liu,[47] M. Liu,[35b] Y. L. Liu,[35b] Y. Liu,[35b] M. Livan,[122a,122b] A. Lleres,[57] J. Llorente Merino,[35a] S. L. Lloyd,[78] F. Lo Sterzo,[152] E. Lobodzinska,[44] P. Loch,[7] W. S. Lockman,[138] F. K. Loebinger,[86] A. E. Loevschall-Jensen,[38] K. M. Loew,[25] A. Loginov,[176] T. Lohse,[17] K. Lohwasser,[44] M. Lokajicek,[128] B. A. Long,[24] J. D. Long,[166] R. E. Long,[74] L. Longo,[75a,75b] K. A. Looper,[112] L. Lopes,[127a] D. Lopez Mateos,[59] B. Lopez Paredes,[140] I. Lopez Paz,[13] A. Lopez Solis,[82] J. Lorenz,[101] N. Lorenzo Martinez,[63] M. Losada,[21] P. J. Lösel,[101] X. Lou,[35a] A. Lounis,[118] J. Love,[6] P. A. Love,[74] H. Lu,[62a] N. Lu,[91] H. J. Lubatti,[139] C. Luci,[133a,133b] A. Lucotte,[57] C. Luedtke,[50] F. Luehring,[63] W. Lukas,[64] L. Luminari,[133a] O. Lundberg,[147a,147b] B. Lund-Jensen,[148] D. Lynn,[27] R. Lysak,[128] E. Lytken,[83] V. Lyubushkin,[67] H. Ma,[27] L. L. Ma,[35d] Y. Ma,[35d] G. Maccarrone,[49] A. Macchiolo,[102] C. M. Macdonald,[140] B. Maček,[77] J. Machado Miguens,[123,127b] D. Madaffari,[87] R. Madar,[36] H. J. Maddocks,[165] W. F. Mader,[46] A. Madsen,[44] J. Maeda,[69] S. Maeland,[15] T. Maeno,[27] A. Maevskiy,[100] E. Magradze,[56] J. Mahlstedt,[108] C. Maiani,[118] C. Maidantchik,[26a] A. A. Maier,[102] T. Maier,[101] A. Maio,[127a,127b,127d] S. Majewski,[117] Y. Makida,[68] N. Makovec,[118] B. Malaescu,[82] Pa. Malecki,[41] V. P. Maleev,[124] F. Malek,[57] U. Mallik,[65] D. Malon,[6] C. Malone,[144] S. Maltezos,[10] S. Malyukov,[32] J. Mamuzic,[167] G. Mancini,[49] B. Mandelli,[32] L. Mandelli,[93a] I. Mandić,[77] J. Maneira,[127a,127b] L. Manhaes de Andrade Filho,[26b] J. Manjarres Ramos,[160b] A. Mann,[101] B. Mansoulie,[137] J. D. Mansour,[35a] R. Mantifel,[89] M. Mantoani,[56] S. Manzoni,[93a,93b] L. Mapelli,[32] G. Marceca,[29] L. March,[51] G. Marchiori,[82] M. Marcisovsky,[128] M. Marjanovic,[14] D. E. Marley,[91] F. Marroquim,[26a] S. P. Marsden,[86] Z. Marshall,[16] S. Marti-Garcia,[167] B. Martin,[92] T. A. Martin,[170] V. J. Martin,[48] B. Martin dit Latour,[15] M. Martinez,[13,s] S. Martin-Haugh,[132] V. S. Martoiu,[28b] A. C. Martyniuk,[80] M. Marx,[139] A. Marzin,[32] L. Masetti,[85] T. Mashimo,[156] R. Mashinistov,[97] J. Masik,[86] A. L. Maslennikov,[110,d] I. Massa,[22a,22b] L. Massa,[22a,22b] P. Mastrandrea,[5] A. Mastroberardino,[39a,39b] T. Masubuchi,[156] P. Mättig,[175] J. Mattmann,[85] J. Maurer,[28b] S. J. Maxfield,[76] D. A. Maximov,[110,d] R. Mazini,[152] S. M. Mazza,[93a,93b] N. C. Mc Fadden,[106] G. Mc Goldrick,[159] S. P. Mc Kee,[91] A. McCarn,[91] R. L. McCarthy,[149] T. G. McCarthy,[31] L. I. McClymont,[80] E. F. McDonald,[90] K. W. McFarlane,[58,a] J. A. Mcfayden,[80] G. Mchedlidze,[56] S. J. McMahon,[132] R. A. McPherson,[169,m] M. Medinnis,[44] S. Meehan,[139] S. Mehlhase,[101] A. Mehta,[76] K. Meier,[60a] C. Meineck,[101] B. Meirose,[43] D. Melini,[167] B. R. Mellado Garcia,[146c] M. Melo,[145a] F. Meloni,[18] A. Mengarelli,[22a,22b] S. Menke,[102] E. Meoni,[162] S. Mergelmeyer,[17] P. Mermod,[51] L. Merola,[105a,105b] C. Meroni,[93a] F. S. Merritt,[33] A. Messina,[133a,133b] J. Metcalfe,[6] A. S. Mete,[163] C. Meyer,[85] C. Meyer,[123] J-P. Meyer,[137] J. Meyer,[108] H. Meyer Zu Theenhausen,[60a] F. Miano,[150] R. P. Middleton,[132] S. Miglioranzi,[52a,52b] L. Mijović,[23] G. Mikenberg,[172] M. Mikestikova,[128] M. Mikuž,[77] M. Milesi,[90] A. Milic,[64] D. W. Miller,[33] C. Mills,[48] A. Milov,[172] D. A. Milstead,[147a,147b] A. A. Minaenko,[131] Y. Minami,[156] I. A. Minashvili,[67] A. I. Mincer,[111] B. Mindur,[40a] M. Mineev,[67] Y. Ming,[173] L. M. Mir,[13] K. P. Mistry,[123] T. Mitani,[171] J. Mitrevski,[101] V. A. Mitsou,[167] A. Miucci,[51] P. S. Miyagawa,[140] J. U. Mjörnmark,[83] T. Moa,[147a,147b] K. Mochizuki,[96] S. Mohapatra,[37] S. Molander,[147a,147b] R. Moles-Valls,[23] R. Monden,[70] M. C. Mondragon,[92] K. Mönig,[44] J. Monk,[38] E. Monnier,[87] A. Montalbano,[149] J. Montejo Berlingen,[32] F. Monticelli,[73] S. Monzani,[93a,93b] R. W. Moore,[3] N. Morange,[118] D. Moreno,[21] M. Moreno Llácer,[56] P. Morettini,[52a] D. Mori,[143] T. Mori,[156] M. Morii,[59] M. Morinaga,[156] V. Morisbak,[120] S. Moritz,[85] A. K. Morley,[151] G. Mornacchi,[32] J. D. Morris,[78] S. S. Mortensen,[38] L. Morvaj,[149] M. Mosidze,[53b] J. Moss,[144] K. Motohashi,[158] R. Mount,[144] E. Mountricha,[27] S. V. Mouraviev,[97,a] E. J. W. Moyse,[88] S. Muanza,[87] R. D. Mudd,[19] F. Mueller,[102] J. Mueller,[126] R. S. P. Mueller,[101] T. Mueller,[30]

D. Muenstermann,[74] P. Mullen,[55] G. A. Mullier,[18] F. J. Munoz Sanchez,[86] J. A. Murillo Quijada,[19] W. J. Murray,[170,132] H. Musheghyan,[56] M. Muškinja,[77] A. G. Myagkov,[131,ff] M. Myska,[129] B. P. Nachman,[144] O. Nackenhorst,[51] K. Nagai,[121] R. Nagai,[68,aa] K. Nagano,[68] Y. Nagasaka,[61] K. Nagata,[161] M. Nagel,[50] E. Nagy,[87] A. M. Nairz,[32] Y. Nakahama,[32] K. Nakamura,[68] T. Nakamura,[156] I. Nakano,[113] H. Namasivayam,[43] R. F. Naranjo Garcia,[44] R. Narayan,[11] D. I. Narrias Villar,[60a] I. Naryshkin,[124] T. Naumann,[44] G. Navarro,[21] R. Nayyar,[7] H. A. Neal,[91] P. Yu. Nechaeva,[97] T. J. Neep,[86] P. D. Nef,[144] A. Negri,[122a,122b] M. Negrini,[22a] S. Nektarijevic,[107] C. Nellist,[118] A. Nelson,[163] S. Nemecek,[128] P. Nemethy,[111] A. A. Nepomuceno,[26a] M. Nessi,[32,gg] M. S. Neubauer,[166] M. Neumann,[175] R. M. Neves,[111] P. Nevski,[27] P. R. Newman,[19] D. H. Nguyen,[6] T. Nguyen Manh,[96] R. B. Nickerson,[121] R. Nicolaidou,[137] J. Nielsen,[138] A. Nikiforov,[17] V. Nikolaenko,[131,ff] I. Nikolic-Audit,[82] K. Nikolopoulos,[19] J. K. Nilsen,[120] P. Nilsson,[27] Y. Ninomiya,[156] A. Nisati,[133a] R. Nisius,[102] T. Nobe,[156] L. Nodulman,[6] M. Nomachi,[119] I. Nomidis,[31] T. Nooney,[78] S. Norberg,[114] M. Nordberg,[32] N. Norjoharuddeen,[121] O. Novgorodova,[46] S. Nowak,[102] M. Nozaki,[68] L. Nozka,[116] K. Ntekas,[10] E. Nurse,[80] F. Nuti,[90] F. O'grady,[7] D. C. O'Neil,[143] A. A. O'Rourke,[44] V. O'Shea,[55] F. G. Oakham,[31,e] H. Oberlack,[102] T. Obermann,[23] J. Ocariz,[82] A. Ochi,[69] I. Ochoa,[37] J. P. Ochoa-Ricoux,[34a] S. Oda,[72] S. Odaka,[68] H. Ogren,[63] A. Oh,[86] S. H. Oh,[47] C. C. Ohm,[16] H. Ohman,[165] H. Oide,[32] H. Okawa,[161] Y. Okumura,[33] T. Okuyama,[68] A. Olariu,[28b] L. F. Oleiro Seabra,[127a] S. A. Olivares Pino,[48] D. Oliveira Damazio,[27] A. Olszewski,[41] J. Olszowska,[41] A. Onofre,[127a,127e] K. Onogi,[104] P. U. E. Onyisi,[11,w] M. J. Oreglia,[33] Y. Oren,[154] D. Orestano,[135a,135b] N. Orlando,[62b] R. S. Orr,[159] B. Osculati,[52a,52b] R. Ospanov,[86] G. Otero y Garzon,[29] H. Otono,[72] M. Ouchrif,[136d] F. Ould-Saada,[120] A. Ouraou,[137] K. P. Oussoren,[108] Q. Ouyang,[35a] M. Owen,[55] R. E. Owen,[19] V. E. Ozcan,[20a] N. Ozturk,[8] K. Pachal,[143] A. Pacheco Pages,[13] C. Padilla Aranda,[13] M. Pagáčová,[50] S. Pagan Griso,[16] F. Paige,[27] P. Pais,[88] K. Pajchel,[120] G. Palacino,[160b] S. Palestini,[32] M. Palka,[40b] D. Pallin,[36] A. Palma,[127a,127b] E. St. Panagiotopoulou,[10] C. E. Pandini,[82] J. G. Panduro Vazquez,[79] P. Pani,[147a,147b] S. Panitkin,[27] D. Pantea,[28b] L. Paolozzi,[51] Th. D. Papadopoulou,[10] K. Papageorgiou,[155] A. Paramonov,[6] D. Paredes Hernandez,[176] A. J. Parker,[74] M. A. Parker,[30] K. A. Parker,[140] F. Parodi,[52a,52b] J. A. Parsons,[37] U. Parzefall,[50] V. R. Pascuzzi,[159] E. Pasqualucci,[133a] S. Passaggio,[52a] Fr. Pastore,[79] G. Pásztor,[31,hh] S. Pataraia,[175] J. R. Pater,[86] T. Pauly,[32] J. Pearce,[169] B. Pearson,[114] L. E. Pedersen,[38] M. Pedersen,[120] S. Pedraza Lopez,[167] R. Pedro,[127a,127b] S. V. Peleganchuk,[110,d] D. Pelikan,[165] O. Penc,[128] C. Peng,[35a] H. Peng,[35b] J. Penwell,[63] B. S. Peralva,[26b] M. M. Perego,[137] D. V. Perepelitsa,[27] E. Perez Codina,[160a] L. Perini,[93a,93b] H. Pernegger,[32] S. Perrella,[105a,105b] R. Peschke,[44] V. D. Peshekhonov,[67] K. Peters,[44] R. F. Y. Peters,[86] B. A. Petersen,[32] T. C. Petersen,[38] E. Petit,[57] A. Petridis,[1] C. Petridou,[155] P. Petroff,[118] E. Petrolo,[133a] M. Petrov,[121] F. Petrucci,[135a,135b] N. E. Pettersson,[88] A. Peyaud,[137] R. Pezoa,[34b] P. W. Phillips,[132] G. Piacquadio,[144] E. Pianori,[170] A. Picazio,[88] E. Piccaro,[78] M. Piccinini,[22a,22b] M. A. Pickering,[121] R. Piegaia,[29] J. E. Pilcher,[33] A. D. Pilkington,[86] A. W. J. Pin,[86] M. Pinamonti,[164a,164c,ii] J. L. Pinfold,[3] A. Pingel,[38] S. Pires,[82] H. Pirumov,[44] M. Pitt,[172] L. Plazak,[145a] M.-A. Pleier,[27] V. Pleskot,[85] E. Plotnikova,[67] P. Plucinski,[92] D. Pluth,[66] R. Poettgen,[147a,147b] L. Poggioli,[118] D. Pohl,[23] G. Polesello,[122a] A. Poley,[44] A. Policicchio,[39a,39b] R. Polifka,[159] A. Polini,[22a] C. S. Pollard,[55] V. Polychronakos,[27] K. Pommès,[32] L. Pontecorvo,[133a] B. G. Pope,[92] G. A. Popeneciu,[28c] D. S. Popovic,[14] A. Poppleton,[32] S. Pospisil,[129] K. Potamianos,[16] I. N. Potrap,[67] C. J. Potter,[30] C. T. Potter,[117] G. Poulard,[32] J. Poveda,[32] V. Pozdnyakov,[67] M. E. Pozo Astigarraga,[32] P. Pralavorio,[87] A. Pranko,[16] S. Prell,[66] D. Price,[86] L. E. Price,[6] M. Primavera,[75a] S. Prince,[89] M. Proissl,[48] K. Prokofiev,[62c] F. Prokoshin,[34b] S. Protopopescu,[27] J. Proudfoot,[6] M. Przybycien,[40a] D. Puddu,[135a,135b] D. Puldon,[149] M. Purohit,[27,jj] P. Puzo,[118] J. Qian,[91] G. Qin,[55] Y. Qin,[86] A. Quadt,[56] W. B. Quayle,[164a,164b] M. Queitsch-Maitland,[86] D. Quilty,[55] S. Raddum,[120] V. Radeka,[27] V. Radescu,[60b] S. K. Radhakrishnan,[149] P. Radloff,[117] P. Rados,[90] F. Ragusa,[93a,93b] G. Rahal,[178] J. A. Raine,[86] S. Rajagopalan,[27] M. Rammensee,[32] C. Rangel-Smith,[165] M. G. Ratti,[93a,93b] F. Rauscher,[101] S. Rave,[85] T. Ravenscroft,[55] I. Ravinovich,[172] M. Raymond,[32] A. L. Read,[120] N. P. Readioff,[76] M. Reale,[75a,75b] D. M. Rebuzzi,[122a,122b] A. Redelbach,[174] G. Redlinger,[27] R. Reece,[138] K. Reeves,[43] L. Rehnisch,[17] J. Reichert,[123] H. Reisin,[29] C. Rembser,[32] H. Ren,[35a] M. Rescigno,[133a] S. Resconi,[93a] O. L. Rezanova,[110,d] P. Reznicek,[130] R. Rezvani,[96] R. Richter,[102] S. Richter,[80] E. Richter-Was,[40b] O. Ricken,[23] M. Ridel,[82] P. Rieck,[17] C. J. Riegel,[175] J. Rieger,[56] O. Rifki,[114] M. Rijssenbeek,[149] A. Rimoldi,[122a,122b] M. Rimoldi,[18] L. Rinaldi,[22a] B. Ristić,[51] E. Ritsch,[32] I. Riu,[13] F. Rizatdinova,[115] E. Rizvi,[78] C. Rizzi,[13] S. H. Robertson,[89,m] A. Robichaud-Veronneau,[89] D. Robinson,[30] J. E. M. Robinson,[44] A. Robson,[55] C. Roda,[125a,125b] Y. Rodina,[87] A. Rodriguez Perez,[13] D. Rodriguez Rodriguez,[167] S. Roe,[32] C. S. Rogan,[59] O. Røhne,[120] A. Romaniouk,[99] M. Romano,[22a,22b] S. M. Romano Saez,[36] E. Romero Adam,[167] N. Rompotis,[139] M. Ronzani,[50] L. Roos,[82] E. Ros,[167] S. Rosati,[133a] K. Rosbach,[50] P. Rose,[138] O. Rosenthal,[142] N.-A. Rosien,[56] V. Rossetti,[147a,147b] E. Rossi,[105a,105b] L. P. Rossi,[52a]

J. H. N. Rosten,[30] R. Rosten,[139] M. Rotaru,[28b] I. Roth,[172] J. Rothberg,[139] D. Rousseau,[118] C. R. Royon,[137] A. Rozanov,[87] Y. Rozen,[153] X. Ruan,[146c] F. Rubbo,[144] M. S. Rudolph,[159] F. Rühr,[50] A. Ruiz-Martinez,[31] Z. Rurikova,[50] N. A. Rusakovich,[67] A. Ruschke,[101] H. L. Russell,[139] J. P. Rutherfoord,[7] N. Ruthmann,[32] Y. F. Ryabov,[124] M. Rybar,[166] G. Rybkin,[118] S. Ryu,[6] A. Ryzhov,[131] G. F. Rzehorz,[56] A. F. Saavedra,[151] G. Sabato,[108] S. Sacerdoti,[29] H. F-W. Sadrozinski,[138] R. Sadykov,[67] F. Safai Tehrani,[133a] P. Saha,[109] M. Sahinsoy,[60a] M. Saimpert,[137] T. Saito,[156] H. Sakamoto,[156] Y. Sakurai,[171] G. Salamanna,[135a,135b] A. Salamon,[134a,134b] J. E. Salazar Loyola,[34b] D. Salek,[108] P. H. Sales De Bruin,[139] D. Salihagic,[102] A. Salnikov,[144] J. Salt,[167] D. Salvatore,[39a,39b] F. Salvatore,[150] A. Salvucci,[62a] A. Salzburger,[32] D. Sammel,[50] D. Sampsonidis,[155] A. Sanchez,[105a,105b] J. Sánchez,[167] V. Sanchez Martinez,[167] H. Sandaker,[120] R. L. Sandbach,[78] H. G. Sander,[85] M. Sandhoff,[175] C. Sandoval,[21] R. Sandstroem,[102] D. P. C. Sankey,[132] M. Sannino,[52a,52b] A. Sansoni,[49] C. Santoni,[36] R. Santonico,[134a,134b] H. Santos,[127a] I. Santoyo Castillo,[150] K. Sapp,[126] A. Sapronov,[67] J. G. Saraiva,[127a,127d] B. Sarrazin,[23] O. Sasaki,[68] Y. Sasaki,[156] K. Sato,[161] G. Sauvage,[5,a] E. Sauvan,[5] G. Savage,[79] P. Savard,[159,e] C. Sawyer,[132] L. Sawyer,[81,r] J. Saxon,[33] C. Sbarra,[22a] A. Sbrizzi,[22a,22b] T. Scanlon,[80] D. A. Scannicchio,[163] M. Scarcella,[151] V. Scarfone,[39a,39b] J. Schaarschmidt,[172] P. Schacht,[102] B. M. Schachtner,[101] D. Schaefer,[32] R. Schaefer,[44] J. Schaeffer,[85] S. Schaepe,[23] S. Schaetzel,[60b] U. Schäfer,[85] A. C. Schaffer,[118] D. Schaile,[101] R. D. Schamberger,[149] V. Scharf,[60a] V. A. Schegelsky,[124] D. Scheirich,[130] M. Schernau,[163] C. Schiavi,[52a,52b] S. Schier,[138] C. Schillo,[50] M. Schioppa,[39a,39b] S. Schlenker,[32] K. R. Schmidt-Sommerfeld,[102] K. Schmieden,[32] C. Schmitt,[85] S. Schmitt,[44] S. Schmitz,[85] B. Schneider,[160a] U. Schnoor,[50] L. Schoeffel,[137] A. Schoening,[60b] B. D. Schoenrock,[92] E. Schopf,[23] M. Schott,[85] J. Schovancova,[8] S. Schramm,[51] M. Schreyer,[174] N. Schuh,[85] M. J. Schultens,[23] H.-C. Schultz-Coulon,[60a] H. Schulz,[17] M. Schumacher,[50] B. A. Schumm,[138] Ph. Schune,[137] A. Schwartzman,[144] T. A. Schwarz,[91] Ph. Schwegler,[102] H. Schweiger,[86] Ph. Schwemling,[137] R. Schwienhorst,[92] J. Schwindling,[137] T. Schwindt,[23] G. Sciolla,[25] F. Scuri,[125a,125b] F. Scutti,[90] J. Searcy,[91] P. Seema,[23] S. C. Seidel,[106] A. Seiden,[138] F. Seifert,[129] J. M. Seixas,[26a] G. Sekhniaidze,[105a] K. Sekhon,[91] S. J. Sekula,[42] D. M. Seliverstov,[124,a] N. Semprini-Cesari,[22a,22b] C. Serfon,[120] L. Serin,[118] L. Serkin,[164a,164b] M. Sessa,[135a,135b] R. Seuster,[169] H. Severini,[114] T. Sfiligoj,[77] F. Sforza,[32] A. Sfyrla,[51] E. Shabalina,[56] N. W. Shaikh,[147a,147b] L. Y. Shan,[35a] R. Shang,[166] J. T. Shank,[24] M. Shapiro,[16] P. B. Shatalov,[98] K. Shaw,[164a,164b] S. M. Shaw,[86] A. Shcherbakova,[147a,147b] C. Y. Shehu,[150] P. Sherwood,[80] L. Shi,[152,kk] S. Shimizu,[69] C. O. Shimmin,[163] M. Shimojima,[103] M. Shiyakova,[67,ll] A. Shmeleva,[97] D. Shoaleh Saadi,[96] M. J. Shochet,[33] S. Shojaii,[93a,93b] S. Shrestha,[112] E. Shulga,[99] M. A. Shupe,[7] P. Sicho,[128] A. M. Sickles,[166] P. E. Sidebo,[148] O. Sidiropoulou,[174] D. Sidorov,[115] A. Sidoti,[22a,22b] F. Siegert,[46] Dj. Sijacki,[14] J. Silva,[127a,127d] S. B. Silverstein,[147a] V. Simak,[129] O. Simard,[5] Lj. Simic,[14] S. Simion,[118] E. Simioni,[85] B. Simmons,[80] D. Simon,[36] M. Simon,[85] P. Sinervo,[159] N. B. Sinev,[117] M. Sioli,[22a,22b] G. Siragusa,[174] S. Yu. Sivoklokov,[100] J. Sjölin,[147a,147b] T. B. Sjursen,[15] M. B. Skinner,[74] H. P. Skottowe,[59] P. Skubic,[114] M. Slater,[19] T. Slavicek,[129] M. Slawinska,[108] K. Sliwa,[162] R. Slovak,[130] V. Smakhtin,[172] B. H. Smart,[5] L. Smestad,[15] J. Smiesko,[145a] S. Yu. Smirnov,[99] Y. Smirnov,[99] L. N. Smirnova,[100,mm] O. Smirnova,[83] M. N. K. Smith,[37] R. W. Smith,[37] M. Smizanska,[74] K. Smolek,[129] A. A. Snesarev,[97] S. Snyder,[27] R. Sobie,[169,m] F. Socher,[46] A. Soffer,[154] D. A. Soh,[152] G. Sokhrannyi,[77] C. A. Solans Sanchez,[32] M. Solar,[129] E. Yu. Soldatov,[99] U. Soldevila,[167] A. A. Solodkov,[131] A. Soloshenko,[67] O. V. Solovyanov,[131] V. Solovyev,[124] P. Sommer,[50] H. Son,[162] H. Y. Song,[35b,nn] A. Sood,[16] A. Sopczak,[129] V. Sopko,[129] V. Sorin,[13] D. Sosa,[60b] C. L. Sotiropoulou,[125a,125b] R. Soualah,[164a,164c] A. M. Soukharev,[110,d] D. South,[44] B. C. Sowden,[79] S. Spagnolo,[75a,75b] M. Spalla,[125a,125b] M. Spangenberg,[170] F. Spanò,[79] D. Sperlich,[17] F. Spettel,[102] R. Spighi,[22a] G. Spigo,[32] L. A. Spiller,[90] M. Spousta,[130] R. D. St. Denis,[55,a] A. Stabile,[93a] R. Stamen,[60a] S. Stamm,[17] E. Stanecka,[41] R. W. Stanek,[6] C. Stanescu,[135a] M. Stanescu-Bellu,[44] M. M. Stanitzki,[44] S. Stapnes,[120] E. A. Starchenko,[131] G. H. Stark,[33] J. Stark,[57] P. Staroba,[128] P. Starovoitov,[60a] S. Stärz,[32] R. Staszewski,[41] P. Steinberg,[27] B. Stelzer,[143] H. J. Stelzer,[32] O. Stelzer-Chilton,[160a] H. Stenzel,[54] G. A. Stewart,[55] J. A. Stillings,[23] M. C. Stockton,[89] M. Stoebe,[89] G. Stoicea,[28b] P. Stolte,[56] S. Stonjek,[102] A. R. Stradling,[8] A. Straessner,[46] M. E. Stramaglia,[18] J. Strandberg,[148] S. Strandberg,[147a,147b] A. Strandlie,[120] M. Strauss,[114] P. Strizenec,[145b] R. Ströhmer,[174] D. M. Strom,[117] R. Stroynowski,[42] A. Strubig,[107] S. A. Stucci,[18] B. Stugu,[15] N. A. Styles,[44] D. Su,[144] J. Su,[126] R. Subramaniam,[81] S. Suchek,[60a] Y. Sugaya,[119] M. Suk,[129] V. V. Sulin,[97] S. Sultansoy,[4c] T. Sumida,[70] S. Sun,[59] X. Sun,[35a] J. E. Sundermann,[50] K. Suruliz,[150] G. Susinno,[39a,39b] M. R. Sutton,[150] S. Suzuki,[68] M. Svatos,[128] M. Swiatlowski,[33] I. Sykora,[145a] T. Sykora,[130] D. Ta,[50] C. Taccini,[135a,135b] K. Tackmann,[44] J. Taenzer,[159] A. Taffard,[163] R. Tafirout,[160a] N. Taiblum,[154] H. Takai,[27] R. Takashima,[71] T. Takeshita,[141] Y. Takubo,[68] M. Talby,[87] A. A. Talyshev,[110,d] K. G. Tan,[90] J. Tanaka,[156] R. Tanaka,[118] S. Tanaka,[68] B. B. Tannenwald,[112] S. Tapia Araya,[34b] S. Tapprogge,[85] S. Tarem,[153]

G. F. Tartarelli,[93a] P. Tas,[130] M. Tasevsky,[128] T. Tashiro,[70] E. Tassi,[39a,39b] A. Tavares Delgado,[127a,127b] Y. Tayalati,[136d] A. C. Taylor,[106] G. N. Taylor,[90] P. T. E. Taylor,[90] W. Taylor,[160b] F. A. Teischinger,[32] P. Teixeira-Dias,[79] K. K. Temming,[50] D. Temple,[143] H. Ten Kate,[32] P. K. Teng,[152] J. J. Teoh,[119] F. Tepel,[175] S. Terada,[68] K. Terashi,[156] J. Terron,[84] S. Terzo,[102] M. Testa,[49] R. J. Teuscher,[159,m] T. Theveneaux-Pelzer,[87] J. P. Thomas,[19] J. Thomas-Wilsker,[79] E. N. Thompson,[37] P. D. Thompson,[19] A. S. Thompson,[55] L. A. Thomsen,[176] E. Thomson,[123] M. Thomson,[30] M. J. Tibbetts,[16] R. E. Ticse Torres,[87] V. O. Tikhomirov,[97,oo] Yu. A. Tikhonov,[110,d] S. Timoshenko,[99] P. Tipton,[176] S. Tisserant,[87] K. Todome,[158] T. Todorov,[5,a] S. Todorova-Nova,[130] J. Tojo,[72] S. Tokár,[145a] K. Tokushuku,[68] E. Tolley,[59] L. Tomlinson,[86] M. Tomoto,[104] L. Tompkins,[144,pp] K. Toms,[106] B. Tong,[59] E. Torrence,[117] H. Torres,[143] E. Torró Pastor,[139] J. Toth,[87,qq] F. Touchard,[87] D. R. Tovey,[140] T. Trefzger,[174] A. Tricoli,[27] I. M. Trigger,[160a] S. Trincaz-Duvoid,[82] M. F. Tripiana,[13] W. Trischuk,[159] B. Trocmé,[57] A. Trofymov,[44] C. Troncon,[93a] M. Trottier-McDonald,[16] M. Trovatelli,[169] L. Truong,[164a,164c] M. Trzebinski,[41] A. Trzupek,[41] J. C-L. Tseng,[121] P. V. Tsiareshka,[94] G. Tsipolitis,[10] N. Tsirintanis,[9] S. Tsiskaridze,[13] V. Tsiskaridze,[50] E. G. Tskhadadze,[53a] K. M. Tsui,[62a] I. I. Tsukerman,[98] V. Tsulaia,[16] S. Tsuno,[68] D. Tsybychev,[149] A. Tudorache,[28b] V. Tudorache,[28b] A. N. Tuna,[59] S. A. Tupputi,[22a,22b] S. Turchikhin,[100,mm] D. Turecek,[129] D. Turgeman,[172] R. Turra,[93a,93b] A. J. Turvey,[42] P. M. Tuts,[37] M. Tyndel,[132] G. Ucchielli,[22a,22b] I. Ueda,[156] R. Ueno,[31] M. Ughetto,[147a,147b] F. Ukegawa,[161] G. Unal,[32] A. Undrus,[27] G. Unel,[163] F. C. Ungaro,[90] Y. Unno,[68] C. Unverdorben,[101] J. Urban,[145b] P. Urquijo,[90] P. Urrejola,[85] G. Usai,[8] A. Usanova,[64] L. Vacavant,[87] V. Vacek,[129] B. Vachon,[89] C. Valderanis,[101] E. Valdes Santurio,[147a,147b] N. Valencic,[108] S. Valentinetti,[22a,22b] A. Valero,[167] L. Valery,[13] S. Valkar,[130] S. Vallecorsa,[51] J. A. Valls Ferrer,[167] W. Van Den Wollenberg,[108] P. C. Van Der Deijl,[108] R. van der Geer,[108] H. van der Graaf,[108] N. van Eldik,[153] P. van Gemmeren,[6] J. Van Nieuwkoop,[143] I. van Vulpen,[108] M. C. van Woerden,[32] M. Vanadia,[133a,133b] W. Vandelli,[32] R. Vanguri,[123] A. Vaniachine,[6] P. Vankov,[108] G. Vardanyan,[177] R. Vari,[133a] E. W. Varnes,[7] T. Varol,[42] D. Varouchas,[82] A. Vartapetian,[8] K. E. Varvell,[151] J. G. Vasquez,[176] F. Vazeille,[36] T. Vazquez Schroeder,[89] J. Veatch,[56] L. M. Veloce,[159] F. Veloso,[127a,127c] S. Veneziano,[133a] A. Ventura,[75a,75b] M. Venturi,[169] N. Venturi,[159] A. Venturini,[25] V. Vercesi,[122a] M. Verducci,[133a,133b] W. Verkerke,[108] J. C. Vermeulen,[108] A. Vest,[46,rr] M. C. Vetterli,[143,e] O. Viazlo,[83] I. Vichou,[166] T. Vickey,[140] O. E. Vickey Boeriu,[140] G. H. A. Viehhauser,[121] S. Viel,[16] L. Vigani,[121] R. Vigne,[64] M. Villa,[22a,22b] M. Villaplana Perez,[93a,93b] E. Vilucchi,[49] M. G. Vincter,[31] V. B. Vinogradov,[67] C. Vittori,[22a,22b] I. Vivarelli,[150] S. Vlachos,[10] M. Vlasak,[129] M. Vogel,[175] P. Vokac,[129] G. Volpi,[125a,125b] M. Volpi,[90] H. von der Schmitt,[102] E. von Toerne,[23] V. Vorobel,[130] K. Vorobev,[99] M. Vos,[167] R. Voss,[32] J. H. Vossebeld,[76] N. Vranjes,[14] M. Vranjes Milosavljevic,[14] V. Vrba,[128] M. Vreeswijk,[108] R. Vuillermet,[32] I. Vukotic,[33] Z. Vykydal,[129] P. Wagner,[23] W. Wagner,[175] H. Wahlberg,[73] S. Wahrmund,[46] J. Wakabayashi,[104] J. Walder,[74] R. Walker,[101] W. Walkowiak,[142] V. Wallangen,[147a,147b] C. Wang,[35c] C. Wang,[35d,87] F. Wang,[173] H. Wang,[16] H. Wang,[42] J. Wang,[44] J. Wang,[151] K. Wang,[89] R. Wang,[6] S. M. Wang,[152] T. Wang,[23] T. Wang,[37] X. Wang,[176] C. Wanotayaroj,[117] A. Warburton,[89] C. P. Ward,[30] D. R. Wardrope,[80] A. Washbrook,[48] P. M. Watkins,[19] A. T. Watson,[19] M. F. Watson,[19] G. Watts,[139] S. Watts,[86] B. M. Waugh,[80] S. Webb,[85] M. S. Weber,[18] S. W. Weber,[174] J. S. Webster,[6] A. R. Weidberg,[121] B. Weinert,[63] J. Weingarten,[56] C. Weiser,[50] H. Weits,[108] P. S. Wells,[32] T. Wenaus,[27] T. Wengler,[32] S. Wenig,[32] N. Wermes,[23] M. Werner,[50] P. Werner,[32] M. Wessels,[60a] J. Wetter,[162] K. Whalen,[117] N. L. Whallon,[139] A. M. Wharton,[74] A. White,[8] M. J. White,[1] R. White,[34b] D. Whiteson,[163] F. J. Wickens,[132] W. Wiedenmann,[173] M. Wielers,[132] P. Wienemann,[23] C. Wiglesworth,[38] L. A. M. Wiik-Fuchs,[23] A. Wildauer,[102] F. Wilk,[86] H. G. Wilkens,[32] H. H. Williams,[123] S. Williams,[108] C. Willis,[92] S. Willocq,[88] J. A. Wilson,[19] I. Wingerter-Seez,[5] F. Winklmeier,[117] O. J. Winston,[150] B. T. Winter,[23] M. Wittgen,[144] J. Wittkowski,[101] S. J. Wollstadt,[85] M. W. Wolter,[41] H. Wolters,[127a,127c] B. K. Wosiek,[41] J. Wotschack,[32] M. J. Woudstra,[86] K. W. Wozniak,[41] M. Wu,[57] M. Wu,[33] S. L. Wu,[173] X. Wu,[51] Y. Wu,[91] T. R. Wyatt,[86] B. M. Wynne,[48] S. Xella,[38] D. Xu,[35a] L. Xu,[27] B. Yabsley,[151] S. Yacoob,[146a] R. Yakabe,[69] D. Yamaguchi,[158] Y. Yamaguchi,[119] A. Yamamoto,[68] S. Yamamoto,[156] T. Yamanaka,[156] K. Yamauchi,[104] Y. Yamazaki,[69] Z. Yan,[24] H. Yang,[35e] H. Yang,[173] Y. Yang,[152] Z. Yang,[15] W-M. Yao,[16] Y. C. Yap,[82] Y. Yasu,[68] E. Yatsenko,[5] K. H. Yau Wong,[23] J. Ye,[42] S. Ye,[27] I. Yeletskikh,[67] A. L. Yen,[59] E. Yildirim,[85] K. Yorita,[171] R. Yoshida,[6] K. Yoshihara,[123] C. Young,[144] C. J. S. Young,[32] S. Youssef,[24] D. R. Yu,[16] J. Yu,[8] J. M. Yu,[91] J. Yu,[66] L. Yuan,[69] S. P. Y. Yuen,[23] I. Yusuff,[30,ss] B. Zabinski,[41] R. Zaidan,[35d] A. M. Zaitsev,[131,ff] N. Zakharchuk,[44] J. Zalieckas,[15] A. Zaman,[149] S. Zambito,[59] L. Zanello,[133a,133b] D. Zanzi,[90] C. Zeitnitz,[175] M. Zeman,[129] A. Zemla,[40a] J. C. Zeng,[166] Q. Zeng,[144] K. Zengel,[25] O. Zenin,[131] T. Ženiš,[145a] D. Zerwas,[118] D. Zhang,[91] F. Zhang,[173] G. Zhang,[35b,nn] H. Zhang,[35c] J. Zhang,[6] L. Zhang,[50] R. Zhang,[23] R. Zhang,[35b,tt] X. Zhang,[35d] Z. Zhang,[118] X. Zhao,[42] Y. Zhao,[35d] Z. Zhao,[35b] A. Zhemchugov,[67] J. Zhong,[121] B. Zhou,[91]

C. Zhou,[47] L. Zhou,[37] L. Zhou,[42] M. Zhou,[149] N. Zhou,[35f] C. G. Zhu,[35d] H. Zhu,[35a] J. Zhu,[91] Y. Zhu,[35b] X. Zhuang,[35a] K. Zhukov,[97] A. Zibell,[174] D. Zieminska,[63] N. I. Zimine,[67] C. Zimmermann,[85] S. Zimmermann,[50] Z. Zinonos,[56] M. Zinser,[85] M. Ziolkowski,[142] L. Živković,[14] G. Zobernig,[173] A. Zoccoli,[22a,22b] M. zur Nedden,[17] G. Zurzolo,[105a,105b] and L. Zwalinski[32]

(ATLAS Collaboration)

[1]*Department of Physics, University of Adelaide, Adelaide, Australia*
[2]*Physics Department, SUNY Albany, Albany, New York, USA*
[3]*Department of Physics, University of Alberta, Edmonton, Alberta, Canada*
[4a]*Department of Physics, Ankara University, Ankara, Turkey*
[4b]*Istanbul Aydin University, Istanbul, Turkey*
[4c]*Division of Physics, TOBB University of Economics and Technology, Ankara, Turkey*
[5]*LAPP, CNRS/IN2P3 and Université Savoie Mont Blanc, Annecy-le-Vieux, France*
[6]*High Energy Physics Division, Argonne National Laboratory, Argonne, Illinois, USA*
[7]*Department of Physics, University of Arizona, Tucson, Arizona, USA*
[8]*Department of Physics, The University of Texas at Arlington, Arlington, Texas, USA*
[9]*Physics Department, University of Athens, Athens, Greece*
[10]*Physics Department, National Technical University of Athens, Zografou, Greece*
[11]*Department of Physics, The University of Texas at Austin, Austin, Texas, USA*
[12]*Institute of Physics, Azerbaijan Academy of Sciences, Baku, Azerbaijan*
[13]*Institut de Física d'Altes Energies (IFAE), The Barcelona Institute of Science and Technology, Barcelona, Spain, Spain*
[14]*Institute of Physics, University of Belgrade, Belgrade, Serbia*
[15]*Department for Physics and Technology, University of Bergen, Bergen, Norway*
[16]*Physics Division, Lawrence Berkeley National Laboratory and University of California, Berkeley, California, USA*
[17]*Department of Physics, Humboldt University, Berlin, Germany*
[18]*Albert Einstein Center for Fundamental Physics and Laboratory for High Energy Physics, University of Bern, Bern, Switzerland*
[19]*School of Physics and Astronomy, University of Birmingham, Birmingham, United Kingdom*
[20a]*Department of Physics, Bogazici University, Istanbul, Turkey*
[20b]*Department of Physics Engineering, Gaziantep University, Gaziantep, Turkey*
[20d]*Istanbul Bilgi University, Faculty of Engineering and Natural Sciences, Istanbul, Turkey, Turkey*
[20e]*Bahcesehir University, Faculty of Engineering and Natural Sciences, Istanbul, Turkey, Turkey*
[21]*Centro de Investigaciones, Universidad Antonio Narino, Bogota, Colombia*
[22a]*INFN Sezione di Bologna, Italy*
[22b]*Dipartimento di Fisica e Astronomia, Università di Bologna, Bologna, Italy*
[23]*Physikalisches Institut, University of Bonn, Bonn, Germany*
[24]*Department of Physics, Boston University, Boston, Massachusetts, USA*
[25]*Department of Physics, Brandeis University, Waltham, Massachusetts, USA*
[26a]*Universidade Federal do Rio De Janeiro COPPE/EE/IF, Rio de Janeiro, Brazil*
[26b]*Electrical Circuits Department, Federal University of Juiz de Fora (UFJF), Juiz de Fora, Brazil*
[26c]*Federal University of Sao Joao del Rei (UFSJ), Sao Joao del Rei, Brazil*
[26d]*Instituto de Fisica, Universidade de Sao Paulo, Sao Paulo, Brazil*
[27]*Physics Department, Brookhaven National Laboratory, Upton, New York, USA*
[28a]*Transilvania University of Brasov, Brasov, Romania, Romania*
[28b]*National Institute of Physics and Nuclear Engineering, Bucharest, Romania*
[28c]*National Institute for Research and Development of Isotopic and Molecular Technologies, Physics Department, Cluj Napoca, Romania*
[28d]*University Politehnica Bucharest, Bucharest, Romania*
[28e]*West University in Timisoara, Timisoara, Romania*
[29]*Departamento de Física, Universidad de Buenos Aires, Buenos Aires, Argentina*
[30]*Cavendish Laboratory, University of Cambridge, Cambridge, United Kingdom*
[31]*Department of Physics, Carleton University, Ottawa, Ontario, Canada*
[32]*CERN, Geneva, Switzerland*
[33]*Enrico Fermi Institute, University of Chicago, Chicago, Illinois, USA*
[34a]*Departamento de Física, Pontificia Universidad Católica de Chile, Santiago, Chile*
[34b]*Departamento de Física, Universidad Técnica Federico Santa María, Valparaíso, Chile*

[35a]Institute of High Energy Physics, Chinese Academy of Sciences, Beijing, China
[35b]Department of Modern Physics, University of Science and Technology of China, Anhui, China
[35c]Department of Physics, Nanjing University, Jiangsu, China
[35d]School of Physics, Shandong University, Shandong, China
[35e]Department of Physics and Astronomy, Shanghai Key Laboratory for Particle Physics and Cosmology, Shanghai Jiao Tong University, Shanghai; (also affiliated with PKU-CHEP), China
[35f]Physics Department, Tsinghua University, Beijing 100084, China
[36]Laboratoire de Physique Corpusculaire, Clermont Université and Université Blaise Pascal and CNRS/IN2P3, Clermont-Ferrand, France
[37]Nevis Laboratory, Columbia University, Irvington, New York, USA
[38]Niels Bohr Institute, University of Copenhagen, Kobenhavn, Denmark
[39a]INFN Gruppo Collegato di Cosenza, Laboratori Nazionali di Frascati, Italy
[39b]Dipartimento di Fisica, Università della Calabria, Rende, Italy
[40a]AGH University of Science and Technology, Faculty of Physics and Applied Computer Science, Krakow, Poland
[40b]Marian Smoluchowski Institute of Physics, Jagiellonian University, Krakow, Poland
[41]Institute of Nuclear Physics Polish Academy of Sciences, Krakow, Poland
[42]Physics Department, Southern Methodist University, Dallas, Texas, USA
[43]Physics Department, University of Texas at Dallas, Richardson, Texas, USA
[44]DESY, Hamburg and Zeuthen, Germany
[45]Institut für Experimentelle Physik IV, Technische Universität Dortmund, Dortmund, Germany
[46]Institut für Kern- und Teilchenphysik, Technische Universität Dresden, Dresden, Germany
[47]Department of Physics, Duke University, Durham, North Carolina, USA
[48]SUPA - School of Physics and Astronomy, University of Edinburgh, Edinburgh, United Kingdom
[49]INFN Laboratori Nazionali di Frascati, Frascati, Italy
[50]Fakultät für Mathematik und Physik, Albert-Ludwigs-Universität, Freiburg, Germany
[51]Section de Physique, Université de Genève, Geneva, Switzerland
[52a]INFN Sezione di Genova, Italy
[52b]Dipartimento di Fisica, Università di Genova, Genova, Italy
[53a]E. Andronikashvili Institute of Physics, Iv. Javakhishvili Tbilisi State University, Tbilisi, Georgia
[53b]High Energy Physics Institute, Tbilisi State University, Tbilisi, Georgia
[54]II Physikalisches Institut, Justus-Liebig-Universität Giessen, Giessen, Germany
[55]SUPA - School of Physics and Astronomy, University of Glasgow, Glasgow, United Kingdom
[56]II Physikalisches Institut, Georg-August-Universität, Göttingen, Germany
[57]Laboratoire de Physique Subatomique et de Cosmologie, Université Grenoble-Alpes, CNRS/IN2P3, Grenoble, France
[58]Department of Physics, Hampton University, Hampton, Virginia, USA
[59]Laboratory for Particle Physics and Cosmology, Harvard University, Cambridge, Massachusetts, USA
[60a]Kirchhoff-Institut für Physik, Ruprecht-Karls-Universität Heidelberg, Heidelberg, Germany
[60b]Physikalisches Institut, Ruprecht-Karls-Universität Heidelberg, Heidelberg, Germany
[60c]ZITI Institut für technische Informatik, Ruprecht-Karls-Universität Heidelberg, Mannheim, Germany
[61]Faculty of Applied Information Science, Hiroshima Institute of Technology, Hiroshima, Japan
[62a]Department of Physics, The Chinese University of Hong Kong, Shatin, N.T., Hong Kong, China
[62b]Department of Physics, The University of Hong Kong, Hong Kong, China
[62c]Department of Physics, The Hong Kong University of Science and Technology, Clear Water Bay, Kowloon, Hong Kong, China
[63]Department of Physics, Indiana University, Bloomington, Indiana, USA
[64]Institut für Astro- und Teilchenphysik, Leopold-Franzens-Universität, Innsbruck, Austria
[65]University of Iowa, Iowa City, Iowa, USA
[66]Department of Physics and Astronomy, Iowa State University, Ames, Iowa, USA
[67]Joint Institute for Nuclear Research, JINR Dubna, Dubna, Russia
[68]KEK, High Energy Accelerator Research Organization, Tsukuba, Japan
[69]Graduate School of Science, Kobe University, Kobe, Japan
[70]Faculty of Science, Kyoto University, Kyoto, Japan
[71]Kyoto University of Education, Kyoto, Japan
[72]Department of Physics, Kyushu University, Fukuoka, Japan
[73]Instituto de Física La Plata, Universidad Nacional de La Plata and CONICET, La Plata, Argentina
[74]Physics Department, Lancaster University, Lancaster, United Kingdom
[75a]INFN Sezione di Lecce, Italy
[75b]Dipartimento di Matematica e Fisica, Università del Salento, Lecce, Italy

[76]*Oliver Lodge Laboratory, University of Liverpool, Liverpool, United Kingdom*
[77]*Department of Physics, Jožef Stefan Institute and University of Ljubljana, Ljubljana, Slovenia*
[78]*School of Physics and Astronomy, Queen Mary University of London, London, United Kingdom*
[79]*Department of Physics, Royal Holloway University of London, Surrey, United Kingdom*
[80]*Department of Physics and Astronomy, University College London, London, United Kingdom*
[81]*Louisiana Tech University, Ruston, Louisiana, USA*
[82]*Laboratoire de Physique Nucléaire et de Hautes Energies, UPMC and Université Paris-Diderot and CNRS/IN2P3, Paris, France*
[83]*Fysiska institutionen, Lunds universitet, Lund, Sweden*
[84]*Departamento de Fisica Teorica C-15, Universidad Autonoma de Madrid, Madrid, Spain*
[85]*Institut für Physik, Universität Mainz, Mainz, Germany*
[86]*School of Physics and Astronomy, University of Manchester, Manchester, United Kingdom*
[87]*CPPM, Aix-Marseille Université and CNRS/IN2P3, Marseille, France*
[88]*Department of Physics, University of Massachusetts, Amherst, Massachusetts, USA*
[89]*Department of Physics, McGill University, Montreal, Québec, Canada*
[90]*School of Physics, University of Melbourne, Victoria, Australia*
[91]*Department of Physics, The University of Michigan, Ann Arbor, Michigan, USA*
[92]*Department of Physics and Astronomy, Michigan State University, East Lansing, Michigan, USA*
[93a]*INFN Sezione di Milano, Italy*
[93b]*Dipartimento di Fisica, Università di Milano, Milano, Italy*
[94]*B.I. Stepanov Institute of Physics, National Academy of Sciences of Belarus, Minsk, Republic of Belarus*
[95]*National Scientific and Educational Centre for Particle and High Energy Physics, Minsk, Republic of Belarus*
[96]*Group of Particle Physics, University of Montreal, Montreal, Québec, Canada*
[97]*P.N. Lebedev Physical Institute of the Russian Academy of Sciences, Moscow, Russia*
[98]*Institute for Theoretical and Experimental Physics (ITEP), Moscow, Russia*
[99]*National Research Nuclear University MEPhI, Moscow, Russia*
[100]*D.V. Skobeltsyn Institute of Nuclear Physics, M.V. Lomonosov Moscow State University, Moscow, Russia*
[101]*Fakultät für Physik, Ludwig-Maximilians-Universität München, München, Germany*
[102]*Max-Planck-Institut für Physik (Werner-Heisenberg-Institut), München, Germany*
[103]*Nagasaki Institute of Applied Science, Nagasaki, Japan*
[104]*Graduate School of Science and Kobayashi-Maskawa Institute, Nagoya University, Nagoya, Japan*
[105a]*INFN Sezione di Napoli, Italy*
[105b]*Dipartimento di Fisica, Università di Napoli, Napoli, Italy*
[106]*Department of Physics and Astronomy, University of New Mexico, Albuquerque, New Mexico, USA*
[107]*Institute for Mathematics, Astrophysics and Particle Physics, Radboud University Nijmegen/Nikhef, Nijmegen, Netherlands*
[108]*Nikhef National Institute for Subatomic Physics and University of Amsterdam, Amsterdam, Netherlands*
[109]*Department of Physics, Northern Illinois University, DeKalb, Illinois, USA*
[110]*Budker Institute of Nuclear Physics, SB RAS, Novosibirsk, Russia*
[111]*Department of Physics, New York University, New York, New York, USA*
[112]*Ohio State University, Columbus, Ohio, USA*
[113]*Faculty of Science, Okayama University, Okayama, Japan*
[114]*Homer L. Dodge Department of Physics and Astronomy, University of Oklahoma, Norman, Oklahoma, USA*
[115]*Department of Physics, Oklahoma State University, Stillwater, Oklahoma, USA*
[116]*Palacký University, RCPTM, Olomouc, Czech Republic*
[117]*Center for High Energy Physics, University of Oregon, Eugene, Oregon, USA*
[118]*LAL, Univ. Paris-Sud, CNRS/IN2P3, Université Paris-Saclay, Orsay, France*
[119]*Graduate School of Science, Osaka University, Osaka, Japan*
[120]*Department of Physics, University of Oslo, Oslo, Norway*
[121]*Department of Physics, Oxford University, Oxford, United Kingdom*
[122a]*INFN Sezione di Pavia, Italy*
[122b]*Dipartimento di Fisica, Università di Pavia, Pavia, Italy*
[123]*Department of Physics, University of Pennsylvania, Philadelphia, Pennsylvania, USA*
[124]*National Research Centre "Kurchatov Institute" B.P.Konstantinov Petersburg Nuclear Physics Institute, St. Petersburg, Russia*
[125a]*INFN Sezione di Pisa, Italy*
[125b]*Dipartimento di Fisica E. Fermi, Università di Pisa, Pisa, Italy*

[126]*Department of Physics and Astronomy, University of Pittsburgh, Pittsburgh, Pennsylvania, USA*
[127a]*Laboratório de Instrumentação e Física Experimental de Partículas - LIP, Lisboa, Portugal*
[127b]*Faculdade de Ciências, Universidade de Lisboa, Lisboa, Portugal*
[127c]*Department of Physics, University of Coimbra, Coimbra, Portugal*
[127d]*Centro de Física Nuclear da Universidade de Lisboa, Lisboa, Portugal*
[127e]*Departamento de Fisica, Universidade do Minho, Braga, Portugal*
[127f]*Departamento de Fisica Teorica y del Cosmos and CAFPE, Universidad de Granada, Granada, Spain*
[127g]*Dep Fisica and CEFITEC of Faculdade de Ciencias e Tecnologia, Universidade Nova de Lisboa, Caparica, Portugal*
[128]*Institute of Physics, Academy of Sciences of the Czech Republic, Praha, Czech Republic*
[129]*Czech Technical University in Prague, Praha, Czech Republic*
[130]*Faculty of Mathematics and Physics, Charles University in Prague, Praha, Czech Republic*
[131]*State Research Center Institute for High Energy Physics (Protvino), NRC KI, Russia*
[132]*Particle Physics Department, Rutherford Appleton Laboratory, Didcot, United Kingdom*
[133a]*INFN Sezione di Roma, Italy*
[133b]*Dipartimento di Fisica, Sapienza Università di Roma, Roma, Italy*
[134a]*INFN Sezione di Roma Tor Vergata, Italy*
[134b]*Dipartimento di Fisica, Università di Roma Tor Vergata, Roma, Italy*
[135a]*INFN Sezione di Roma Tre, Italy*
[135b]*Dipartimento di Matematica e Fisica, Università Roma Tre, Roma, Italy*
[136a]*Faculté des Sciences Ain Chock, Réseau Universitaire de Physique des Hautes Energies - Université Hassan II, Casablanca, Morocco*
[136b]*Centre National de l'Energie des Sciences Techniques Nucleaires, Rabat, Morocco*
[136c]*Faculté des Sciences Semlalia, Université Cadi Ayyad, LPHEA-Marrakech, Morocco*
[136d]*Faculté des Sciences, Université Mohamed Premier and LPTPM, Oujda, Morocco*
[136e]*Faculté des sciences, Université Mohammed V, Rabat, Morocco*
[137]*DSM/IRFU (Institut de Recherches sur les Lois Fondamentales de l'Univers), CEA Saclay (Commissariat à l'Energie Atomique et aux Energies Alternatives), Gif-sur-Yvette, France*
[138]*Santa Cruz Institute for Particle Physics, University of California Santa Cruz, Santa Cruz, California, USA*
[139]*Department of Physics, University of Washington, Seattle, Washington, USA*
[140]*Department of Physics and Astronomy, University of Sheffield, Sheffield, United Kingdom*
[141]*Department of Physics, Shinshu University, Nagano, Japan*
[142]*Fachbereich Physik, Universität Siegen, Siegen, Germany*
[143]*Department of Physics, Simon Fraser University, Burnaby, British Columbia, Canada*
[144]*SLAC National Accelerator Laboratory, Stanford, California, USA*
[145a]*Faculty of Mathematics, Physics & Informatics, Comenius University, Bratislava, Slovak Republic*
[145b]*Department of Subnuclear Physics, Institute of Experimental Physics of the Slovak Academy of Sciences, Kosice, Slovak Republic*
[146a]*Department of Physics, University of Cape Town, Cape Town, South Africa*
[146b]*Department of Physics, University of Johannesburg, Johannesburg, South Africa*
[146c]*School of Physics, University of the Witwatersrand, Johannesburg, South Africa*
[147a]*Department of Physics, Stockholm University, Sweden*
[147b]*The Oskar Klein Centre, Stockholm, Sweden*
[148]*Physics Department, Royal Institute of Technology, Stockholm, Sweden*
[149]*Departments of Physics & Astronomy and Chemistry, Stony Brook University, Stony Brook, New York, USA*
[150]*Department of Physics and Astronomy, University of Sussex, Brighton, United Kingdom*
[151]*School of Physics, University of Sydney, Sydney, Australia*
[152]*Institute of Physics, Academia Sinica, Taipei, Taiwan*
[153]*Department of Physics, Technion: Israel Institute of Technology, Haifa, Israel*
[154]*Raymond and Beverly Sackler School of Physics and Astronomy, Tel Aviv University, Tel Aviv, Israel*
[155]*Department of Physics, Aristotle University of Thessaloniki, Thessaloniki, Greece*
[156]*International Center for Elementary Particle Physics and Department of Physics, The University of Tokyo, Tokyo, Japan*
[157]*Graduate School of Science and Technology, Tokyo Metropolitan University, Tokyo, Japan*
[158]*Department of Physics, Tokyo Institute of Technology, Tokyo, Japan*
[159]*Department of Physics, University of Toronto, Toronto, Ontario, Canada*
[160a]*TRIUMF, Vancouver, British Columbia, Canada*
[160b]*Department of Physics and Astronomy, York University, Toronto, Ontario, Canada*

[161]*Faculty of Pure and Applied Sciences, and Center for Integrated Research in Fundamental Science and Engineering, University of Tsukuba, Tsukuba, Japan*
[162]*Department of Physics and Astronomy, Tufts University, Medford, Massachusetts, USA*
[163]*Department of Physics and Astronomy, University of California Irvine, Irvine, California, USA*
[164a]*INFN Gruppo Collegato di Udine, Sezione di Trieste, Udine, Italy*
[164b]*ICTP, Trieste, Italy*
[164c]*Dipartimento di Chimica, Fisica e Ambiente, Università di Udine, Udine, Italy*
[165]*Department of Physics and Astronomy, University of Uppsala, Uppsala, Sweden*
[166]*Department of Physics, University of Illinois, Urbana, Illinois, USA*
[167]*Instituto de Fisica Corpuscular (IFIC) and Departamento de Fisica Atomica, Molecular y Nuclear and Departamento de Ingeniería Electrónica and Instituto de Microelectrónica de Barcelona (IMB-CNM), University of Valencia and CSIC, Valencia, Spain*
[168]*Department of Physics, University of British Columbia, Vancouver, British Columbia, Canada*
[169]*Department of Physics and Astronomy, University of Victoria, Victoria, British Columbia, Canada*
[170]*Department of Physics, University of Warwick, Coventry, United Kingdom*
[171]*Waseda University, Tokyo, Japan*
[172]*Department of Particle Physics, The Weizmann Institute of Science, Rehovot, Israel*
[173]*Department of Physics, University of Wisconsin, Madison, Wisconsin, USA*
[174]*Fakultät für Physik und Astronomie, Julius-Maximilians-Universität, Würzburg, Germany*
[175]*Fakultät für Mathematik und Naturwissenschaften, Fachgruppe Physik, Bergische Universität Wuppertal, Wuppertal, Germany*
[176]*Department of Physics, Yale University, New Haven, Connecticut, USA*
[177]*Yerevan Physics Institute, Yerevan, Armenia*
[178]*Centre de Calcul de l'Institut National de Physique Nucléaire et de Physique des Particules (IN2P3), Villeurbanne, France*

[a]Deceased.
[b]Also at Department of Physics, King's College London, London, United Kingdom.
[c]Also at Institute of Physics, Azerbaijan Academy of Sciences, Baku, Azerbaijan.
[d]Also at Novosibirsk State University, Novosibirsk, Russia.
[e]Also at TRIUMF, Vancouver BC, Canada.
[f]Also at Department of Physics & Astronomy, University of Louisville, Louisville, KY, USA.
[g]Also at Department of Physics, California State University, Fresno CA, USA.
[h]Also at Department of Physics, University of Fribourg, Fribourg, Switzerland.
[i]Also at Departament de Fisica de la Universitat Autonoma de Barcelona, Barcelona, Spain.
[j]Also at Departamento de Fisica e Astronomia, Faculdade de Ciencias, Universidade do Porto, Portugal.
[k]Also at Tomsk State University, Tomsk, Russia.
[l]Also at Universita di Napoli Parthenope, Napoli, Italy.
[m]Also at Institute of Particle Physics (IPP), Canada.
[n]Also at National Institute of Physics and Nuclear Engineering, Bucharest, Romania.
[o]Also at Department of Physics, St. Petersburg State Polytechnical University, St. Petersburg, Russia.
[p]Also at Department of Physics, The University of Michigan, Ann Arbor MI, USA.
[q]Also at Centre for High Performance Computing, CSIR Campus, Rosebank, Cape Town, South Africa.
[r]Also at Louisiana Tech University, Ruston LA, USA.
[s]Also at Institucio Catalana de Recerca i Estudis Avancats, ICREA, Barcelona, Spain.
[t]Also at Graduate School of Science, Osaka University, Osaka, Japan.
[u]Also at Department of Physics, National Tsing Hua University, Taiwan.
[v]Also at Institute for Mathematics, Astrophysics and Particle Physics, Radboud University Nijmegen/Nikhef, Nijmegen, Netherlands.
[w]Also at Department of Physics, The University of Texas at Austin, Austin TX, USA.
[x]Also at Institute of Theoretical Physics, Ilia State University, Tbilisi, Georgia.
[y]Also at CERN, Geneva, Switzerland.
[z]Also at Georgian Technical University (GTU),Tbilisi, Georgia.
[aa]Also at Ochadai Academic Production, Ochanomizu University, Tokyo, Japan.
[bb]Also at Manhattan College, New York NY, USA.
[cc]Also at Hellenic Open University, Patras, Greece.
[dd]Also at Academia Sinica Grid Computing, Institute of Physics, Academia Sinica, Taipei, Taiwan.
[ee]Also at School of Physics, Shandong University, Shandong, China.
[ff]Also at Moscow Institute of Physics and Technology State University, Dolgoprudny, Russia.
[gg]Also at Section de Physique, Université de Genève, Geneva, Switzerland.

[hh]Also at Eotvos Lorand University, Budapest, Hungary.
[ii]Also at International School for Advanced Studies (SISSA), Trieste, Italy.
[jj]Also at Department of Physics and Astronomy, University of South Carolina, Columbia SC, USA.
[kk]Also at School of Physics and Engineering, Sun Yat-sen University, Guangzhou, China.
[ll]Also at Institute for Nuclear Research and Nuclear Energy (INRNE) of the Bulgarian Academy of Sciences, Sofia, Bulgaria.
[mm]Also at Faculty of Physics, M.V.Lomonosov Moscow State University, Moscow, Russia.
[nn]Also at Institute of Physics, Academia Sinica, Taipei, Taiwan.
[oo]Also at National Research Nuclear University MEPhI, Moscow, Russia.
[pp]Also at Department of Physics, Stanford University, Stanford CA, USA.
[qq]Also at Institute for Particle and Nuclear Physics, Wigner Research Centre for Physics, Budapest, Hungary.
[rr]Also at Flensburg University of Applied Sciences, Flensburg, Germany.
[ss]Also at University of Malaya, Department of Physics, Kuala Lumpur, Malaysia.
[tt]Also at CPPM, Aix-Marseille Université and CNRS/IN2P3, Marseille, France.